Finite-size and thermal effects in effective models : phase transitions and summability

Erich Cavalcanti

PhD Thesis

Advisors:
Adolfo Malbouisson
Cesar Linhares

Rio de Janeiro, RJ
2019

Erich Cavalcanti

Finite-size and thermal effects in effective models : phase transitions and summability

Ph.D. Thesis

Thesis submitted in fulfillment of the requirements of the degree of Ph.D. at Centro Brasileiro de Pesquisas Físicas (CBPF).

Advisors:
Adolfo Malbouisson
Cesar Linhares

Rio de Janeiro, RJ
2019

CBPF 70 ANOS

MINISTÉRIO DA
CIÊNCIA, TECNOLOGIA,
INOVAÇÕES E COMUNICAÇÕES

"FINITE-SIZE AND THERMAL EFFECTS IN EFFECTIVE MODELS:
PHASE TRANSITIONS AND SUMMABILITY"

ERICH MONTEIRO BAILLY ANDERSEN CAVALCANTI

Tese de Doutorado em Física apresentada no Centro Brasileiro de Pesquisas Físicas do Ministério da Ciência Tecnologia e Inovação. Fazendo parte da banca examinadora os seguintes professores:

Adolfo Pedro Carvalho Malbouisson – Presidente/Orientador/CBPF

César Augusto Linhares da Fonseca Junior – Coorientador/UERJ

Eduardo Souza Fraga - UFRJ

Bruno Werneck Mintz - UERJ

José Abdalla Helayel Neto - CBPF

Sérgio José Barbosa Duarte - CBPF

Rio de Janeiro, 22 de agosto de 2019.

Centro Brasileiro de Pesquisas Físicas
Rua Doutor Xavier Sigaud, 150, URCA, Rio de Janeiro, Brasil
Tel.: +55 21 2141-7100 CEP:22290-180
http://www.cbpf.br

Resumo

Ao longo deste trabalho, investigamos o comportamento de alguns modelos de teoria de campos considerando a influência de variáveis e restrições termodinâmicas como a temperatura, o potencial químico, tamanho finito, e diferentes tipos de condições de contorno. Assumimos o ponto de vista de que é possível extrair aspectos não perturbativos de um modelo a partir da sua série perturbativa, o que nos traz à discussão de somabilidade em teoria de campos e que, por sua vez, nos levou à investigação do tópico de redução dimensional. Além disto, adotamos outro ponto de vista e consideramos teorias de campo efetivas por uma perspectiva fenomenológica para descrever interações hadrônicas em colisões de altas energias.
Palavras chave: Temperatura finita, condições de contorno, modelos efetivos, somabilidade de Borel, redução dimensional

Abstract

Throughout this work, we endeavor some investigation on the behavior of some field theoretical models taking into account the influence of thermodynamical variables and constraints as the temperature, chemical potential, finite size, and different kinds of boundary conditions. We assume the point of view that we can extract the nonperturbative aspects of a model from its perturbative series, which brings us to the topic of summability in field theories and introduced us to the topic of dimensional reduction. Moreover, we take a different viewpoint and study effective field theories from a phenomenological perspective to describe hadronic interplay at high-energy collisions.

Keywords: Finite temperature, boundary conditions, effective models, Borel summability, dimensional reduction

To the Magnum Khaos

Agradecimentos

Apesar de esta tese ser em inglês, os agradecimentos serão na minha língua-mãe. Nunca fui uma pessoa boa em comemorar ou agradecer, e a informalidade permeia minha escrita. A apresentação desta tese marca não um encerramento, pois minhas dúvidas não foram sanadas, mas sim um princípio, pois agora pareço ter amadurecido o suficiente para formular minhas perguntas e trilhar uma resposta a elas.

Agradeço ao meu avô Roberto, pois foi ele quem financiou meus estudos primários sem os quais não sei onde estaria. À minha avó Elbanira, que até hoje tem uma pilha de fotos da minha infância e é uma referência de mulher forte. À minha avó Zenith, pelo apoio que me deu tanto na graduação como no principio da pós-graduação. Agradeço aos meus pais, Roberto e Irani, que me deram recursos e incentivo para que eu me dedicasse aos meus estudos, que me ensinaram a valorizar o conhecimento, que me ensinaram a ser crítico e depois me ensinaram que não se deve exagerar tanto. Agradeço aos conselhos que me foram dados, inclusive àqueles que ignorei e depois percebi serem de extrema importância. Agradeço ao meu irmão Caio, pois não importa o caminho que trilhemos, sei que sempre poderemos contar um com o outro.

Agradeço aos meus orientadores e amigos, Adolfo e Cesar, que me acompanham desde o início do mestrado. Foram seis proveitosos anos que contribuíram fortemente para minha formação não somente como pesquisador, mas também como pessoa. Agradeço ao companheiro de pesquisa e amigo Zé Andre, que chegou no grupo injetando novas perguntas. Agradeço ao professor Luciano, com quem tive a oportunidade de trabalhar em uma linha de pesquisa distinta do que eu vinha fazendo. Agradeço à receptividade do Instituto de Física da UFBA. Agradeço a Erick, amigo e que foi companheiro de pesquisa durante o mestrado. Agradeço também aos meus orientadores do período da graduação. A Delson que foi meu primeiro orientador e a Franz Peter, sob supervisão do qual escrevi a monografia.

Agradeço aos professores da minha formação e de convívio. Agradeço a Franz Peter, Reiner, Fredson, Gilney, José Carlos, Delson, Iranderly, Miltão, Helayël, Tião, Gilvan, Tobias, Sérgio, ... Em especial àqueles que não simplesmente ensinaram, mas criaram uma atmosfera agradável para meu desenvolvimento próprio. É interessante perceber, em retrospectiva, que aprendi mais com aqueles que me deram tempo para ir além ao invés de me prender a um programa estático e imutável.

Agradeço a todos os companheiros e amigos da pós-graduação. Agradeço a Erick, GuilheRme, Zé Fernando, Thalis, Luciana, Daniel, Jade, Grécia, Miguel, Gabi, Max, Fábio, Lais, Guilherme, Isadora, Francisco, Jaime, Arthur, Gabriel, ... e tantos outros que não estou citando. Agradeço aos que colaboram com manter a APG-CBPF viva. Agradeço aos companheiros que demonstram ser a esperança de um futuro saudável para a ciência brasileira.

Em respeito ao meu passado e à minha história, agradeço à Ivana, que me acompanhou durante vários anos e que viu tanto minha calmaria quanto meu desespero diante da vida. Vivemos, ganhamos, sofremos, lutamos, perdemos.

Agradeço à bela comunidade do acroyoga, yoga, circo e calistenia. Às pessoas cheias de boa vontade e para as quais o treino é um prazer. Agradeço a Rafha, Wellington, Guga, Pat, Danilo, Manu, Susy, ...

Agradeço às pessoas que fazem o CBPF funcionar. Em especial, agradeço à super secretária Sônia e agradeço a Denise, Mônica, Bete e Cláudia.

Agradeço ao CNPq pela bolsa, sem a qual o doutorado não teria sido possível.

Agradeço a todos com quem tive contato e convivi pelas correções, debates, conselhos e críticas construtivas que recebi ao longo da minha trajetória. Sem isso, não teria aberto os olhos para várias das minhas falhas de julgamento. E neste ponto, agradeço a minha terapeuta, que tem me ajudado a refletir.

Se cheguei até aqui, reconheço, foi por ter dado sorte em vários momentos e por escolhas às vezes boas, às vezes ingênuas, que fiz ao longo do meu trajeto. E, portanto, agradeço ao meu Deus, qual chamo de Acaso.

À frente, não sei o que me aguarda.

And the vision
that was planted in my brain
Still remains
Within the sound of silence

– Simon & Garfunkel
The Sound Of Silence

Contents

Chapter 1

Introduction

When you follow two separate chains of thought, Watson, you will find some point of intersection which should approximate the truth.

– SHERLOCK HOLMES,
The disappearance of Lay Francis Carfax
Sir Arthur Conan Doyle

There is nothing like looking, if you want to find something. You certainly usually find something, if you look, but it is not always quite the something you were after.

– J.R.R. TOLKIEN *The Hobbit*

1.1 Opening remarks

The general framework of this thesis is an investigation of aspects of finite temperature quantum field theory (QFT). Three different research lines were considered during my Ph.D. studies: phase transitions; finiteness and summability of perturbative QFT; and hadron phenomenology. These studies have produced a few published articles [1–6] and motivates some further studies for future research. These opening remarks intend to clarify the structure of the thesis.

This thesis comes from a collection of previous works, and it is structured as follows:

- **Introduction**. In this chapter, I intend to clarify the motivation for the research lines followed and sketch the general picture. Also, to improve clarity, I make an overview of each publication. This is motivated by the fact that, for example, the articles [5, 6] are intimately related to the findings both in Ref. [2] and Ref. [3].

- **Research Lines**. Each chapter exhibits a published article. I have chosen not to show the article [1] about phase transitions in a scalar field theory under the influence of the magnetic field, temperature, chemical potential, and finite size, since it is very closely connected to the exposition in my master thesis.

- **Conclusions**. In this final chapter, I present some unpublished studies and give final remarks and perspectives for each research line.

The flow chart in Fig. 1.1 is a sketch on how this thesis should be read and understood. The underlying motivation is the investigation of aspects from highly interacting field theories, as QCD. Not in the sense to directly study QCD, but in the sense of investigating formal aspects that arise when one is interested in nonperturbative phenomena of QCD and that are also relevant in a broader perspective. There are plenty of paths to deal with nonperturbative phenomena in QCD and related theories, here we assume the perspective of effective models. This must be understood in the sense that effective models can isolate an aspect (formal or phenomenological) from the fundamental theory. The first aspect that drove some attention is regarding the problem of phase transitions. The research group I came into has some experience on the investigation of phase transitions for many different field-theoretical models under the influence of thermodynamical effects as temperature, finite size, chemical potential, and external magnetic field. Following the same spirit, it was produced the article in Ref. [1] - not exhibited here - and also the paper in Ref. [2]. This second paper come as a proposal to consider a simple and direct extension of the known formalism (of quantum field theories in toroidal topologies): the influence of boundary conditions on the spatial directions on the phase transitions of field-theoretical models.

A new perspective was inserted in the panorama with the research line of hadronic phenomenology. At first, we considered it as a complementary point of view to understand the physics of phase transition and, perhaps, assume a more phenomenological approach near QCD. The main concern was the behavior of the charmonium meson, a probe of the quark-gluon plasma. An initial step towards this produced the paper in Ref. [4]. However, a complete union between both research lines were not attained. One reason was that the initial approach needs to by modified to consider a lagrangian more intimately related to the recent findings in the ultrarelativistic colliders. Nevertheless, this study and the investigation of this topic allowed a better understanding of the recent developments in hadronic phenomenology.

The last research line arose as a consequence of the previous ones. We can say, in generic and general terms, that the papers in Refs. [1, 2, 4] assume some kind of effective model whose consequences are investigated through some perturbative series using some method that intends to obtain nonperturbative information. Therefore, the necessity to investigate the perturbative series to obtain the nonperturbative exact solution is a common aspect of both perspectives. This leads us to the problem of finitess in quantum field theory and then to take into account - as a first step - the summability of a scalar field model in the presence of finite temperature, resulting in the published paper in Ref. [3]. However, at this point some inquiries arose that seemed to be lacking an explanation. Therefore, instead of taking a step further in the effort to study of summability for some field theoretical model with some phase transition or apply it to study some phenomenological model, we studied the topic of dimensional reduction in the context of finite temperature and finite size. This investigation produced the papers in Ref. [5, 6].

The present chapter is structured as follows. At first, I sketch the general picture that motivates the use of effective models for Quantum Chromodynamics (QCD). Then, I specify, related to this broad picture, my topics of interest: phase transitions, summability of quantum field theory and application to hadronic phenomenology. I also add a section commenting on the problem of dimensional reduction. The last section exhibits the errata from the published articles.

1.1.1 Contribution to each paper included

I was intimately involved in the development of all five papers outlined in this paper-based thesis. The entire computation was done by myself and the results where

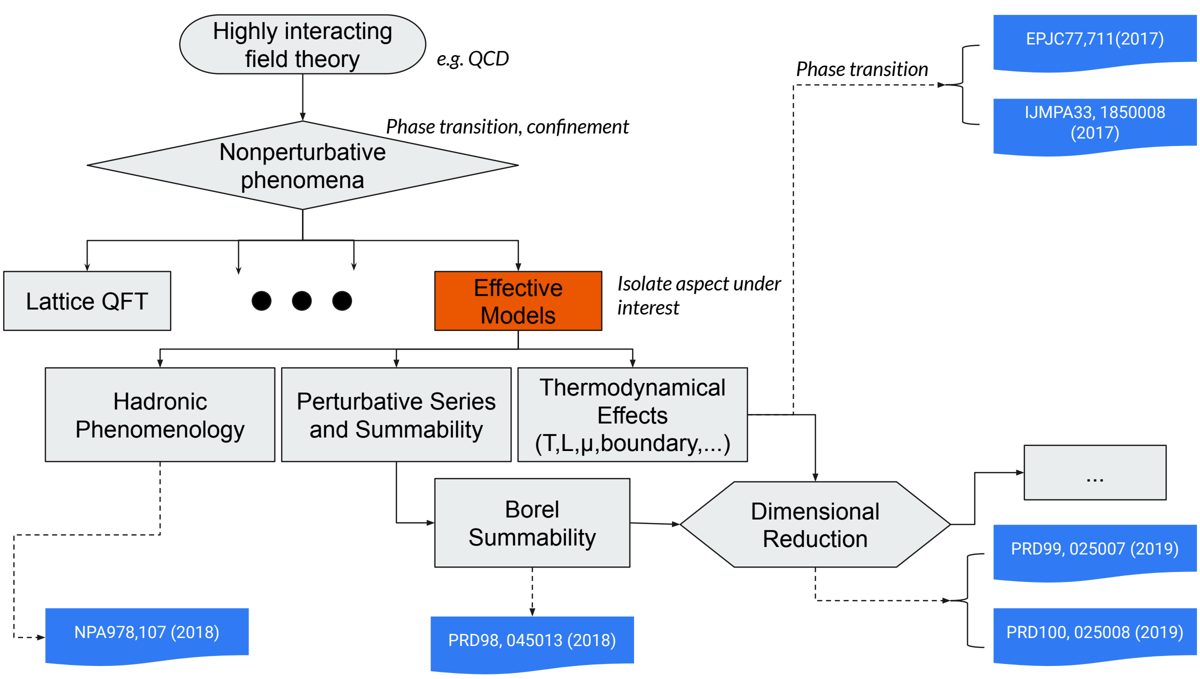

Figure 1.1: Representative flow chart of the developed work. It relates the published articles with the research lines under interest.

fruitfully discussed and analyzed during the meetings with the other members of the research group. These discussions were a necessary and important contribution so that the initial idea took a palatable and comprehensible form as to become publishable material.

Regarding the original proposal of each paper, I directly proposed what became the published articles in Refs. [2, 5, 6]. The project on the topic of scalar renormalons was originally proposed by the collaborator José André, but what motivated the publication in Ref. [3] were my findings on a way to compute the relevant Feynman diagrams for a self-interacting scalar field model at finite temperature in a large N approximation. The project on hadron phenomenology was proposed by the collaborator Luciano Abreu, I studied in detail the proposed model, applied it to our specific scenario and implemented a routine to obtain the cross-sections of all process that occurs as is presented in Ref. [4].

The research group followed the philosophy that I, being a Ph.D. student, should be responsible for the entire writing process of each article. This experience was essential for my formation as my supervisors were remarking each grammar mistake, misleading expression or lack of clarity that they could find in the paper. At each new project, I managed to 'converge' a bit faster to the final form of the paper due to the guidance of my supervisors.

1.2 The general picture: the underlying motivation

Quantum Chromodynamics (QCD) is the assumed theory of strongly interacting quarks and gluons. Although it is a complete and fundamental theory, some of its fundamental features such as chiral symmetry breaking and color confinement have not been fully understood up to now. Chiral symmetry breaking is responsible for almost all mass in the luminous universe as it is the mechanism of mass generation to the fundamental constituents of ordinary matter like protons and neutrons. Color confinement, on the other hand, is one of the fundamental puzzles of nature. The full determination of the QCD phase diagram remains one of the most challenging topics in high-energy physics and would mean an understanding of the conversion from the hadronic phase to the quark-gluon plasma. These aspects are contained in the larger problem of the development and study of nonperturbative techniques able to describe nonperturbative phenomena in general.

There are plentiful procedures developed over the past decades to explore QCD [7, 8]: perturbative QCD (pQCD) [9, 10], large-N QCD [11], sum rules [12, 13], lattice QCD [14–17], effective models [18–21], ...Perhaps the most practical method to obtain nonperturbative results is by lattice techniques [14–16, 22], although it faces some difficulties in certain aspects, as the evaluation of dynamical phenomena and the use of chemical potential that introduces the so called 'sign problem' - for details on this we refer to

Ref. [17]. However, there are also other perspectives, such as the use of effective models that reproduce some relevant aspects of the complete theory and have a low degree of complexity compared to the full theory. In the context of effective field theories, we raise two simple and common inquiries when it comes to their applicability.

1 - Considering that what we really can access is a perturbative expansion in some parameter, how we can obtain the nonperturbative information in such a way that we can discuss nonperturbative phenomena from the perturbative expansion?

2 - Furthermore, how can thermodynamic effects (such as temperature, finite size, chemical potential,...) modify the behavior of a quantum-field model?

The first question is formal. The second question can be viewed as a "matter of pure curiosity" but becomes of importance once one takes into account processes occurring at extreme conditions, as in the large colliders or inside neutron stars, where temperature, chemical potential, finite size, external magnetic field, and other parameters might play a significant role. Also, in "not so extreme" conditions one might be interested if there remains some influence of these "macro" effects.

The path to approach the first question brings us to the topic of finiteness in quantum field theory which introduces itself as the problem of *summability* of the perturbative series. As already pointed out by many authors, perturbative series are in most cases divergent, and there is a need to make sense out of them as an asymptotic series [23]. Let us emphasize this point a little bit more. Take a quantum field theory with some interaction, a hard problem. To solve this hard problem we make a perturbative expansion for "small" values of the coupling constant, meaning that we make a perturbation around the free theory. As we know, the contribution of each Feynman diagram must be regulated and renormalized. In many theories, this is a nontrivial problem. However, we are discussing a different kind of problem. Assuming that renormalization holds, there is no divergence problem popping in at each new order. This somewhat ideal scenario can be an "illusion". It turns out that for the majority of cases, even if the model is renormalizable, the perturbative series is not well defined. It is divergent, which means that the perturbative series is not summable. Of course, there are alternatives for this. We continue to elaborate on this topic in Sec. 1.3.

We let the second inquiry to be discussed in Sec. 1.4. From a formal perspective, the question itself justifies the endeavor as we do not know the answer yet. However, we must be careful in identifying in which scenarios thermodynamic effects as finite volume, chemical potential, temperature,... might play any role at all. We choose to elaborate our discussion by having a specific physical process in mind: the ultrarelativistic collision of heavy ions in large colliders (as RHIC and LHC) and its outcomes. As can be expected, we shall apply some effective models that simplify many aspects of the initial discussion.

In addition, we enforce that: - Although QCD might come as an underlying motivation we do not apply it nor use effective models intended to reproduce a physical aspect of it; - We are mainly interested in the investigation of formal aspects that arise in the scenario of QCD and that also arises in other contexts; - The topic on hadronic phenomenology is an intermediate step towards future studies more connected to experimental findings.

1.3 Summability

As we have discussed in the previous section, we start this topic with the simple - yet profound - question "can we make sense out of the perturbative series in quantum field theory?". Notice that this is a formal and "generic" perspective. Suppose we have some arbitrary quantum field theory with an interaction controlled by the coupling constant g. Consider that we want to extract some information from this theory. Let us call this information that is dependent on the coupling constant as a function $F(g)$. In an ideal scenario, we would solve the problem nonperturbatively and obtain the exact solution. Of course, there are always options under development to study the nonperturbative solution. However, in most cases, this path is not possible and it is a "hard problem". Another alternative is to make a perturbative expansion in the coupling constant g (or in some other parameter, like in the large-N expansion). However, this is not necessarily a one-to-one path. We can say that the exact solution $F(g)$, which is unknown, is *represented* by a perturbative series $\sum_n a_n g^n$. They are *equal* only if the perturbative series is convergent. Let us take two simple examples (A) and (B):

$$(A): \quad F_A(g) \sim \sum_{n=1}^{\infty} \frac{n!}{n}(-g)^n, \tag{1.1}$$

$$(B): \quad F_B(g) \sim \sum_{n=0}^{\infty} n! g^n; \tag{1.2}$$

both examples are not summable because of the $n!$ growth. One way to relate the perturbative series with the complete theory is by the "Borel summability"; let us discuss it a little. First, we make a "Borel transform" of the original perturbative series, which introduces a term $n!$ in the denominator. Then, we define a new series $\mathcal{B}(F;b)$ in the "Borel plane". Let us take a look at our examples (A) and (B):

$$(A): \quad \mathcal{B}(F_A;b) = \sum_{n=1}^{\infty} \frac{1}{n}(-b)^n = -\ln(1+b), \tag{1.3}$$

$$(B): \quad \mathcal{B}(F_B;b) = \sum_{n=0}^{\infty} b^n = \frac{1}{1-b}; \tag{1.4}$$

after performing the Borel transform, the new series is well defined and summable.

The final step is to make the "inverse Borel transform" which defines a function $\widetilde{F}(g)$ by an integral in the complex Borel plane. If this integration can be well defined, the function $\widetilde{F}(g)$ can be related to the nonperturbative solution $F(g)$. To illustrate this, we look again at our two examples:

$$(A): \quad \widetilde{F}_A(g) = -\frac{1}{g}\int_0^\infty db\, e^{-\frac{b}{g}} \ln(1+b) = e^{\frac{1}{g}}\mathrm{Ei}\left(-\frac{1}{g}\right), \tag{1.5}$$

$$(B): \quad \widetilde{F}_B(g) = \frac{1}{g}\int_0^\infty db\, e^{-\frac{b}{g}} \frac{1}{1-b} = \begin{cases} e^{-\frac{1}{g}}\left[\mathrm{Ei}\left(1/g\right)+i\pi\right], b+i0^+ \\ e^{-\frac{1}{g}}\left[\mathrm{Ei}\left(1/g\right)-i\pi\right], b+i0^- \end{cases} ; \tag{1.6}$$

$\mathrm{Ei}(z)$ is the exponential integral function. Case (A) is well defined, as the singularities (a cut) in the Borel plane occur only on the negative real axis. However, for case (B) there is a pole on the positive real axis. Therefore, the inverse Borel transform becomes dependent on the choice of the integration contour.

Case (A) is an ideal scenario, where the study of Borel summability of the theory solves the problem of "making sense out of the perturbative expansion". On the other hand, case (B) has poles in the Borel plane that introduce ambiguities in the inverse Borel transform. In the context of a quantum field theory, these are the so-called "renormalons", which comes from the sum of a class of diagrams. As should be expected, there is a program to "cure" these ambiguities and take into account these renormalons [1]. However, this falls out of the scope of this thesis as none of the published articles we reproduced in the following chapters has dealt with this.

To motivate this topic a little bit more, I exhibit in Fig. 1.2a and Fig. 1.2b the comparison between the perturbative series and the function $\widetilde{F}(g)$, respectively for cases (A) and (B). Both curves, perturbative and nonperturbative, agree for low values of the coupling constant g. However, as expected, the perturbative solution diverges for large values of g.

Before taking into account the problem of solving the renormalon ambiguities, we are interested in determining the presence of poles or cuts. Moreover, we are foremost interested in possible thermal effects of a quantum field theory. Therefore, we study the influence of temperature on the existence of the renormalons (see Ref. [3] or Chap. 4). Sec. 1.9 presents an overview of the published article.

1.4 Ultrarelativistic collisions - a quick overview

In this section, let us try to visualize how ultrarelativistic collisions occur in colliders such as LHC and RHIC. The configuration is that two opposite particle beams (with a heavy ion "A" or particle "p") are accelerated up to ultrarelativistic velocities and col-

[1]This program is the so-called *resurgence*.

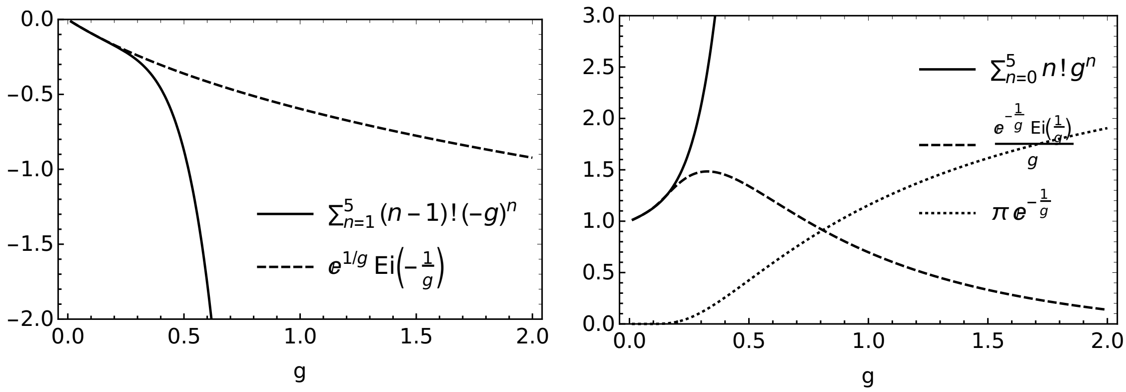

(a) (b)

Figure 1.2: Comparison between the perturbative series (thick curve) and the nonperturbative function (dashed curve) for both cases (A) (left) and (B) (right). The dotted curve in (B) is the imaginary part of the solution and the source of the ambiguity. Its sign is positive if the integration contour path is above the pole and negative otherwise.

lides with each other. Therefore we consider pp (proton-proton), pA (proton-nuclei) or AA (nuclei-nuclei) collisions.

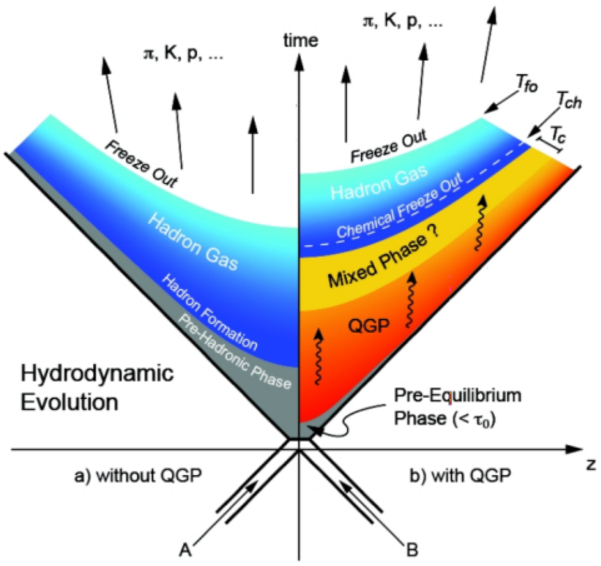

Figure 1.3: Time evolution after a heavy-ion collision in a scenario without (left) and with (right) the QGP phase. Source: Ref. [24]

In Fig.1.3 we exhibit a light-cone sketch of a collision between two particles. First, let us consider the simpler scenario on the left. The higher the scattering energy, more particles are formed in the final state. After these first processes occur, the generated particles can collide with each other (rescattering) or decay to subproducts. Therefore, the abundance of hadrons may change during the "hadron-gas" phase where the formed hadrons interact. After some time, the rescattering inside of the hadron gas stops due to energy loss, which is called the "kinetical freeze-out". After this, the remaining particles go to the detectors.

In the second scenario, there is a new phase of matter called the "quark-gluon plasma" (QGP), where the *partons* (quarks and gluons) move deconfined inside a fireball [2] formed immediately after the initial collision. This fireball has a finite size and survives for a small amount of time. When it cools down, there is a hadronization process that gives rise to the outgoing hadrons. For a thorough and complete review on this topic from both historical and conceptual perspectives see Ref. [28].

It was expected that the QGP phase would be formed only in AA collisions and did not take place in pp nor pA collisions. Therefore, the investigation of QGP formation is in general done using pp collision as a control data that do not have QGP formation. However, recent experimental findings seem to indicate that a QGP-droplet might occur in pA collisions depending on the scattering energy [29–31].

Regarding the QGP phase and the collision process, the aspects of interest for ourselves are:

1 - What is the QCD phase diagram? How this formally motivates the investigation of some parameters?

2 - What are the probes of the QGP? How are they influenced by other processes during the evolution of the dynamics sketched in Fig.1.3?

In Sec. 1.7, we discuss some aspects on the formal exploration of a phase diagram and motivate the investigation of the phase diagram in quantum field models. In Sec. 1.5, we discuss the problem of the QGP probes and motivate the use of the charmonium J/ψ as QGP and QCD probe.

1.5 Quak-gluon plasma (QGP) probe

Heavy quarks, like the charm and bottom quarks, are an excellent probe to investigate the QGP phase and in-medium behavior. These particles are produced after the initial collision and survive the whole process. Contrarily to photons, they also interact with the medium and carry signatures of this interaction. One signature is the charmonium $c\bar{c}$ suppression when comparing AA collisions with pp collisions. The observable R_{AA} gives the ratio between the number of particles in a AA collision and a reference pp collision; it can then compare a scenario with and without a QGP phase and isolate its effects. In a scenario with QGP formation, the abundance of charmonium is expected to be suppressed ($R_{AA} < 1$) due to the mechanism of color screening. Due to this, the measurement of J/ψ suppression in the PHENIX experiment at RHIC was an indication of the existence of the QGP phase. Furthermore, this mechanism turns charmonium into

[2] This fireball is understood as a fluid and so far it seems to have the viscosity of a perfect fluid [22, 25–27]

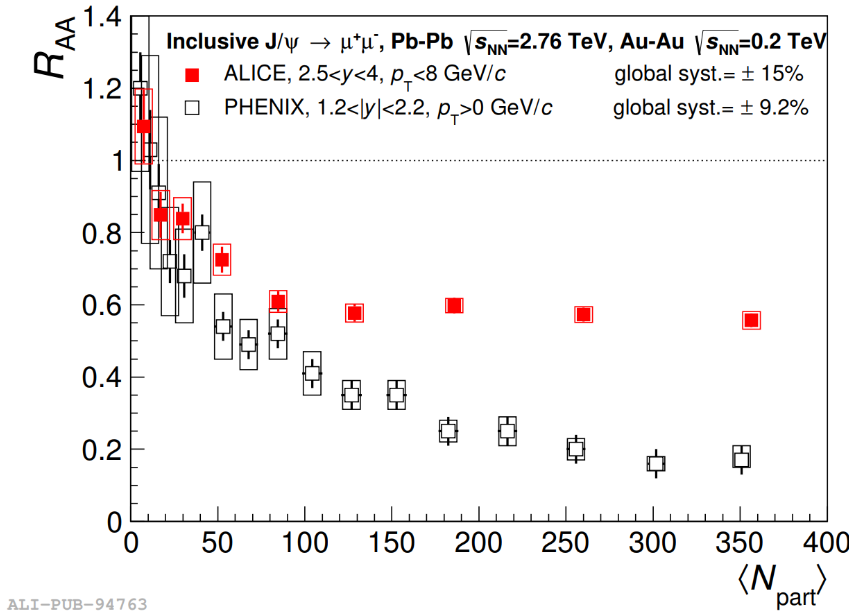

Figure 1.4: Comparison between measured R_{AA} in ALICE and PHENIX of the J/ψ at $\sqrt{s_{\mathrm{NN}}} = 2.76$ TeV as a function of number of participants, Ref. [35]

.

a "QGP thermometer" as each $c\bar{c}$ resonance, depending on its binding energy, "melts" at a different temperature [32–35].

At LHC energies, however, several experiments have reported a less suppressed scenario. In Fig. 1.4, we exhibit a comparison between PHENIX (at RHIC) and ALICE (at LHC) measurements on the J/ψ suppression. It is visible from the graph that there is a regeneration of charmonium, which indicates the existence of a new mechanism taking place.

Some of the nonprompt[3] mechanisms that may increase J/ψ abundance are photoproduction, color recombination, b-hadron decays, and cold nuclear matter (CNM) effects. The mechanism of photoproduction contributes only to very low transverse momentum p_T [35], and the contribution from b-hadron decays can be isolated [36]. Therefore, we can discard both. Some results coming from AA collisions indicate that color recombination mechanisms in the QGP are the main "missing" source to explain the regeneration [35]. However, a similar phenomenon occurs in pA collisions [37], where there a QGP formation was not expected and there is also a charmonium suppression ($R_{pA} \neq 1$) [4]. A possibility is the existence of nuclear matter effects. A comparison between AA collisions and pA collisions might give more clues about these effects. Some preliminary, and yet inconclusive, data from RHIC and LHC are beginning to be reported [38, 39]. Beyond that, the CMB/FAIR collaboration intends to explore QGP with higher baryon density, which can

[3] a prompt production occurs at the initial collision; a nonprompt production refers to any mechanism taking place after the initial collision

[4] Recent findings seems to indicate that, indeed, there might be a QGP-droplet formation in pA collisions [29–31].

introduce new information about the evolution of J/ψ abundance.

Following this discussion, we can investigate the influence of the hadronic medium on the charmonium J/ψ. As sketched in Fig. 1.3 this medium occurs in both AA and pA scenarios. In the past two decades, phenomenological studies have shown that the basic ingredients to study hadronic resonances are chiral symmetry and unitarization in coupled channels. Therefore, in Chap. 3 (a reproduction of Ref. [4]), we apply the use of unitarized chiral theory with coupled channels to investigate the interaction of the charmonium with the hadronic medium composed of light pseudoscalars (π, K, η) and light vector mesons (ρ, K^*, ω). Furthermore, we study the cross-sections for absorption/production processes and investigate which channels are the most relevant.

1.6 Hadronic phenomenology

In Chap. 3 we consider an extension of the lowest order chiral perturbation theory in which we consider that the relevant degrees of freedom are pseudoscalar mesons and vectorial mesons. Moreover, as we are mainly interested in charmonium, we take into account the charm flavor and the lighter ones (u, d, s) using a pseudoscalar 15-plet and a vectorial 15-plet of mesons. Of course, the lagrangian under consideration is a *very* simple and restrictive approximation. Moreover, the $SU(4)$ symmetry of the model must be explicitly broken. In our scenario, we employ three different procedures to break the symmetry:

1. The use of the physical masses of the mesons in the 15-plet.

2. The coupling constant must be modified each time the internal legs connect to charmed mesons.

3. We assume that all interactions have some “mediator” that adds a suppression factor. It means that a four-leg interaction is understood as the combination of two 3-leg interaction and the mediating particle is ‘hidden’. We take control of this looking at the structure constant.

To extend the range of applicability, we require unitarization of the model. The central idea is that a complete theory would be unitarized and, therefore, the imposition could force the model to behave better. Furthermore, to reproduce the idea of interaction in the hadron gas, it is also considered the coupled channel approach. What we mean by a coupled channel is that all pairs of mesons with the same combined quantum numbers can transit from one to another. With both concepts, we produce the unitarization in coupled channels, that has been employed to take into account the observation of resonances.

In our scenario, the use of this methodology is responsible both for: the nonzero cross-section between more pairs of particles (this arises as a consequence of the nonunitarized subprocesses); and the cross-section controlled behavior for high values of energy. Also, as a result of the investigation, we get that the most relevant processes are those where a $c\bar{c}$ pair remains in the initial and final states.

Measurements from ALICE/LHC [35] on the J/ψ behavior in Pb-Pb collision at low p_T seems to support models that assume that suppression and regeneration compete during QGP. Despite that, it is not possible to distinguish which model correctly describes the process. Furthermore, models studying production and absorption of J/ψ in a hot hadronic gas seems to indicate that this interaction does not contribute to a change in J/ψ multiplicity; one more signal that what dominates the production is the QGP dynamics [40].

The CMS collaboration measured the behavior for higher p_T [36]. At this range, the only nonprompt source of J/ψ considered is from b-hadrons decay and is isolated from the prompt production in the results. The prompt production is more suppressed then the nonprompt one, which indicates different mechanisms. For example, an expectation is that the suppression of nonprompt J/ψ produced by b-meson decay is related to the energy loss of the b quark.

Although J/ψ suppression in AA collisions seems so far to be explained entirely by QGP dynamics (color screening and regeneration), there is also an observed suppression in pA collisions, although a QGP phase is not expected. Therefore, pA collisions present themselves as a good scenario to investigate the contribution of suppression mechanisms that are not related to a QGP phase but are, instead, a Cold Nuclear Matter (CNM) effect. The observation that $R_{pA} \neq 1$ was first done in 2013 by several experiments (see Ref. [37] and references therein).

1.7 Phase diagram

First-principle calculations with lattice QCD provide a profound insight into the phase structure of QCD [14–17, 22, 41]. However, for a non-zero chemical potential, the lattice QCD framework faces some difficulties, although a variety of techniques have been developed to circumvent such problems [17]. Lattice QCD also faces difficulties with dynamical phenomena. Moreover, the relevant parameters that are responsible for some phenomena might stay hidden in the lattice framework as it solves the “full” theory. An alternative to gain insight into the phase diagram is to use QCD-inspired models [18–21, 42]. These effective models intend to isolate one aspect and study its consequences.

Nowadays the findings in lattice QCD indicate that the “transition” at small baryon chemical potential is a cross-over [22]. Therefore, what we call a “phase” would be

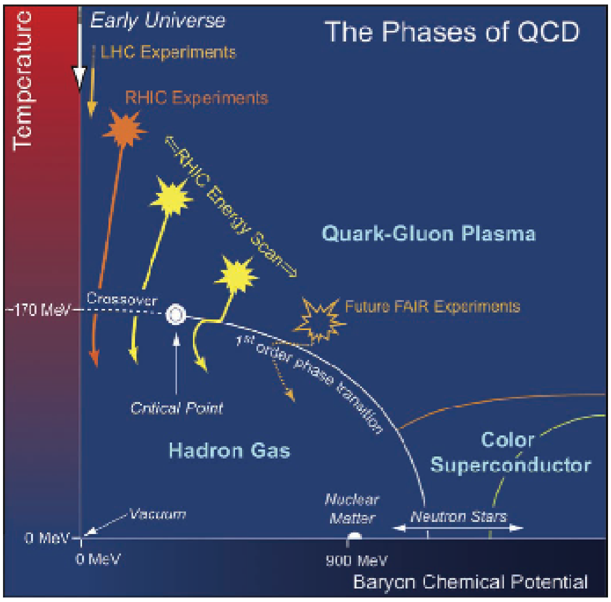

Figure 1.5: The conjectured sketch for the QCD phase diagram. Source: Ref. [24].

understood as indicating the dominant degree of freedom. The pseudocritical temperature that marks the chiral transition is around $T_c = 150\text{MeV}$ [41]. In Fig. 1.5 a conjectured sketch of the QCD phase diagram is exhibited. It is based on results obtained in the past decades, see for instance Ref. [22, 24, 26, 27].

There are recent investigation of the phase structure under the influence of the system size. For example, recent works point out the existence of finite-size effects on the position of the critical endpoint (CEP, tricritical point for the chiral limit) for effective models as the Nambu–Jona-Lasinio (NJL) and Linear Sigma Model (LSM) [43–48]. In this context, both periodic and antiperiodic spatial boundary conditions are used to perform the investigations and it is found a disagreement between the finite-volume behavior of different effective models [42].

The applicability of these spatial boundary conditions to study effective models motivates the investigation of different kinds of boundary conditions. On a formal level and as first step towards this goal, we consider quasiperiodic boundary conditions (also called anyonic or twisted boundary conditions) that interpolate between the periodic and antiperiodic using a “contour parameter” θ (usually called a phase parameter). We consider the influence of the contour parameter in a finite-size system in the paper at Ref. [2], this is reproduced in Chap. 2. Besides the formal motivation, the use of quasiperiodic boundary condition can be related to some physical scenarios as the presence of an external magnetic field in a plane [49]; a magnetic flux through a cyllinder [50]; or an Aharanov-Bohm phase due to a constant vector field [51].

1.8 Quasiperiodic boundary conditions

In the context of Quantum Field Theories in Toroidal Topologies, see review in Ref. [52], there are plenty of studies and investigation on the topic of phase transitions of finite-temperature models considering finite-size effects. These studies employ periodic boundary conditions in space for bosons and antiperiodic for fermions, even though there is a formal freedom of choice.

The Kubo-Martin-Schwinger (KMS) condition impose periodic (antiperiodic) boundary conditions on the imaginary time for bosons (fermions) as a direct consequence of the definition of the thermal Green's function [53–55] [5]. However, there is no fundamental restriction imposed on the boundary condition of the spatial directions. The primary motivation of the paper reproduced in Chap. 2 was to investigate the influence of the imposed boundary conditions when one is interested in a finite-size model that undergoes a phase transition.

The idea employed is to take into account a quasiperiodic boundary condition (b.c). This condition have a parameter θ and interpolates between the periodic scenario ($\theta = 0$) and the antiperiodic scenario ($\theta = 1$). It is very straightforward to introduce this parameter using the perspective of quantum field theory at toroidal topologies [52, 56].

Although we introduce the quasiperiodic b.c. from a formal perspective, there are some possible physical motivations. One possible scenario, proposed by Yoshioka et al. [49] and adopted by plenty of subsequent authors, is to consider a rectangular cell with periodic boundary conditions in the presence of an external magnetic field perpendicular to the surface of the cell. In this scenario, the Landau levels introduce a quasiperiodic b.c. in the spatial directions of the surface. Notice that in this scenario there are *two* spatial directions with quasiperiodic boundary conditions.

Another perspective where these boundary conditions are useful is in the study of Casimir energy as an attractive or repulsive behavior depends on space boundaries. One example is the use of general boundary conditions by Ref. [57] and the many works that employ quasiperiodic b.c. [58–62] in the context of Casimir effect. One proposal of a physical implementation in this context is the relationship with nanotubes [61, 63].

Concerning superconducting cylinders it is known since the 60's that the quantized magnetic flux produces a twisted/quasiperiodic boundary condition, see Ref. [50] and the plenty of subsquent papers through the decades.The phase θ that interpolates between periodic and antiperiodic b.c. is related to the magnetic flux that passes through the ring.

In the context of large-N lattice QFT, twisted b.c. are also introduced with a

[5] The thermal Green's function is the thermal average over of the imaginary-time ordered product of fields. The boundary condition cames as a consequence of the cyclicity of the trace and that the *statistical density matrix* $e^{-\beta H}$ is the generator of imaginary-time evolution. Therefore, it *does not* have any effect when it comes to the spatial directions.

formal motivation to avoid a symmetry breaking. [64, 65].

One last perspective that the quasiperiodic/twisted b.c. are produced by a constant background vector field, just like an Aharanov-Bohm phase [66]. This used in the context of lattice simulations of QCD [67]. Also, it is exhibited that this Aharanov-Bohm phase can induce a transmutation between fermions and bosons due to the presence of a quasiperiodic/twisted boundary condition [51, 68–71]. This is the relationship discussed at Sec.5 of Chap. 2. In special, Ref. [51] presents a detailed investigation on how the statistical phase emerges from the gauge field. For the interested reader Ref. [72] follows the same line of thought and explain the concept of a quasiperiodic boundary condition in the context of quantum mechanics.

In order to make the study a bit more complete, we choose to take into account different models that depend both on a finite temperature and finite size and undergoes a phase transition. We have considered a self-interacting scalar model with both a ϕ^4 and a ϕ^6 interaction term, and also a Gross-Neveu model. To make the analysis comprehensible, we investigate how the critical size (minimal thickness) behaves concerning the change in the boundary condition. The concept of a critical size, meaning some finite size that drives a phase transition, is known from both an experimental and a theoretical perspective [73–86]. This is well known both from the formalism of quantum field theory on toroidal topologies [73–83], from a more general framework from a condensed-matter perspective [84–86].

1.8.1 Phase transition

It is well known that a phase transition is defined in the thermodynamical limit, therefore the investigation of finite-size effects in the context of phase transitions must be taken carefully. To a simple demonstration that there ir no spontaneous symmetry breaking for finite V we refer to the textbook in Ref. [87]; we point that the acceptable scenario occurs when one considers a large V dynamics. In spite of this, we can take the perspective one *compactified dimension* as discussed in the textbook in Ref. [88]. The proposal is that, instead of taking the space volume as $V = L^D$ we consinder some a longitudinal size $\ell \neq L$ (therefore we are dealing in reality with $V = L^{D-1}\ell$). On this scenario, we can have a definition of phase transition with ordering if the correlation length ξ_L is greater then the system length L ($\xi_L \geq L$), as $L \to \infty$, for models in $D \geq 2$. Therefore, as long as we do not consider a *fully* compactified scenario, our definition of phase transition is always related to the correlation length in the *non-compactified* directions. And, therefore, we should bear in mind that a fully compactified scenario would be a purely formal extrapolation of the mathematics with no physical meaning.

A result shared by all models considered in Chap. 2 is that the choice of contour indeed affects observed parameters. Furthermore, we note the existence of a critical value of the parameter θ at which the minimal length goes to zero. Although the result depends on the dimensionality of the model, it seems that it is independent of the physical nature of the system. For example, for $D = 4$ we obtain $\theta = 0.422650$ and for $D = 3$ we obtain the critical value $\theta = 1/3$ both for a bosonic and a fermionic model, for other dimensions we refer to Table 1 in Chap. 2.

An aspect worth mentioning and that was missing in the published article reproduced in Chap. 2 is the discussion of $D \leq 2$ phase transitions. It is well known that the ground state of $D \leq 2$ systems with a continuous group of symmetry is symmetric, meaning the inexistence of symmetry breaking in this scenario. This was proved in the context of statical physics by Hohenberg-Mermin-Wagner [89, 90] and in the context of quantum field theory by Coleman [91], this theorem is connected to the inexistence of Nambu-Goldstone modes in $D \leq 2$ dimensions. This topic is well discussed in the standard literature [88, 92–94]. However, one must notice that:

- Not all phase transitions are related to a symmetry breaking. A system with a unique ground state may have a non-analytic thermodynamic function, which characterizes a phase transition. One such example is the Berezinski-Kasterlitz-Thouless (BKT) transition in the XY model [87, 94].

- Systems where a *discrete* symmetry is broken may have phase transition in $D = 2$. Therefore, the dynamical symmetry breaking of the chiral symmetry in the Gross-Neveu (GN) model does not violate the Mermin-Wagner theorem [87, 93].

- Models with dimensions *effectively* reduced might circumvent the theorem. One illustration is a system where a constant magnetic field induces a dimensional reduction: $D \to D - 2$. However, this reduction occurs only for charged fields while Nambu-Goldstone modes are neutral. Therefore, they still exist in the D-dimensional space, so the Mermin-Wagner theorem does not apply [95, 96].

In Chap. 2 the theorem is not violated because we considered the breaking of discrete symmetries: chiral symmetry for the GN model and the parity symmetry for the Ginzburg-Landau (GL) model.

1.9 Renormalon poles

The concept of Borel summability was shown in Sec. 1.3. Keeping this explanation in mind, we can discuss the study of the renormalon poles in a thermal-dependent model. The primary purpose of the published paper – reproduced in Chap. 4 – is to determine the position and residues of the renormalon poles. The main contribution to the literature is that we find some temperature-dependent poles that seemed to be unknown.

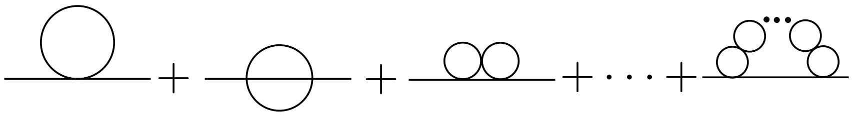

Figure 1.6: Sum over necklace digrams. Reproduced from Ref. [3].

The motivation for the study of renormalons has already been taken into account in Sec. 1.3. Perturbative series in quantum field theory are generally asymptotic and do not converge. One can usually get through this by using some summation technique, as the Borel sum. The general idea is that after we obtain a perturbative series, we can sum it up in the Borel plane and, afterward, use the inverse Borel transform to obtain the nonperturbative result. However, for some field theoretical models, the sum-up of a class of diagrams[6] produces poles in Borel plane, the so-called renormalons. These renormalons add ambiguities in the inverse Borel transform and forbid its direct use. Therefore, the interest in renormalons is related to the interest in summing the perturbative series.

The investigation of the behavior of renormalons at finite temperature has two primary motivations. The first one is practical: the extensive use of thermal field theories to investigate nonperturbative phenomena like phase transitions [22, 97–99]. The second one is more subtle and is related to the growing field of resurgence and transseries [100–102]. Recent literature [102–108] has taken into account some effective models with one spatial restriction L (or a finite temperature T). Moreover, it is found that the renormalons poles disappear for small L (high temperatures), and the model becomes summable in this regime [102, 104–106, 108].

The paper, reproduced in Chap. 4, investigates a scalar field model with a quartic self-interaction term and with N fields in $D = 4$ dimensions. Using a large-N expansion the sum of the perturbative series becomes a sum over the class of "necklace" diagrams, see Fig.1.6.

The model is defined in a space $\mathbb{R}^3 \times \mathbb{S}^1$ where the circle compactification introduces the thermal dependence $\beta = 1/T$. The existence of renormalons at $T = 0$ is well known in the usual literature [88]. What drives attention is what happens when we vary the temperature, and this is illustrated in Fig. 1.7. At zero temperature there are only two poles on the real positive axis of the Borel plane, represented by a blue circle (positive residue) and a red circle (negative residue). If the temperature increases, we observe the appearance of two countably infinite sets of poles. For the first set, marked with blue and red circles (to indicate the sign of the residue), the position of the poles is independent of the temperature although the residues are thermal dependent. The size of the circles indicates the value of the residue; this scale is not exact and only used as an illustration. For the second set, marked as green circles, both the location and residues of the renormalon poles are thermal dependent. All residues have a positive sign, and the

[6] in the sense that all considered diagrams are at the same order in some parameter expansion

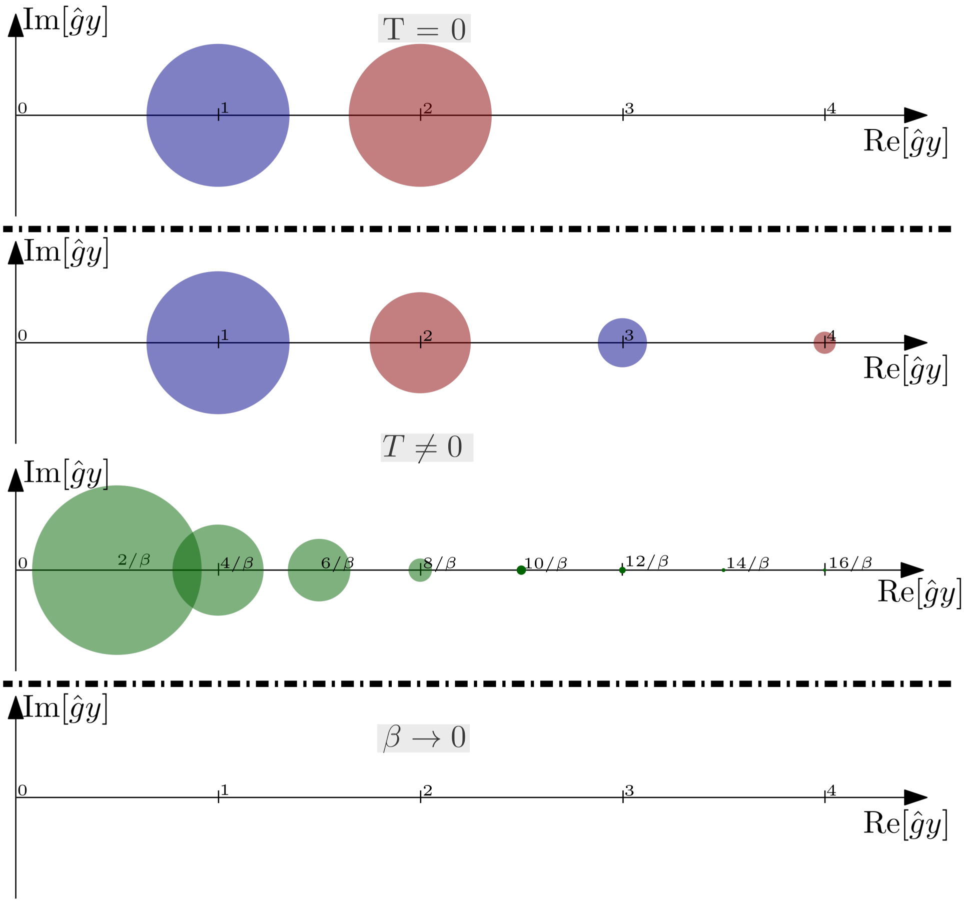

Figure 1.7: Illustration of renormalons poles for a scalar field model with self-interaction ϕ_4^4 at large N and finite temperature. Filled circles are centered at the position of renormalon pole, the size of the circle represents the value of the residue. Green circles have positive residues, and its position depends on the temperature. The last illustration, $\beta \to 0$ is the limit of extremely high temperature where we observe no renormalon.

size of the circle is off-scale. As could be inferred, the renormalons from zero temperature belong to the set of renormalons with a thermal-independent location. Finally, in the limit of extremely high temperatures, a dimensional reduction occurs and all renormalon poles disappear.

We can take all this discussion from another perspective and consider the scenario with one spatial direction with a circle compactification with length L. It means to replace $1/T = \beta \leftrightarrow L$, and the consequences are the same. The interpretation is in agreement with the current results in the literature [102, 104–106, 108].

Chapter 4 exhibits these results with greater detail. The discussion continues in Chap. 7, where we show some further developments that fall outside the scope of the published article.

1.10 Dimensional reduction

When it comes to the summation of the perturbative series to obtain the nonperturbative result, it is well known that field theories have a summability problem, as we discussed in the last section about the renormalon poles.

In recent years, a renewed interest in the topic of summability arose due to the development of the resurgence program and transseries as they intend to cure the problem. We do not get into details on this topic and we refer to some reviews that are intended to have a pedagogical approach [109–113].

A particular model under interest is adjoint QCD with a length compactification and 'inverted' boundary conditions in space[7] (periodic for fermions, antiperiodic for bosons) [103, 107, 108, 114]. The interest on the 'inverted' boundary conditions arose as a consequence of the so-called 'adiabatic continuity conjecture' [102, 105, 106, 115, 116]. The conjecture, initially proposed by Refs. [105, 106], and explicitly stated by Refs. [100, 101], states that if a field theory *does not* have a phase transition when varying, for example, the value of the length compactification L, the information obtained at some value of L could be related to the one at a different value. Why does this matter? If a theory is summable for some value of L and then gives the 'exact' nonperturbative solution and does not have a phase transition with a variation of the length parameter L, the conjecture states that the solution found is valid for all range of the L. Therefore, a procedure is to take some theory (as adjoint QCD) add a length compactification, explore some domain where phase transitions are avoided (as applying the 'inverted' boundary conditions) and study the range of low length ($L \to 0$) [102]. As a result, the renormalons disappear in this limit and, therefore, the series is summable without the ambiguity problem [102, 104–106, 108].

The adiabatic continuity is still a matter of discussion. So far, recent studies with quasiperiodic/twisted boundary conditions [116–119] and a comparison with lattice techniques [117, 118] indicate the continuity conjecture holds.

We remark that, with regard to the adiabatic continuity conjecture, the mathematical process of a dimensional reduction plays a significant role when one is interested in the disappearance of renormalons. All renormalons disappear when one takes the limit of extremely high temperatures. This feature is reproduced not only in our work but throughout the literature [102, 104–106, 108]. Naturally, in the case treated in Chap. 4 this behavior is not anomalous, as the model under study has renormalons at $D = 4$ but is summable at $D = 3$. A natural extension of our previous analysis, and also connected with recent years investigations, is to consider the dependence of the renormalons with other parameters as a finite length of the system, the chemical potential, and different

[7] We already commented in Sec.1.8 that there is a formal freedom in the choice of boundary conditions in space

kinds of boundary conditions. However, this raises some questions that were not yet fully clarified in the literature:

- Is the renormalon disappearance for the $L \to 0$ limit a mathematical property shared by all models, or is it a coincidence of some specific models?
- How does a thermal field theory model behave when the length goes to zero?
- How do the boundary conditions influence the renormalons? Do they have any significance at all in the renormalon disappearance?

The knowledge of a thermal dimensional reduction is not something new and has been investigated, for example, in a seminal paper by Landsman [53]. By analogy, the same study can be applied to the limit $L \to 0$ in zero-temperature field theory. However, there seemed to be no investigation on dimensional reduction so far considering a system with a finite temperature and restricted to a finite length. This motivated our research on the topic of dimensional reduction, which produced the publications in Refs. [5, 6]. In this way, the research of dimensional reduction is, in fact, a small preparatory study so that we can consider with more efficiency the behavior of renormalon poles in field theories with imposed boundary conditions. Nevertheless, this is a work under active development during the writing of this thesis and is only cited here for completeness and a better understanding of the motivations.

The theme of dimensional reduction is relevant in a broader context than what initially motivate the study. We can build effective models, as Hot QCD, that reduce the complexity of the original theory. It can be used to explore the effects of higher-dimensional field theories. There is also the perspective in the context of condensed-matter field theories to compare thin films and surfaces modelss.

Let us consider a bit the scenario of thin films and surfaces – that seems further away from our discussion in this thesis. The topic of phase transitions in thin films has a vast literature and is subjected to a diversity of approaches. Both 2D (surfaces) or 3D (films with some thickness) models are widely employed. As an example, we cite some published works by the research group on toroidal topologies here at CBPF [73–83]. A planar model would mean that the relevant degrees of freedom are in the surface. However, we can raise the somewhat naive question on how to distinguish between a surface or a film description. From another perspective, we can ask if we can describe a thin film as a planar model. Alternatively, in a stronger viewpoint, if we can understand a planar model as the limit of a film model.

Usually, some authors mix both perspectives and consider a combination of a thickness-dependent component and a surface contribution [84, 85]. On the other hand, some studies on thin films, both from a theoretical and experimental perspective, have shown the existence of a critical size [84–86]. The former is reproduced using the formalism of toroidal topologies and even have an agreement with some experimental results [73]. In this context, the consequence is that thin-film models have a critical size below which there is no phase transition. All that said, we point out that we do not attain a strict dimensional reduction ($L = 0$) in the context of phase transitions, and we are interested in the effective behavior of the model in this regime.

What we mean by a dimensional reduction is simply the investigation on the behavior of some field theoretical models with a spatial restriction L in the limit where this length goes zero ($L \to 0$). This relates with the usual consideration on thermal dimensional reduction if we consider a compactification on the imaginary time giving the inverse temperature $1/T = \beta$. Let us, for clarity on this topic, take into account a scalar one-loop Feynman diagram with ν internal lines and consider the presence of a finite temperature T introduced via imaginary-time Matsubara formalism

$$\int d^D p \frac{1}{(p^2+m^2)^\nu} \to T \sum_{n\in\mathbb{Z}} \int d^{D-1} p \frac{1}{(p^2+4\pi^2 n^2 T^2+m^2)^\nu}. \tag{1.7}$$

In the limit of very high temperatures this decouples, following the Appelquist-Carazzone theorem [120], between a static contribution with mass m and a nonstatic contribution with a thermal mass,

$$T \int d^{D-1} p \frac{1}{(p^2+m^2)^\nu} + 2T \sum_{n\in\mathbb{N}} \int d^{D-1} p \frac{1}{(p^2+(4\pi^2 n^2 T^2+m^2))^\nu}. \tag{1.8}$$

The static contribution gives a dimensionally-reduced theory that is valid in the limit of very high temperatures. Naturally, this logic is valid for the bosonic case because we must use a periodic boundary condition in the imaginary time. However, when one deals with fermions, the antiperiodic boundary condition gives a Matsubara frequency as $\omega_n = (2n+1)\pi T$, which implies the nonexistence of a static mode, and therefore, there is no decoupling.

The typical result, therefore, is that bosons and fermions behave differently in the process of a thermal dimensional reduction. Although this topic is not a new one, the investigation on this procedure of dimensional reduction was not extensively explored and, as far as we know, there are just a few reports on thermally-reduced fermionic models. In Ref.[121] a procedure is proposed to give a *partial* thermal dimensional reduction for fermions, and the authors themselves express this as an "ill-defined" dimensional reduction as the procedure is not straightforward. In Ref. [122], the authors introduce another perspective on this topic when they exhibit that the procedure of restricting a $5D$ fermionic model to $4D$ introduces new contributions as an inheritance of $5D$. It seems that computing the loop corrections and dimensionally reducing a fermionic model *does not commute*.

As far as we know, there is also another gap in the literature concerning this theme: the use of different kinds of boundary conditions. The case of a thermal dimensional reduction did not have the freedom to explore this aspect because of the restriction imposed by the KMS condition [56]. However, as we are interested in a spatial restriction, there is formal mathematical freedom of choice on the imposed spatial boundary condition.

As a first step, we consider the particular case of a scalar field theory with periodic boundary conditions, and we obtain the comparison between Path I and Path II for any real value of the dimension D. The first paper has a careful explanation of used methodology and is reproduced in Chap. 5. The succeeding paper, reproduced in Chap. 6, took into account the case of both scalar and fermionic field theories (spin 0 and 1/2), subjected to a diversity of boundary conditions: periodic, antiperiodic, Dirichlet and Neumann.

In Fig. 1.8, we illustrate the procedure of both articles. We start with the original tree-level model that was assumed to be a self-interacting scalar field theory or a self-interacting fermionic field theory. Then, we can follow two different paths. The first path is to remove one dimension of the model and then obtain the one-loop correction $\mathcal{I}_{\rho}^{D}(M)$. This is a formal correction in D dimensions with ρ internal lines in the diagram that can be used to compute the effective potential of the model. Naturally, this path is independent of the choice of spatial boundary conditions. The second path is to obtain the one-loop contribution, which shall be different for each chosen boundary condition, and then remove one dimension. While *Path I* gives just one result, *Path II* has four different possibilities depending on the choice of boundary condition. We then compare both paths to understand what happens.

In the bosonic case, a direct comparison between both paths is attainable. If we assume a simple model with quartic interaction, we can make an identification between the coupling constant in the initially reduced scenario (Path I, λ_{D-1}) and the scenario where the reduction occurs afterward (Path II, λ_D).

- **Periodic b.c.** $\lambda_{D-1} = \frac{\lambda_D}{L}$
- **Dirichlet b.c.** $\lambda_{D-1} = -\frac{\lambda_D}{4L}$
- **Neumann b.c.** $\lambda_{D-1} = \frac{3\lambda_D}{4L}$
- **Antiperiodic b.c.** gives no reduced model

The result for periodic boundary condition was already exhibited in the first paper (Ref. [5], Chap. 5) and is the standard identification found in the literature when one is interested in thermal dimensional reduction [53]. The nonexistence of a reduced model when we consider antiperiodic boundary condition is a remarkable finding that raises more

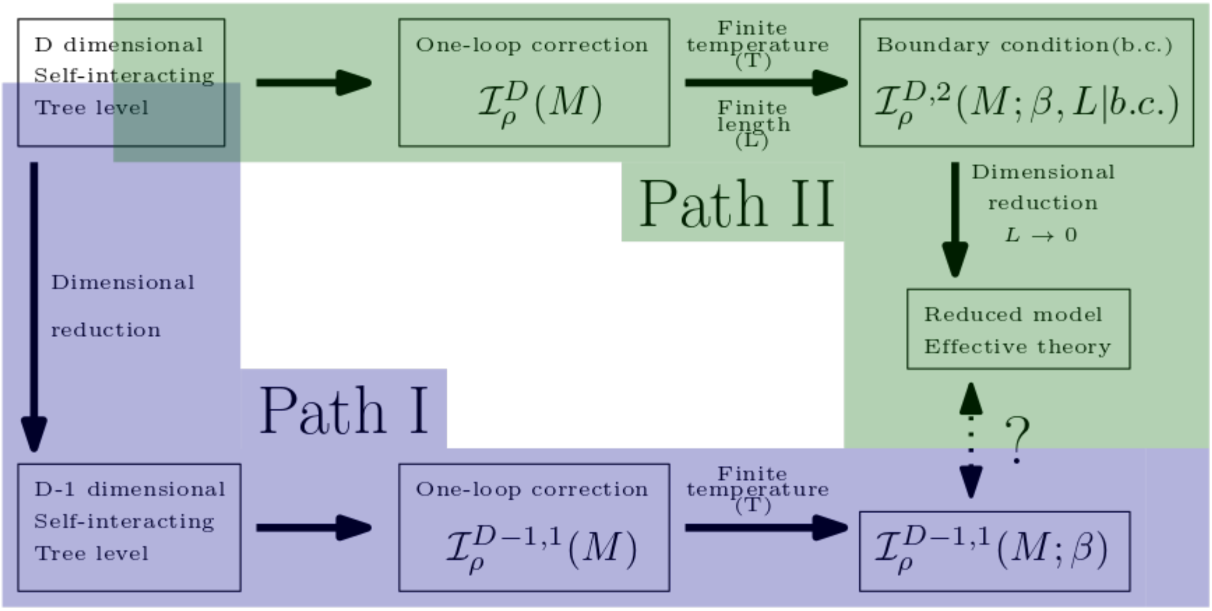

Figure 1.8: The two paths that are followed and then compared. The function $\mathcal{I}_\rho^{D,d}$ is a formal one-loop correction in D dimensions, d of then compactified and with ρ internal lines. M is the mass of the field.

questions. Moreover, the change of sign in the coupling constant when we consider the Dirichlet boundary condition might also be responsible for some effect[8].

When it comes to the fermionic model, the results are a bit more intricate. An aspect that still holds is the nonexistence of a reduced model when we consider antiperiodic boundary conditions in space, which raises the question of whether this is a topological property independent of initial lagrangian. The self-interacting fermionic field with a periodic boundary condition in space can attain a dimensional reduction, but to a new model that has no relation with the first path. Therefore, for the fermionic field, *Path I* and *Path II* from the illustration in Fig. 1.8 do not commute and are not even proportional. The solutions in the scenarios of Dirichlet and Neumann boundary conditions are linear combinations of the solution obtained following *Path I* and the solution produced in *Path II* using periodic boundary conditions.

We find that a dimensional reduction is attainable, but it depends both on the nature of the field and on the boundary conditions imposed. The idea that the boundary conditions affect the behavior of systems with small size is understandable as we might be dealing with border effects. The considered model can yet be enhanced but it already gives some information about the system. The main limitation is that we are considering, in both articles, only the one-loop contribution. The second limitation is that we only took into account self-interacting models. In the final chapter, we discuss some further developments that intend to exhaust the theme.

[8]We could, for example, naively imagine some model that undergoes a second-order phase transition in D dimensions and that, because of the change of sign, undergoes a first-order phase transition in the dimensionally-reduced model.

1.11 Errata

Unfortunately, it is always possible that some misprints can survive the publication process. This section is a collection of corrections in the text of the following chapters, that are reproductions of the published papers.

1.11.1 Chapter 2

Mermin-Wagner theorem

It was missing in the paper an explanation about the validity to consider some models in two spatial dimensions to investigate phase transitions. The discussion of this in the light of the Mermin-Wagner theorem can be found at the end of Sec. 1.8.

Quasiperiodic boundary condition for Ginzburg-Landau

Unfortunately, due to a desire to shorten notation there was a major mistake in the beginning of the paper that passed unnoticed during the revision of the manuscript. The mistake occurs when defining a quasiperiodic boundary condition for a *generic* field Φ as

$$\Phi(\ldots, x_i + L, \ldots) = e^{i\pi\theta_i}\Phi(\ldots, x_i, \ldots).$$

By this definition the field Φ have to be complex so that it can manage the multiplication by a complex number. Fortunately, this mistake does not affect any result and modifies just a couple of equations. The relation holds for the Gross-Neveu model and must be modified to consider the neutral Ginzburg-Landau model. A proper definition in the scalar scenario is

$$\Phi(\ldots, x_i + L, \ldots) = \cos(\pi\theta_i)\Phi(\ldots, x_i, \ldots).$$

The consequence is that the associated Matsubara frequencies can be $\omega_n^i = \frac{2\pi n_i}{L_i} \pm \frac{\theta_i \pi}{L}$. However, the sign of θ is not relevant (*and would simply mean a double counting of each mode*) and we can - without loss - adopt the sign convention of the article.

We emphasize that the neutral scalar model is chosen because we intended to compare the phase transition of models with a discrete symmetry breaking, such that Mermin-Wagner theorem is not violated when we consider $D = 2$ dimensions.

Imaginary chemical potential

We remark that the *imaginary chemical potential*, commented in section 2, is just formal and is not related to any conserved charge.

Figures

For all figures in this chapter, the parameters are adimensional by convention. We remark that the major concern was with the formal behavior and that no comparison was made with possible experiments, which justifies keeping adimensional units.

There is a misprint in section 3.1.1 when referring to Fig. 2. It is written in the text that “in Fig. 2, for $D = 2, 3, 4$ an periodic [...]”, but it should read “in Fig. 2, for $D = 4, 5, 6$ an periodic [...]”. This was correctly indicated in the caption of the figure.

Misleading statement

There is a misleading statement in the conclusion that can introduce some confusion. It is written “The observed independence of $\theta^\star$ shows that there is a common substrate of models having quasiperiodic boundary conditions independent of its physical nature”, but it should be completely rephrased to ‘ The observed independence of $\theta^\star$ with regard to the nature of the field and order of the phase transition seems to indicate that there is a formal and general aspect shared by field-theoretical models with quasiperiodic boundary conditions.”

1.11.2 Chapter 4

At equation (9) instead of $(q + \ell)^2$ in the denominator we should have $(q - \ell)^2$. This misprint does not modify the following equations in the paper.

At equations (10), (11) instead of $(4\pi^2)$ it should read $(4\pi)^2$. In the following formulas this misprint is absent.

We emphasize that the discussion is valid for $D = 4$ Euclidean dimensions. Although commented during Chapter, we believe this point is not completely explicit in the text.

References

[1] E. Cavalcanti, E. Castro, C. A. Linhares, and A. P. C. Malbouisson, “Influence of external magnetic field, finite-size effects and chemical potential on the phase transition of a complex scalar field”, Eur. Phys. J. **C77**, 711 (2017).

[2] E. Cavalcanti, C. A. Linhares, and A. P. C. Malbouisson, “Properties of size-dependent models having quasiperiodic boundary conditions”, Int. J. Mod. Phys. **A33**, 1850008 (2018).

[3] E. Cavalcanti, J. A. Lourenço, C. A. Linhares, and A. P. C. Malbouisson, “Appearance and disappearance of thermal renormalons”, Phys. Rev. **D98**, 045013 (2018).

[4]L. M. Abreu, E. Cavalcanti, and A. P. C. Malbouisson, "Impact of unitarization on the J/ψ-light meson cross section", Nucl. Phys. **A978**, 107–122 (2018).

[5]E. Cavalcanti, J. A. Lourenço, C. A. Linhares, and A. P. C. Malbouisson, "Dimensional reduction of a finite-size scalar field model at finite temperature", Phys. Rev. **D99**, 025007 (2019).

[6]E. Cavalcanti, C. A. Linhares, J. A. Lourenço, and A. P. C. Malbouisson, "Effect of boundary conditions on dimensionally reduced field-theoretical models at finite temperature", Phys. Rev. **D100**, 025008 (2019).

[7]N. Brambilla et al., "QCD and Strongly Coupled Gauge Theories: Challenges and Perspectives", Eur. Phys. J. **C74**, 2981 (2014).

[8]M. Tanabashi et al., "Review of Particle Physics", Phys. Rev. **D98**, 030001 (2018).

[9]R. Brock et al., "Handbook of perturbative QCD: Version 1.0", Rev. Mod. Phys. **67**, 157–248 (1995).

[10]X.-N. Wang, "pQCD based approach to parton production and equilibration in high-energy nuclear collisions", Phys. Rept. **280**, 287–371 (1997).

[11]E. Witten, "Baryons in the 1/n Expansion", Nucl. Phys. **B160**, 57–115 (1979).

[12]L. J. Reinders, H. Rubinstein, and S. Yazaki, "Hadron Properties from QCD Sum Rules", Phys. Rept. **127**, 1 (1985).

[13]M. Nielsen, F. S. Navarra, and S. H. Lee, "New Charmonium States in QCD Sum Rules: A Concise Review", Phys. Rept. **497**, 41–83 (2010).

[14]F. Karsch, "Lattice results on QCD thermodynamics", Nucl. Phys. **A698**, 199–208 (2002).

[15]D. H. Rischke, "The Quark gluon plasma in equilibrium", Prog. Part. Nucl. Phys. **52**, 197–296 (2004).

[16]E. Laermann and O. Philipsen, "The Status of lattice QCD at finite temperature", Ann. Rev. Nucl. Part. Sci. **53**, 163–198 (2003).

[17]P. de Forcrand, "Simulating QCD at finite density", PoS **LAT2009**, 010 (2009).

[18]U. G. Meissner, "Recent developments in chiral perturbation theory", Rept. Prog. Phys. **56**, 903–996 (1993).

[19]T. Hatsuda and T. Kunihiro, "QCD phenomenology based on a chiral effective Lagrangian", Phys. Rept. **247**, 221–367 (1994).

[20]M. Buballa, "NJL model analysis of quark matter at large density", Phys. Rept. **407**, 205–376 (2005).

[21]M. G. Alford, A. Schmitt, K. Rajagopal, and T. Schäfer, "Color superconductivity in dense quark matter", Rev. Mod. Phys. **80**, 1455–1515 (2008).

[22]K. Fukushima and T. Hatsuda, "The phase diagram of dense QCD", Rept. Prog. Phys. **74**, 014001 (2011).

[23]G. 't Hooft, "Can we make sense out of "quantum chromodynamics"?", in *The whys of subnuclear physics*, edited by A. Zichichi (Springer US, Boston, MA, 1979), pp. 943–982.

[24]B. Mohanty, "Exploring the QCD phase diagram through high energy nuclear collisions: An overview", PoS **CPOD2013**, 001 (2013).

[25]M. A. Stephanov, "QCD phase diagram and the critical point", Prog. Theor. Phys. Suppl. **153**, [Int. J. Mod. Phys.A20,4387(2005)], 139–156 (2004).

[26]M. A. Stephanov, "QCD phase diagram: An Overview", PoS **LAT2006**, 024 (2006).

[27]E. Shuryak, "Physics of Strongly coupled Quark-Gluon Plasma", Prog. Part. Nucl. Phys. **62**, 48–101 (2009).

[28]J. Rafelski, ed., *Melting Hadrons, Boiling Quarks - From Hagedorn Temperature to Ultra-Relativistic Heavy-Ion Collisions at CERN* (Springer, 2016).

[29]H. Song, "Hydrodynamic modelling for relativistic heavy-ion collisions at RHIC and LHC", Pramana **84**, 703–715 (2015).

[30]R. Pasechnik and M. Šumbera, "Phenomenological Review on Quark–Gluon Plasma: Concepts vs. Observations", Universe **3**, 7 (2017).

[31]W. Busza, K. Rajagopal, and W. van der Schee, "Heavy Ion Collisions: The Big Picture, and the Big Questions", Ann. Rev. Nucl. Part. Sci. **68**, 339–376 (2018).

[32]W. Cassing and E. L. Bratkovskaya, "Hadronic and electromagnetic probes of hot and dense nuclear matter", Phys. Rept. **308**, 65–233 (1999).

[33]T. Matsui and H. Satz, "J/ψ Suppression by Quark-Gluon Plasma Formation", Phys. Lett. **B178**, 416–422 (1986).

[34]J. Adams et al., "Experimental and theoretical challenges in the search for the quark gluon plasma: The STAR Collaboration's critical assessment of the evidence from RHIC collisions", Nucl. Phys. **A757**, 102–183 (2005).

[35]V. Feuillard, "Charmonium production in Pb–Pb collisions measured by ALICE at the LHC", Nucl. Part. Phys. Proc. **289-290**, 389–392 (2017).

[36]A. M. Sirunyan et al., "Measurement of prompt and nonprompt charmonium suppression in PbPb collisions at 5.02 TeV", Eur. Phys. J. **C78**, 509 (2018).

[37]B. Paul, "Charmonium production in p-Pb collisions with ALICE at the LHC", PoS **EPS-HEP2017**, 182 (2017).

[38]T. Todoroki, "Measurements of charmonium production in p+p, p+Au, and Au+Au collisions at $\sqrt{s_{NN}}$= 200 GeV with the STAR experiment", Nucl. Phys. **A967**, 572–575 (2017).

[39]J. A. López López, “Measurement of charmonium production in heavy-ion collisions with the ATLAS detector”, Nucl. Phys. **A967**, 584–587 (2017).

[40]L. M. Abreu, K. P. Khemchandani, A. Martínez Torres, F. S. Navarra, and M. Nielsen, “Update on J/ψ regeneration in a hadron gas”, Phys. Rev. **C97**, 044902 (2018).

[41]S. Borsanyi, Z. Fodor, C. Hoelbling, S. D. Katz, S. Krieg, and K. K. Szabo, “Full result for the QCD equation of state with 2+1 flavors”, Phys. Lett. **B730**, 99–104 (2014).

[42]B.-L. Li, Z.-F. Cui, B.-W. Zhou, A. Sun, L.-P. Zhang, and H.-S. Zong, “Finite volume effects on chiral phase transition from Dyson-Schwinger equations of QCD”, (2017).

[43]L. F. Palhares, E. S. Fraga, and T. Kodama, “Chiral transition in a finite system and possible use of finite size scaling in relativistic heavy ion collisions”, J. Phys. **G38**, 085101 (2011).

[44]A. Bhattacharyya, P. Deb, S. K. Ghosh, R. Ray, and S. Sur, “Thermodynamic Properties of Strongly Interacting Matter in Finite Volume using Polyakov-Nambu-Jona-Lasinio Model”, Phys. Rev. **D87**, 054009 (2013).

[45]A. Bhattacharyya, R. Ray, and S. Sur, “Fluctuation of strongly interacting matter in the Polyakov–Nambu–Jona-Lasinio model in a finite volume”, Phys. Rev. **D91**, 051501 (2015).

[46]A. Bhattacharyya, S. K. Ghosh, R. Ray, K. Saha, and S. Upadhaya, “Polyakov–Nambu–Jona-Lasinio model in finite volumes”, EPL **116**, 52001 (2016).

[47]Z. Pan, Z.-F. Cui, C.-H. Chang, and H.-S. Zong, “Finite-volume effects on phase transition in the Polyakov-loop extended Nambu–Jona-Lasinio model with a chiral chemical potential”, Int. J. Mod. Phys. **A32**, 1750067 (2017).

[48]A. Juricic and B.-J. Schaefer, “Chiral thermodynamics in a finite box”, Acta Phys. Polon. Supp. **10**, 609 (2017).

[49]D. Yoshioka, B. I. Halperin, and P. A. Lee, “Ground state of two-dimensional electrons in strong magnetic fields and 1/3 quantized hall effect”, Phys. Rev. Lett. **50**, 1219–1222 (1983).

[50]N. Byers and C. Yang, “Theoretical considerations concerning quantized magnetic flux in superconducting cylinders”, Physical review letters **7**, 46 (1961).

[51]S. Forte, “Quantum mechanics and field theory with fractional spin and statistics”, Rev. Mod. Phys. **64**, 193–236 (1992).

[52]F. C. Khanna, A. P. C. Malbouisson, J. M. C. Malbouisson, and A. E. Santana, “Quantum field theory on toroidal topology: Algebraic structure and applications”, Phys. Rept. **539**, 135–224 (2014).

[53]N. P. Landsman, “Limitations to Dimensional Reduction at High Temperature”, Nucl. Phys. **B322**, 498–530 (1989).

[54]J. I. Kapusta and C. Gale, *Finite-temperature field theory: Principles and applications*, Cambridge Monographs on Mathematical Physics (Cambridge University Press, 2011).

[55]M. L. Bellac, *Thermal Field Theory*, Cambridge Monographs on Mathematical Physics (Cambridge University Press, 2011).

[56]F. C. Khanna, A. P. C. Malbouisson, J. M. C. Malbouisson, and A. R. Santana, *Thermal quantum field theory - Algebraic aspects and applications* (World Scientific Publishing Company, Singapore, 2009).

[57]M. Asorey and J. M. Munoz-Castaneda, "Attractive and Repulsive Casimir Vacuum Energy with General Boundary Conditions", Nucl. Phys. **B874**, 852–876 (2013).

[58]S. S. Bayin, J. P. Krisch, and M. Ozcan, "The Casimir energy of the twisted string loop: Uniform and two segment loops", J. Math. Phys. **37**, 3662–3674 (1996).

[59]P. F. Borges, H. Boschi-Filho, and C. Farina, "Generalized partition functions for quasiperiodic fields", Mod. Phys. Lett. **A13**, 843–852 (1998).

[60]P. F. Borges, H. Boschi-Filho, and C. Farina, "Quasiperiodic fields and Bose-Einstein condensation", (1998).

[61]C.-J. Feng, X.-Z. Li, and X.-H. Zhai, "Casimir Effect under Quasi-Periodic Boundary Condition Inspired by Nanotubes", Mod. Phys. Lett. **A29**, 1450004 (2014).

[62]S. Bellucci, A. A. Saharian, and N. A. Saharyan, "Casimir effect for scalar current densities in topologically nontrivial spaces", Eur. Phys. J. **C75**, 378 (2015).

[63]X.-H. Zhai, R.-H. Lin, C.-J. Feng, and X.-Z. Li, "Some Developments of the Casimir Effect in p-Cavity of $(D+1)$-Dimensional Spacetime", Int. J. Mod. Phys. **A29**, 1430068 (2014).

[64]A. Gonzalez-Arroyo and M. Okawa, "The Twisted Eguchi-Kawai Model: A Reduced Model for Large N Lattice Gauge Theory", Phys. Rev. **D27**, 2397 (1983).

[65]A. Gonzalez-Arroyo and M. Okawa, "A twisted model for large n lattice gauge theory", Physics Letters B **120**, 174–178 (1983).

[66]Y. Aharonov and D. Bohm, "Significance of electromagnetic potentials in the quantum theory", Phys. Rev. **115**, [,95(1959)], 485–491 (1959).

[67]C. T. Sachrajda and G. Villadoro, "Twisted boundary conditions in lattice simulations", Phys. Lett. **B609**, 73–85 (2005).

[68]A. M. Polyakov, "Fermi-Bose Transmutations Induced by Gauge Fields", Mod. Phys. Lett. **A3**, [,214(1988)], 325 (1988).

[69]E. H. Fradkin and F. A. Schaposnik, "The Fermion - boson mapping in three-dimensional quantum field theory", Phys. Lett. **B338**, 253–258 (1994).

[70]G. V. Dunne, "Aspects of Chern-Simons theory", in Topological Aspects of Low-dimensional Systems: Proceedings, Les Houches Summer School of Theoretical Physics, Session 69: Les Houches, France, July 7-31 1998 (1998).

[71]P. F. Borges, H. Boschi-Filho, and C. Farina, "The effect of a topological gauge field on Bose-Einstein condensation", Phys. Lett. **B460**, 376–382 (1999).

[72]E. Abdalla, M. C. B. Abdalla, and K. D. Rothe, *Nonperturbative methods in two-dimensional quantum field theory* (1991).

[73]C. A. Linhares, A. P. C. Malbouisson, Y. W. Milla, and I. Roditi, "First-order phase transitions in superconducting films: A Euclidean model", Phys. Rev. **B73**, 214525 (2006).

[74]L. M. Abreu, A. P. C. Malbouisson, J. M. C. Malbouisson, and A. E. Santana, "Large N transition temperature for superconducting films in a magnetic field", Phys. Rev. **B67**, 212502 (2003).

[75]L. M. Abreu, A. P. C. Malbouisson, J. M. C. Malbouisson, and A. E. Santana, "Finite-size effects on the chiral phase diagram of four-fermion models in four dimensions", Nucl. Phys. **B819**, 127–138 (2009).

[76]L. M. Abreu, A. P. C. Malbouisson, and J. M. C. Malbouisson, "Finite-size effects on the phase diagram of difermion condensates in two-dimensional four-fermion interaction models", Phys. Rev. **D83**, 025001 (2011).

[77]L. M. Abreu, A. P. C. Malbouisson, and J. M. C. Malbouisson, "Nambu-Jona-Lasinio model in a magnetic background: Size-dependent effects", Phys. Rev. **D84**, 065036 (2011).

[78]C. A. Linhares, A. P. C. Malbouisson, and M. L. Souza, "A note on the infrared behavior of the compactified Ginzburg–Landau model in a magnetic field", EPL **96**, 31002 (2011).

[79]C. A. Linhares, A. P. C. Malbouisson, J. M. C. Malbouisson, and I. Roditi, "Spontaneous symmetry restoration in a field theory at finite chemical potential in a toroidal topology", Phys. Rev. **D86**, 105022 (2012).

[80]F. C. Khanna, A. P. C. Malbouisson, J. M. C. Malbouisson, and A. E. Santana, "Finite-size effects on the phase transition in the three-dimensional Gross-Neveu model", EPL **97**, 11002 (2012).

[81]F. C. Khanna, A. P. C. Malbouisson, J. M. C. Malbouisson, and A. E. Santana, "Phase transition in the massive Gross-Neveu model in toroidal topologies", Phys. Rev. **D85**, 085015 (2012).

[82]L. M. Abreu, C. A. Linhares, A. P. C. Malbouisson, and J. M. C. Malbouisson, "Magnetic effects on spontaneous symmetry breaking/restoration in a toroidal topology", Phys. Rev. **D88**, 107701 (2013).

[83]E. B. S. Corrêa, C. A. Linhares, and A. P. C. Malbouisson, "Finite-size, magnetic and chemical-potential effects on first-order phase transitions", Phys. Lett. **A377**, 1984–1990 (2013).

[84]W. L. Zhong, Y. G. Wang, P. L. Zhang, and B. D. Qu, "Phenomenological study of the size effect on phase transitions in ferroelectric particles", Phys. Rev. B **50**, 698–703 (1994).

[85]W. L. Zhong, B. D. Qu, P. L. Zhang, and Y. G. Wang, "Thickness dependence of the dielectric susceptibility of ferroelectric thin films", Phys. Rev. B **50**, 12375–12380 (1994).

[86]A. V. Bune, V. M. Fridkin, S. Ducharme, L. M. Blinov, S. P. Palto, A. V. Sorokin, S. Yudin, and A. Zlatkin, "Two-dimensional ferroelectric films", Nature **391**, 874 (1998).

[87]V. A. Miransky, *Dynamical symmetry breaking in quantum field theories* (Singapore, Singapore: World Scientific (1993) 533 p, 1994).

[88]J. Zinn-Justin, *Quantum field theory and critical phenomena*, 4th ed. (Clarendon Press, Oxford, 2002).

[89]N. D. Mermin and H. Wagner, "Absence of ferromagnetism or antiferromagnetism in one-dimensional or two-dimensional isotropic Heisenberg models", Phys. Rev. Lett. **17**, 1133–1136 (1966).

[90]P. C. Hohenberg, "Existence of Long-Range Order in One and Two Dimensions", Phys. Rev. **158**, 383–386 (1967).

[91]S. R. Coleman, "There are no Goldstone bosons in two-dimensions", Commun. Math. Phys. **31**, 259–264 (1973).

[92]C. Itzykson and J. B. Zuber, *Quantum Field Theory*, International Series In Pure and Applied Physics (McGraw-Hill, New York, 1980).

[93]S. Coleman, *Aspects of Symmetry* (Cambridge University Press, Cambridge, U.K., 1985).

[94]J. Glimm and A. M. Jaffe, *QUANTUM PHYSICS. A FUNCTIONAL INTEGRAL POINT OF VIEW* (1987).

[95]V. P. Gusynin, V. A. Miransky, and I. A. Shovkovy, "Dimensional reduction and dynamical chiral symmetry breaking by a magnetic field in (3+1)-dimensions", Phys. Lett. **B349**, 477–483 (1995).

[96]V. P. Gusynin, V. A. Miransky, and I. A. Shovkovy, "Dimensional reduction and catalysis of dynamical symmetry breaking by a magnetic field", Nucl. Phys. **B462**, 249–290 (1996).

[97]L. Dolan and R. Jackiw, "Symmetry Behavior at Finite Temperature", Phys. Rev. **D9**, 3320–3341 (1974).

[98]D. J. Gross, R. D. Pisarski, and L. G. Yaffe, “QCD and Instantons at Finite Temperature”, Rev. Mod. Phys. **53**, 43 (1981).

[99]J. Gasser and H. Leutwyler, “Chiral Perturbation Theory to One Loop”, Annals Phys. **158**, 142 (1984).

[100]G. V. Dunne and M. Ünsal, “Continuity and Resurgence: towards a continuum definition of the $\mathbb{CP}$(N-1) model”, Phys. Rev. **D87**, 025015 (2013).

[101]G. V. Dunne and M. Unsal, “Resurgence and Trans-series in Quantum Field Theory: The CP(N-1) Model”, JHEP **11**, 170 (2012).

[102]A. Cherman, D. Dorigoni, and M. Unsal, “Decoding perturbation theory using resurgence: Stokes phenomena, new saddle points and Lefschetz thimbles”, JHEP **10**, 056 (2015).

[103]M. Shifman and M. Unsal, “QCD-like Theories on R(3) x S(1): A Smooth Journey from Small to Large r(S(1)) with Double-Trace Deformations”, Phys. Rev. **D78**, 065004 (2008).

[104]M. Unsal and L. G. Yaffe, “Center-stabilized Yang-Mills theory: Confinement and large N volume independence”, Phys. Rev. **D78**, 065035 (2008).

[105]P. Argyres and M. Unsal, “A semiclassical realization of infrared renormalons”, Phys. Rev. Lett. **109**, 121601 (2012).

[106]P. C. Argyres and M. Unsal, “The semi-classical expansion and resurgence in gauge theories: new perturbative, instanton, bion, and renormalon effects”, JHEP **08**, 063 (2012).

[107]M. M. Anber and T. Sulejmanpasic, “The renormalon diagram in gauge theories on $\mathbb{R}^3 \times \mathbb{S}^1$”, JHEP **01**, 139 (2015).

[108]T. Misumi and T. Kanazawa, “Adjoint QCD on $\mathbb{R}^3 \times S^1$ with twisted fermionic boundary conditions”, JHEP **06**, 181 (2014).

[109]E. Caliceti, M. Meyer-Hermann, P. Ribeca, A. Surzhykov, and U. D. Jentschura, “From useful algorithms for slowly convergent series to physical predictions based on divergent perturbative expansions”, Phys. Rept. **446**, 1–96 (2007).

[110]M. Mariño, “Lectures on non-perturbative effects in large N gauge theories, matrix models and strings”, Fortsch. Phys. **62**, 455–540 (2014).

[111]D. Dorigoni, “An Introduction to Resurgence, Trans-Series and Alien Calculus”, (2014).

[112]G. V. Dunne and M. Ünsal, “What is QFT? Resurgent trans-series, Lefschetz thimbles, and new exact saddles”, PoS **LATTICE2015**, 010 (2016).

[113]G. V. Dunne and M. Ünsal, “New Nonperturbative Methods in Quantum Field Theory: From Large-N Orbifold Equivalence to Bions and Resurgence”, Ann. Rev. Nucl. Part. Sci. **66**, 245–272 (2016).

[114]T. Kanazawa, M. Ünsal, and N. Yamamoto, "Phases of circle-compactified QCD with adjoint fermions at finite density", Phys. Rev. **D96**, 034022 (2017).

[115]P. Kovtun, M. Unsal, and L. G. Yaffe, "Volume independence in large N(c) QCD-like gauge theories", JHEP **06**, 019 (2007).

[116]T. Sulejmanpasic, "Global Symmetries, Volume Independence, and Continuity in Quantum Field Theories", Phys. Rev. Lett. **118**, 011601 (2017).

[117]A. Cherman, S. Sen, M. L. Wagman, and L. G. Yaffe, "Exponential reduction of finite volume effects with twisted boundary conditions", Phys. Rev. **D95**, 074512 (2017).

[118]P. V. Buividovich and S. N. Valgushev, "Lattice study of continuity and finite-temperature transition in two-dimensional SU(N) x SU(N) Principal Chiral Model", (2017).

[119]M. Hongo, T. Misumi, and Y. Tanizaki, "Phase structure of the twisted $SU(3)/U(1)^2$ flag sigma model on $\mathbb{R} \times S^1$", JHEP **02**, 070 (2019).

[120]T. Appelquist and R. D. Pisarski, "High-Temperature Yang-Mills Theories and Three-Dimensional Quantum Chromodynamics", Phys. Rev. **D23**, 2305 (1981).

[121]S.-z. Huang and M. Lissia, "Dimensional reduction at high temperature for fermions", Phys. Lett. **B349**, 484–490 (1995).

[122]L. P. R. Ospedal and J. A. Helayël-Neto, "Fermion interparticle potentials in 5D and a dimensional restriction prescription to 4D", Phys. Rev. **D97**, 056014 (2018).

Chapter 2

Properties of size-dependent models having quasiperiodic boundary conditions

Published as:
E. Cavalcanti, C.A. Linhares, and A.P.C. Malbouisson. International Journal of Modern Physics A **33**, 1850008 (2018) *Properties of size-dependent models having quasiperiodic boundary conditions*

International Journal of Modern Physics A
Vol. 33, No. 1 (2018) 1850008 (18 pages)

DOI: 10.1142/S0217751X18500082

Properties of size-dependent models having quasiperiodic boundary conditions

E. Cavalcanti,[*,‡] C. A. Linhares[†,§] and A. P. C. Malbouisson[*,¶]

[*] *Centro Brasileiro de Pesquisas Físicas/MCTI, Rio de Janeiro, RJ 22290-180, Brazil*
[†] *Instituto de Física, Universidade do Estado do Rio de Janeiro, Rio de Janeiro, RJ 20559-900, Brazil*
[‡] *erich@cbpf.br*
[§] *linharescesar@gmail.com*
[¶] *adolfo@cbpf.br*

Received 3 October 2017
Accepted 11 December 2017
Published 9 January 2018

Boundary condition effects are explored for size-dependent models in thermal equilibrium. Scalar and fermionic models are used for $D = 1 + 3$ (films), $D = 1 + 2$ (hollow cylinder) and $D = 1 + 1$ (ring). For all models, a minimal length is found, below which no thermally-induced phase transition occurs. Using quasiperiodic boundary condition controlled by a contour parameter θ ($\theta = 0$ is a periodic boundary condition and $\theta = 1$ is an antiperiodic condition), it results that the minimal length depends directly on the value of θ. It is also argued that this parameter can be associated to an Aharonov–Bohm phase.

Keywords: Quasiperiodic boundary conditions; finite-temperature field theory; finite-size effects; phase transition; Aharonov–Bohm effect; Casimir effect.

PACS numbers: 11.30.Qc, 11.10.Wx, 11.10.Kk, 03.65.Ta

1. Introduction

The question of the influence of the size of a system is of importance in many situations: e.g. consequences on the transition temperature for systems having some dimensions of finite size, as films, wires and grains in condensed matter; also in higher dimensional systems with some compactified dimensions.

In previous works,[1–14] when investigating phase transitions in films, periodic or antiperiodic boundary conditions for spatial coordinates have been used in analogy

[‡]Corresponding author.

with the imposed condition on the imaginary-time variable. According to the KMS condition,[15] the boundary conditions on imaginary time are restricted to be periodic for bosons and antiperiodic for fermions. However, there are no similar restrictions on the spatial boundary conditions. As a generalization, we can study a whole new class of models whose spatial boundary conditions are between the perfect periodic and the perfect antiperiodic boundary conditions, which is a way of generalizing the boundary conditions within the framework of quantum field theory (QFT) on spaces with toroidal topologies. Although we choose to refer to this as a quasi-periodic boundary condition, it follows along lines similar to those used in *anyonic* systems[16–23] and models with twisted boundary conditions[24–34] and have been found to be useful in many fields, e.g. the Casimir effect,[16,34–36] condensed matter systems,[37–39] string theories[25–27] and also effective and phenomenological models for high-energy physics.[28–32]

The study of thermal phase transitions in a quantum field theoretical approach is usually done through either the imaginary-time Matsubara formalism[40] or the real-time formalism.[41] Throughout this paper, we use an extension of the imaginary-time formalism. We consider a D-dimensional Euclidean space and introduce periodic/antiperiodic boundary conditions on d of its coordinates, effectively compactifying them, and generating a toroidal topology $\Gamma_D^d = (\mathbb{S}^1)^d \times \mathbb{R}^{D-d}$ with $1 \leq d \leq D$. This defines the so-called QFT on toroidal topologies[42] which has been applied in the recent literature.[1–14]

In this paper, the phase transition for these models is studied by constructing and analyzing the effective potential of the theory through the 2PI formalism. The existence of a nontrivial minimum of the effective potential corresponds in this case to a phase transition and defines for some models a criticality condition. For instance, for models undergoing a second-order phase transition, the criticality is related to a vanishing effective mass.

Before approaching specific problems, we present the general formalism for a scalar field in Sec. 2 and study its general consequences. Then, we apply the formalism both for a scalar and a fermionic model. In Sec. 3, we present a scalar model, which is of the Ginzburg–Landau-type, and consider some special cases which allow to take into account first-order and second-order phase transitions. The fermionic model is introduced in Sec. 4. The results are presented throughout the paper and are synthesized in the conclusions, Sec. 5.

We emphasize that we are dealing with phase transitions from a purely theoretical point of view. We are not directly concerned with comparison with experiments. In fact, we are mainly concerned with the mathematical consistency of our approach. Quasiperiodic boundary conditions are similar to *anyonic* statistics largely used over the last years, in connection, in particular, with the quantum Hall effect. Here, differently, we are interested in phase transitions occurring in systems obeying quasiperiodic boundary conditions from a mathematical physics point of view. However, in Sec. 5, we present a discussion in which we interpret the contour parameter as related to an Aharonov–Bohm phase.

2. The Formalism

Let us take a generic field Φ for which the boundary condition imposed on the x_i spatial variable is

$$\Phi(\ldots, x_i + L, \ldots) = e^{i\pi\theta_i}\Phi(\ldots, x_i, \ldots)\,, \tag{1}$$

where $\theta_i = 0$ corresponds to a periodic condition and $\theta_i = 1$ to an antiperiodic condition. The parameter θ_i is called the *boundary parameter*. Mathematically, the only change in the general formalism is that the frequencies associated with the spatial compactification become

$$p_i \to \omega_n^i = \frac{2\pi n_i}{L_i} + \frac{\theta_i \pi}{L_i}\,. \tag{2}$$

This feature can be absorbed into the formalism by introducing an *imaginary chemical potential* that takes into account the quasiperiodic boundary conditions. We then write

$$\omega_n^i = \frac{2\pi n_i}{L_i}\,, \quad \mu_i = i\frac{\theta_i \pi}{L_i}\,. \tag{3}$$

The following integral:

$$\mathcal{I}_\nu^D(M^2) = \int \frac{d^D p}{(2\pi)^D}\frac{1}{(p^2+M^2)^\nu} \tag{4}$$

plays an important role in the formalism we develop. It is to be evaluated on a D-dimensional Euclidean space, with M^2 being the squared field mass. By introducing periodic, antiperiodic or quasiperiodic boundary conditions on d coordinates, we effectively map our theory from a Euclidean space ($\mathbb{R}^D$) onto a *toroidal space* ($(\mathbb{S}^1)^d \times \mathbb{R}^{D-d}$). The compactification of imaginary time introduces the temperature $T = \beta^{-1} = L_0$ and compactifications of the spatial coordinates introduce characteristic lengths L_i. We apply periodic or antiperiodic conditions to imaginary time if the model is, respectively, bosonic or fermionic, and apply the quasiperiodic boundary conditions to the compactified spatial coordinates. By using a condensed notation in which $i = 0$ is associated to the imaginary time, and computing the remaining integral on the $(D-d)$-dimensional subspace using dimensional regularization,[43,44] we get

$$\begin{aligned}
&\mathcal{I}_\nu^D(M^2; L_\alpha, \mu_\alpha, \theta_\alpha)\\
&\quad = \frac{\sum_{n_0,\ldots,n_{d-1}=-\infty}^{\infty}}{\prod_{\alpha=0}^{d-1} L_\alpha}\int \frac{d^{D-d}q}{(2\pi)^{D-d}}\frac{1}{\left[q^2 + M^2 + \sum_{\alpha=0}^{d-1}\left(\frac{2\pi n_\alpha}{L_\alpha} - i\mu_\alpha\right)^2\right]^\nu}\\
&\quad = \frac{\sum_{n_0,\ldots,n_{d-1}=-\infty}^{\infty}}{\prod_{\alpha=0}^{d-1} L_\alpha}\frac{\Gamma\left[\nu - \frac{D}{2} + \frac{d}{2}\right]}{(4\pi)^{\frac{D}{2}-\frac{d}{2}}\Gamma[\nu]}\frac{1}{\left[M^2 + \sum_{\alpha=0}^{d-1}\left(\frac{2\pi n_\alpha}{L_\alpha} - i\mu_\alpha\right)^2\right]^{\nu-\frac{D}{2}+\frac{d}{2}}}\,,
\end{aligned}$$

where $\Gamma(\nu)$ is the Euler gamma function. In the above formula, the summations over n_0 and $\{n_i\}$ correspond to compactification of, respectively, the imaginary time and the spatial coordinates.

We define the quantity $\mu_0 = \mu + i\theta_0\pi/\beta$, which depends on the chemical potential μ and also on whether the model describes bosons ($\theta_0 = 0$) or fermions ($\theta_0 = 1$). The remaining infinite sum can be identified as an Epstein–Hurwitz zeta function, which can be regularized by the use of a Jacobi identity for theta functions, leading to sums of modified Bessel functions of the second kind $K_\nu(X)$ (see Ref. 45),

$$\begin{aligned}
&\mathcal{I}_\nu^D(M^2; L_\alpha, \mu_\alpha, \theta_\alpha) \\
&\quad = \frac{(M^2)^{-\nu+\frac{D}{2}}\Gamma\left[\nu - \frac{D}{2}\right]}{(4\pi)^{\frac{D}{2}}\Gamma[\nu]} + \frac{1}{(2\pi)^{\frac{D}{2}}2^{\nu-2}\Gamma[\nu]} \\
&\quad \times \Bigg\{ \sum_{\alpha=0}^{d-1}\sum_{n_\alpha=1}^{\infty}\left(\frac{n_\alpha L_\alpha}{M}\right)^{\nu-\frac{D}{2}} \cosh(n_\alpha L_\alpha \mu^\alpha) K_{\nu-\frac{D}{2}}(n_\alpha L_\alpha M) + \cdots \\
&\quad + 2^{d-1}\sum_{n_0,\ldots,n_{d-1}=1}^{\infty}\left(\frac{\sqrt{\sum_{\alpha=0}^{d-1} n_\alpha^2 L_\alpha^2}}{M}\right)^{\nu-\frac{D}{2}} \\
&\quad \times \prod_{\alpha=0}^{d-1}\cosh(n_\alpha L \mu^\alpha) K_{\nu-\frac{D}{2}}\left(M\sqrt{\sum_{\alpha=0}^{d-1} n_\alpha^2 L_\alpha^2}\right)\Bigg\}. \qquad (5)
\end{aligned}$$

In the following, we restrict ourselves to the $d = 2$ case, so that the compactifications introduce the temperature $L_0 = \beta^{-1}$; a characteristic length $L_1 = L$; the parameter $\mu_0 = \mu + i\theta_0\pi/\beta$, which carries information about the chemical potential μ and the imaginary-time boundary condition; and the parameter $\mu_1 = i\theta\pi/L$, which carries information about the spatial quasiperiodic boundary condition.

The function $\mathcal{I}_\nu^D$ in Eq. (5) can be rewritten as

$$\mathcal{I}_\nu^D(M^2; \beta, \mu, \theta_0; L, \theta) = \frac{(M^2)^{-\nu+\frac{D}{2}}\Gamma\left[\nu - \frac{D}{2}\right]}{(4\pi)^{\frac{D}{2}}\Gamma[\nu]} + \frac{W_{\frac{D}{2}-\nu}[M^2; \beta, \mu, \theta_0; L, \theta]}{(2\pi)^{\frac{D}{2}}2^{\nu-2}\Gamma[\nu]}, \qquad (6)$$

where the function W_ρ, introduced to simplify notations, is defined by

$$\begin{aligned}
&W_\rho[M^2; \beta, \mu, \theta_0; L, \theta] \\
&\quad = \sum_{n=1}^{\infty}\left\{\left(\frac{M}{n\beta}\right)^\rho (-1)^{n\theta_0}\cosh(n\beta\mu)K_\rho(n\beta M) + \left(\frac{M}{nL}\right)^\rho \cos(n\pi\theta)K_\rho(nLM)\right\} \\
&\qquad + 2\sum_{n_0,n_1=1}^{\infty}\frac{M^\rho(-1)^{n_0\theta_0}\cosh(n_0\beta\mu)\cos(n_1\pi\theta)}{\left(n_0^2\beta^2 + n_1^2L^2\right)^{\rho/2}} K_\rho\left(M\sqrt{n_0^2\beta^2 + n_1^2L^2}\right), \qquad (7)
\end{aligned}$$

which is positive and monotonically decreasing with L and β. Its derivatives are computed by means of the recurrence formula

$$\frac{d^k}{dX^k}W_\nu[X, \beta, L, \mu, \theta] = \left(-\frac{1}{2}\right)^k W_{\nu-k}[X, \beta, L, \mu, \theta]. \qquad (8)$$

Table 1. Root $\theta^\star$ of the polylogarithm function depending on the parameter $\rho = D/2 - \nu$.

ρ	0	1/2	1	3/2	2	5/2	$\cdots$	∞
$\theta^\star$	0	1/3	0.422650	0.461659	0.480670	0.490238	$\cdots$	1/2

With respect to the function W_ρ, which contains all size and temperature dependencies, it turns out that an expression for $M^2 = 0$ is useful in many occasions. For $\rho > 0$, we obtain, by taking the modified Bessel function of the second kind in the limit $M \to 0$ and computing the sum over the frequencies,

$$W_\rho[0;\beta,\mu,\theta_0;L,\theta] = \Gamma[\rho]2^{\rho-2}\left\{\frac{\Re[\mathrm{Li}_{2\rho}\big((-1)^{\theta_0}e^{\beta\mu}\big)]}{\beta^{2\rho}} + \frac{\Re\big[\mathrm{Li}_{2\rho}\big(e^{i\pi\theta}\big)\big]}{L^{2\rho}}\right.$$
$$\left. + 4\sum_{n_0,n_1=1}^{\infty}\frac{(-1)^{n_0\theta_0}\cosh(n_0\beta\mu)\cos(n_1\pi\theta)}{\big(n_0^2\beta^2 + n_1^2L^2\big)^\rho}\right\},$$

where Li_s is the polylogarithm function of order s. For $\rho = 0$, we have, instead, in the $T = 0$ case,

$$W_0[M \to 0; L,\theta] = \frac{\gamma}{2} + \frac{1}{2}\ln\frac{ML}{2} + \frac{\mathrm{Li}_0'(-e^{-i\pi\theta}) + \mathrm{Li}_0'(-e^{i\pi\theta})}{2}\,. \tag{9}$$

As $\Re\big[\mathrm{Li}_{2\rho}\big(e^{i\pi\theta}\big)\big] = \big[\mathrm{Li}_{2\rho}\big(e^{+i\pi\theta}\big) + \mathrm{Li}_{2\rho}\big(e^{-i\pi\theta}\big)\big]/2$, it is always possible to define a *critical parameter* $\theta^\star$ for which the polylogarithm function vanishes. Its value depends only on α $\big(\rho = \frac{D}{2} - \nu$, as in Eq. (6)$\big)$. Some of these values are exhibited in Table 1.

Note that the maximal possible value for $\theta^\star$ is 1/2, representing the intermediate point between the periodic and antiperiodic boundary conditions.

3. Ginzburg–Landau Model

As a first example, we take a Ginzburg–Landau (GL) model with a 6th-order polynomial potential in D-dimensions,

$$S_E(\phi) = \int d^Dx\left[\frac{1}{2}(\partial\phi)^2 + V_0(\phi)\right], \tag{10}$$

$$V_0(\phi) = m_0^2\frac{\phi^2}{2} + \lambda_0\frac{\phi^4}{4!} + g_0\frac{\phi^6}{6!}\,. \tag{11}$$

By employing the 2PI formalism[46] in the Hartree–Fock approximation, we are restricted to diagrams with only one vertex; then the effective action is written as

$$\Gamma_{\mathrm{eff}}(\phi,G) = S_E(\phi) + \frac{1}{2}\big[V_0''(\phi) - m^2\big]\,\mathrm{Tr}\,G + \frac{1}{2}\,\mathrm{Tr}\ln G^{-1}$$
$$+ \sum_{n=2}^{\infty}\frac{V_0^{(2n)}(\phi)}{(2n)!!}(\mathrm{Tr}\,G)^n\,, \tag{12}$$

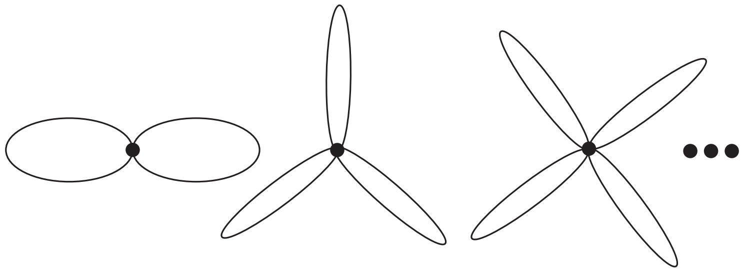

Fig. 1. Contributions of the *petal* diagrams.

where G is the full propagator, which depends on the thermal mass, and the trace Tr is taken over the D-dimensional spatial coordinates and momenta. The last term is the sum over all *petal* diagrams in Fig. 1.

We assume that ϕ is a constant field and then define the effective potential as the effective action divided by the D-dimensional volume. All size and temperature dependencies are contained in $\mathrm{tr}\, G$ (see Sec. 2 for a detailed explanation), and the remaining trace tr is only over the D-momenta. The ϕ-dependent effective potential is simply

$$\begin{aligned} V_{\mathrm{eff}}(\phi) = {} & \left[m_0^2 + \frac{\lambda_0}{2}\mathcal{I}_1^D(m^2;\beta,\mu,0;L,\theta)\right]\frac{\phi^2}{2} \\ & + \left[\lambda_0 + \frac{g_0}{2}\mathcal{I}_1^D(m^2;\beta,\mu,0;L,\theta)\right]\frac{\phi^4}{4!} + g_0\frac{\phi^6}{6!}\,, \end{aligned} \tag{13}$$

where $\mathcal{I}_\nu^D$ is defined in Eq. (6).

The phase transition analysis consists in determining the value φ that minimizes V_{eff}. We must use in parallel the relation $\partial V_{\mathrm{eff}}/\partial\phi|_{\phi=\varphi\neq 0} = 0$, defining extrema, and $\partial^2 V_{\mathrm{eff}}/\partial\phi^2|_{\phi=\varphi} = m^2$, which is the recurrence equation defining the thermal dependent mass. The symmetric phase $\varphi = 0$ is an acceptable extremum and the mass in this phase evolves as

$$m_{\mathrm{sym}}^2 = m_0^2 + \frac{\lambda_0}{2}\mathcal{I}_1^D\left(m_{\mathrm{sym}}^2;\beta,\mu,0;L,\theta\right). \tag{14}$$

Similarly, in the broken phase, we can always find a recurrence relation for the properly defined mass m_{brk}^2 by using a nontrivial minimum $\varphi \neq 0$.

3.1. *Phase transitions*

3.1.1. *Second-order phase transition*

In this section, we consider a theory as described in Eq. (10) with $g_0 = 0$. Thus, in the absence of the ϕ^6 coupling, the system undergoes a second-order phase transition at $m^2 = 0$.[47] Considering the mass evolution from the symmetric phase given in Eq. (14), the critical condition is

$$m_0^2 + \frac{\lambda_0}{2}\mathcal{I}_1^D\left(0;\beta_c,\mu,0;L,\theta\right) = 0\,. \tag{15}$$

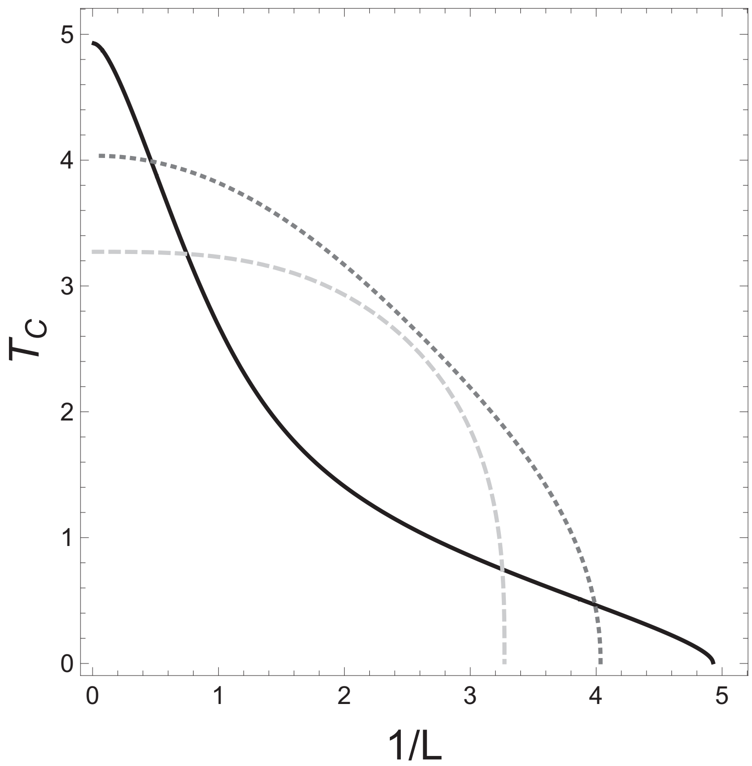

Fig. 2. Critical temperature as a function of the inverse length for $D = 4$ (full black line), $D = 5$ (dashed light gray line), $D = 6$ (dotted gray line) for the GL model with quartic interaction. These phase diagrams are for the second-order phase transition and exhibits the minimal length (maximal inverse length) below which no phase transition occurs. In each case, the broken phase lies below the respective curve.

Using this condition, we construct a phase diagram giving the critical temperature as a function of the size of the system, in Fig. 2, for $D = 2, 3, 4$ and periodic boundary condition $\theta = 0$, which exhibits a minimal length for $T_c = 0$, below which no thermally induced phase transition occurs. For systems subject to external influence (for instance, an applied magnetic field, pressure$, \ldots$), phase transitions can occur even for $T = 0$, known in the literature as quantum phase transitions;[48] however, these situations are beyond the scope of the present work. The behavior in Fig. 2 is mathematically expected as all size and temperature dependencies are contained in $W_\rho[M^2; \beta, \mu, 0; L, 0]$, which is monotonically decreasing in L and β; to sustain a fixed value for W when $T \to 0$ ($\beta \to \infty$), the parameter L must decrease. Therefore, for $T_c = 0$, the system has its minimal possible length $L_{\min}$ and the critical condition becomes

$$0 = m_0^2 + \frac{\lambda_0}{2}\left(\frac{m^{D-2}\Gamma\left[1-\frac{D}{2}\right]}{(4\pi)^{\frac{D}{2}}} + \frac{2}{(2\pi)^{\frac{D}{2}}}\frac{\Gamma\left[\frac{D}{2}-1\right]2^{\frac{D}{2}-2}}{L_{\min}^{D-2}}\Re\left[\mathrm{Li}_{D-2}\left(e^{i\pi\theta}\right)\right]\right). \quad (16)$$

For some critical value of the contour parameter $\theta = \theta^\star$, the minimal length becomes zero, meaning that the size restriction was removed. The evolution of the minimal length with respect to the contour parameter is presented in Fig. 3

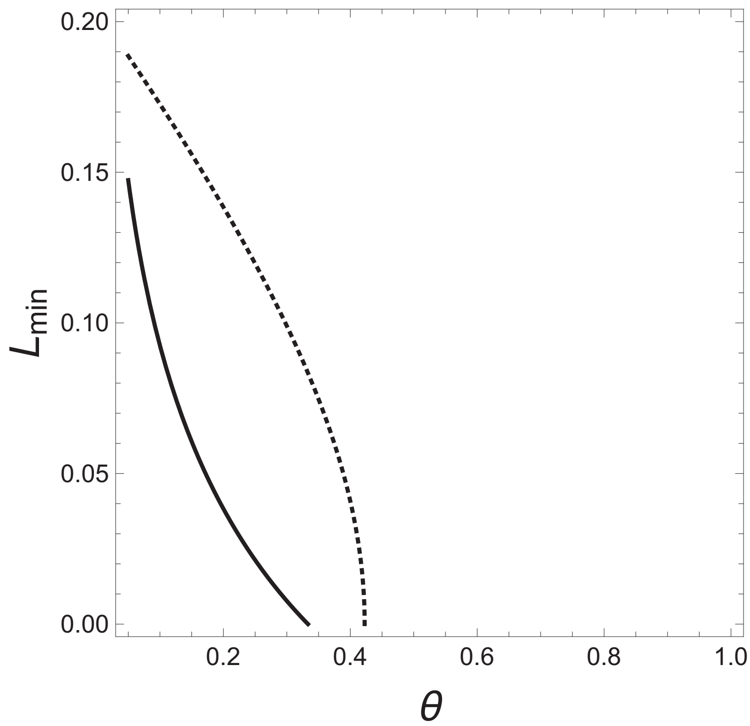

Fig. 3. Dependence of the ratio $L_{\min}$ on the contour parameter for $D = 1 + 2$ (full line) and $D = 1 + 3$ (dotted line) in the quartic GL model. The region below each curve corresponds to the symmetric phase. The length L has mass dimensions, which is equivalent to take $m_0^2 = -1$, and we are assuming $\lambda = 1$.

for a hollow cylinder ($D = 1 + 2$) and a film ($D = 1 + 3$). Under the critical curve $L_{\min}(\theta)$, a thermally-induced phase transition cannot exist. This justifies the name *minimal length*; under this critical size, the system no longer exhibits a phase transition. Above the critical curve $L_{\min}(\theta)$, the phase is broken and there may be a thermally-induced phase transition at some critical temperature.

We emphasize the important contribution of the contour parameter θ that controls the periodicity; its value determines whether the system exhibits a minimal length. The critical parameter varies with dimensionality: for $D = 2, 3, 4$, we have, respectively, $\theta^\star = 0$, $\frac{1}{3}$, 0.42265. Therefore, the behavior is present for the film model, controlling the minimal film thickness, and for the cylindrical model (a tube), controlling its radius. For the ring model, the contour parameter has no influence; mathematically, this happens because of the property $\mathrm{Li}_0(e^x) + \mathrm{Li}_0(e^{-x}) = -1$; so there is no θ-dependence. This suggests that the contour condition does not modify the minimal radius of a ring ($D = 1 + 1$).

For clarity, we show in Fig. 4 the meaning of a vanishing minimal length: in this case, we have $D = 4$ and a critical contour parameter $\theta^\star = 0.42265$. For $\theta = 0$, 0.2, $0.4 < \theta^\star$, there is still a minimal length; however, when $\theta = 0.6 > \theta^\star$ (dot-dashed curve), we no longer have a minimal length and the behavior of the critical temperature as a function of the length is completely changed.

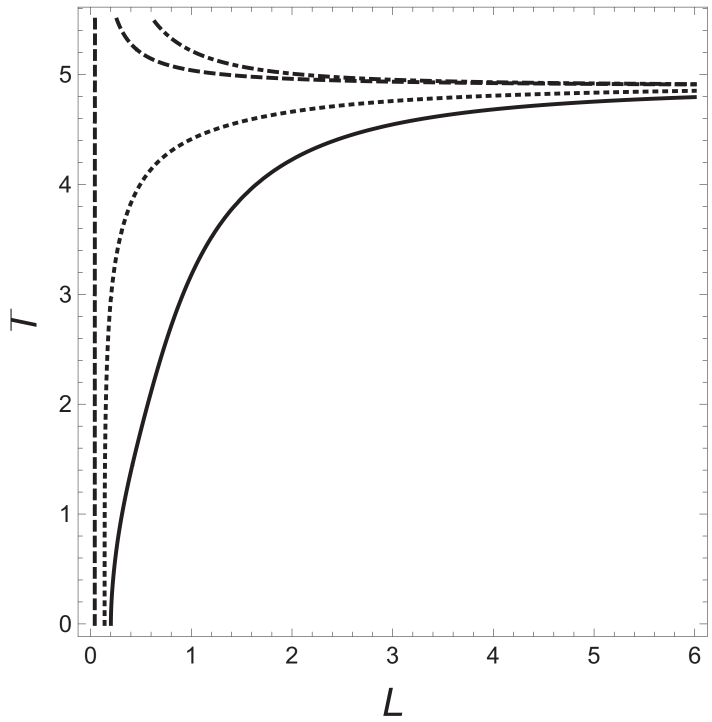

Fig. 4. Phase diagram for $D = 4$, critical temperature T_c of a bosonic second-order phase transition as a function of the length L for values of the contour parameter $\theta = 0$, 0.2, 0.4, 0.6, respectively, the full, dotted, dashed and dot-dashed curves. The broken phase is the region below each curve.

3.1.2. *First-order phase transition*

In this section, we consider $g_0 \neq 0$, and $\lambda_0 < 0$. In this case, there is a first-order transition in the GL model of Eq. (10). Its critical region is determined by the coexistence $V_{\text{eff}}(\varphi \neq 0) = V_{\text{eff}}(\varphi = 0)$, with φ defined as an extremum. From the perspective of the symmetric phase, the critical condition is obtained, after some algebraic manipulations, as

$$\mathcal{I}_1^D\left(5m_0^2 - \frac{5\lambda_0^2}{2g}; \beta_c, \mu, 0; L, \theta\right) = -\frac{2\lambda_0}{g} \pm \frac{4\lambda_0}{g}\sqrt{\frac{2gm_0^2}{\lambda_0^2} - 1}\,. \tag{17}$$

As before, the minimal length $L_{\min}$ is defined as the size of the system at which the critical temperature vanishes ($T_c = 0$) which, as already mentioned, means that there is no thermally induced phase transition for lengths below $L_{\min}$. Then, by taking this limit, we obtain $\lim_{\beta\to\infty} \mathcal{I}_1^D(m^2; \beta, \mu, 0; L, \theta) = \mathcal{I}_1^D(m^2; L, \theta)$. In this case, the condition expressed in Eq. (17) becomes

$$\begin{aligned}\frac{2W_{\frac{D}{2}-1}\left[m^2; L_{\min}, \theta\right]}{(2\pi)^{\frac{D}{2}}} &= \frac{m^{\frac{D}{2}-1}}{2^{\frac{D}{2}-1}\pi^{\frac{D}{2}} L_{\min}^{\frac{D}{2}-1}} \sum_{n=1}^{\infty} \frac{\cos(n\pi\theta)}{n^{\frac{D}{2}-1}} K_{\frac{D}{2}-1}(nL_{\min}m) \\ &= -\frac{2\lambda_0}{g} \pm \frac{4\lambda_0}{g}\sqrt{\frac{2gm_0^2}{\lambda_0^2} - 1}\,.\end{aligned} \tag{18}$$

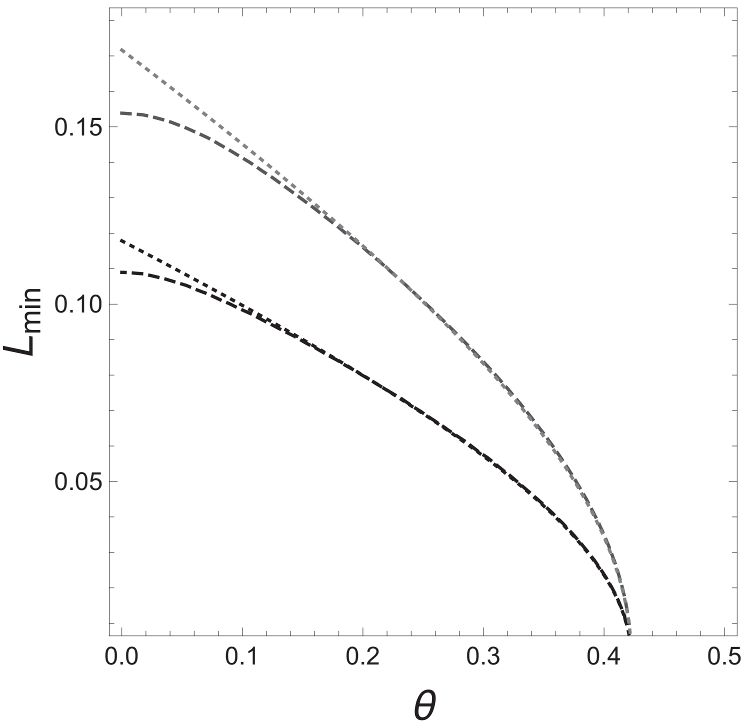

Fig. 5. Minimal thickness $L_{\min}$, in $D = 1 + 3$, as a function of the contour parameter θ in the extended GL model. The dashed curve uses the full equation with a truncated series, the dotted curve uses the approximation for low $L_{\min}$. For all curves $m_0^2 = 1$ and $g = 1$. The black curves have $\lambda_0 = -1$, implying $gm_0^2/\lambda_0^2 = 1 > 5/8$ which is symmetric at the tree level. The gray curves have $\lambda_0 = -\sqrt{2}$ implying $gm_0^2/\lambda_0^2 = 1/2 < 5/8$ (broken phase at the tree level).

As an example, we consider $D = 1 + 3$ (a film) and investigate the critical contour parameter $\theta^\star$ at which there is no minimal length, see Fig. 5. This can be done by taking in Eq. (18) $L_{\min} \approx 0$ and using an asymptotic formula for $K_\nu(z)$ for $z \sim 0$, so that,

$$L_{\min} = \left(-\frac{2\lambda_0}{g} \pm \frac{4\lambda_0}{g}\sqrt{\frac{2gm_0^2}{\lambda_0^2} - 1}\right)^{-\frac{1}{2}} \sqrt{\frac{\Re\left[\mathrm{Li}_2(e^{i\pi\theta})\right]}{2\pi^2}}\,. \tag{19}$$

In this case, we obtain the value $\theta^\star = 0.42265$. We see that, although we are dealing with a first-order phase transition, this is the same result of the previous section where we dealt with a second-order phase transition. This means that the critical contour parameter seems to be a natural characteristic of the compactified scalar model, regardless the order of the phase transition.

In Fig. 5, we compare the approximation for a low value of $L_{\min}$ (dotted line) and the full equation (dashed line), note that they only disagree for very low values of θ. The presence of the critical contour parameter at which the minimal length goes to zero is made evident. Let us consider two different initial conditions at the tree level, one ensuring that the phase is symmetric (black lines) and the other one ensuring that the phase is broken (gray lines); both exhibit the same behavior when taking $T_c = 0$ and varying the minimal length with respect to the contour parameter.

4. The Bosonized Gross–Neveu Model

In this section, we extend the massless Gross–Neveu model originally established for $D = 1+1$,[49] to generic D dimensions where the model is not renormalizable but can be viewed under some circumstances as an effective model for QCD.[11,12] In this case, perturbative renormalizability is not an absolute criterion for the existence of the model.[50–52] We point out that for $D = 1+2$, although not perturbatively renormalizable, the model has been shown to exist and was constructed.[53] We take into account temperature, chemical potential, finite-size effects and the contour condition. Both the fermion ring (1+1) and the fermion tube (1+2) are constructed by identifying a space point (compactifying the space) which modifies its topology; this compactification is controlled by the contour parameter. We find that the system exhibits a dynamical generation of mass[54] that here characterizes a second-order phase transition. A minimal length below which no thermally induced phase transition occurs is found in both cases, which means that the fermion ring does not become a point and that the fermion tube does not become a line and both have dependencies on the contour parameter.

We consider a colorless and flavorless fermionic system with an interaction of the Gross–Neveu-type,

$$S(\bar{\psi}, \psi) = \int d^D x \left[\bar{\psi}\partial\!\!\!/\psi + g_0^2(\bar{\psi}\psi)^2\right]. \tag{20}$$

In our convention, we use Euclidean γ matrices.[55] We consider the bosonization given by the scalar field $\sigma = \bar{\psi}\psi$. To find the new Lagrangian density, we then employ the substitution $(\bar{\psi}\psi)^2 = 2\bar{\psi}\psi\sigma - \sigma^2$, which ensures that the relation $\delta S/\delta\sigma = 0$ leads to the identity $\sigma = \bar{\psi}\psi$. We then obtain that the action is

$$S(\bar{\psi}, \psi, \sigma) = \int d^D x \left[\bar{\psi}(\partial\!\!\!/ + g_0^2\sigma)\psi - \frac{g_0^2}{2}\sigma^2\right] \tag{21}$$

and the generating function is

$$Z = \int \mathcal{D}[\bar{\psi}, \psi, \sigma] e^{-S(\bar{\psi}, \psi, \sigma)}.$$

Integrating over the fermionic field, we construct the effective potential,

$$V_{\text{eff}}(\sigma) = \frac{g_0^2}{2}\sigma^2 - \operatorname{Tr}\ln\left[\partial\!\!\!/ + g_0^2\sigma\right],$$

where the trace is to be evaluated over the Dirac indices and the momentum space. Using that $\operatorname{Tr}\ln = \ln\operatorname{Det}$ and taking the determinant over the Dirac indices, we get

$$V_{\text{eff}} = \frac{g_0^2}{2}\sigma^2 - \int \frac{d^D p}{(2\pi)^D}\ln\left[p^2 + g_0^4\sigma^2\right].$$

The logarithm can be expressed as a derivative

$$\ln x = -\frac{\partial}{\partial \nu} x^{-\nu}\Big|_{\nu=0},$$

which allows us to employ Eq. (6) and then obtain

$$V_{\text{eff}} = \frac{g_0^2}{2}\sigma^2 + \frac{\Gamma\left[-\frac{D}{2}\right]}{(4\pi)^{\frac{D}{2}}}(g_0^2\sigma)^D + \frac{4}{(2\pi)^{\frac{D}{2}}} W_{\frac{D}{2}}\left[\left(g_0^2\sigma\right)^2; \beta, \mu, 1; L, \theta\right],$$

where we have used that

$$\frac{\partial}{\partial \nu}\frac{f(\nu)}{\Gamma(\nu)}\Big|_{\nu=0} = f(0)$$

for a function $f(\nu)$ with no poles at $\nu = 0$. The function W_ν was defined in Eq. (7). The term $\theta_0 = 1$ corresponds to the antiperiodic boundary condition on the imaginary time, which is used since we are dealing with a fermionic model.

The dynamically generated mass is $m = g_0^2\sigma$, so we can rewrite the effective potential as

$$V_{\text{eff}} = \frac{m^2}{2g_0^2} + \frac{\Gamma\left[-\frac{D}{2}\right]}{(4\pi)^{\frac{D}{2}}}|m|^D + \frac{4}{(2\pi)^{\frac{D}{2}}} W_{\frac{D}{2}}[m^2; \beta, \mu, 1; L, \theta].$$

By applying the renormalization condition

$$\frac{\partial^2 V_{\text{eff}}}{\partial m^2}(m = m_R; \beta \to \infty) = \frac{1}{g_R}, \tag{22}$$

we exchange the effective potential dependence from g_0 and m to g_R and m_R, leading to

$$V_{\text{eff}} = \frac{m^2}{2g_R^2} + \frac{\Gamma\left[-\frac{D}{2}\right]}{(4\pi)^{\frac{D}{2}}}\left(|m|^D - \frac{m^2 D(D-1)}{2}|m_R|^{D-2}\right) + \frac{4}{(2\pi)^{\frac{D}{2}}} W_{\frac{D}{2}}[m^2; \beta, \mu, 1; L, \theta].$$

Alternatively, we express the effective potential in terms of the dynamically generated mass defined by the condition $\partial V_{\text{eff}}/\partial m|_{m=\tilde{m}} = 0$, taking the point at zero temperature $\tilde{m}\big(T = 0, \mu = 0, \frac{1}{L} = 0\big) = m_0$. Then, the effective potential is written as

$$V_{\text{eff}} = m^2 \frac{\Gamma\left[-\frac{D}{2}\right]}{(4\pi)^{\frac{D}{2}}}\left(|m|^{D-2} - \frac{D}{2}|m_0|^{D-2}\right) + \frac{4}{(2\pi)^{\frac{D}{2}}} W_{\frac{D}{2}}\left[m^2; \beta, \mu, 1; L, \theta\right]. \tag{23}$$

This result is valid for any dimensionality, but in principle, only applicable for $D \leq 3$. In $1+1$ dimensions, the theory is renormalizable and in $1+2$ dimensions, although not perturbatively renormalizable, it was shown that the theory can be defined through the methods of constructive QFT.[53]

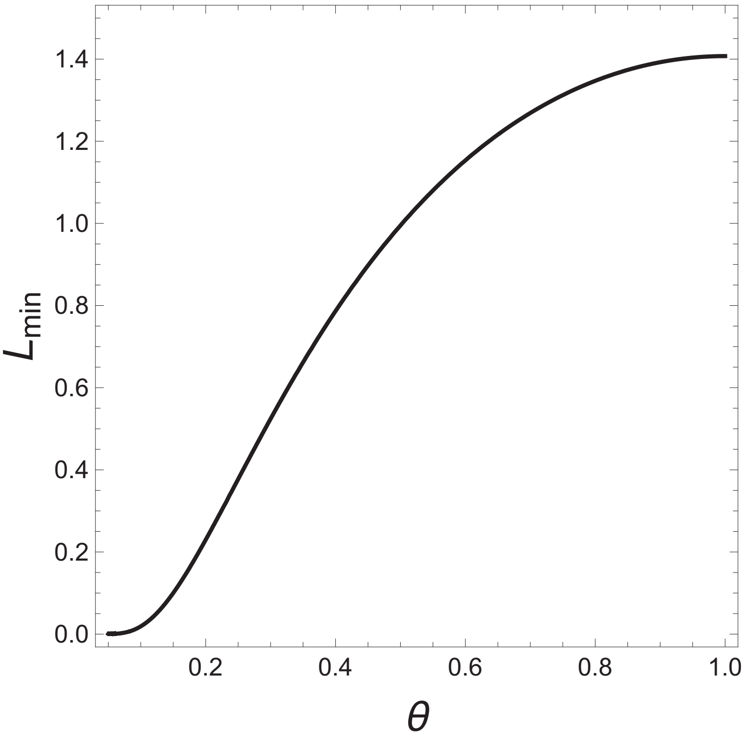

Fig. 6. Minimal length as a function of the contour parameter in the GN model for $D = 1 + 1$. Only for $\theta = 0$, the minimal length turns out to be zero. Under the curve, the phase is *always* symmetric and there is no thermally induced transition.

4.1. $\mathbf{GN_{1+1}}$, *fermion on a ring*

For $D = 1 + 1$, the effective potential is

$$V_{\text{eff}}^{D=2} = \frac{m^2}{4\pi}\left(\ln\frac{m^2}{m_0^2} - 1\right) + \frac{2}{\pi}W_1[m^2;\beta,\mu,1;L,\theta]\,. \tag{24}$$

Its first derivative with respect to m gives all extrema. Discarding the known $m = 0$ result of the symmetric phase, we have the mass gap equation

$$\ln\frac{m}{m_0} = 2W_0[m^2;\beta,\mu,1;L,\theta]\,. \tag{25}$$

To investigate the existence of a minimal length, we go directly to the critical condition $m = 0$ and take a zero critical temperature $T_c = 0$. We then find, after some manipulations [see Eq. (9)], that

$$\ln\frac{2}{m_0 L_{\min}} = \gamma + \mathrm{Li}_0'\big(e^{-i\pi\theta}\big) + \mathrm{Li}_0'\big(e^{i\pi\theta}\big)\,. \tag{26}$$

The minimal length is controlled by the contour parameter, and as we take lower values of θ, the value of L diminishes, see Fig. 6. It becomes zero only for $\theta^\star = 0$, the fully periodic case. We must remark that this is the same result we obtained for the bosonic case: for $D = 2$ ($\rho = 0$), we obtain the value $\theta^\star = 0$. This seems to point out a property of the formalism, independently of whether we use bosonic or fermionic models.

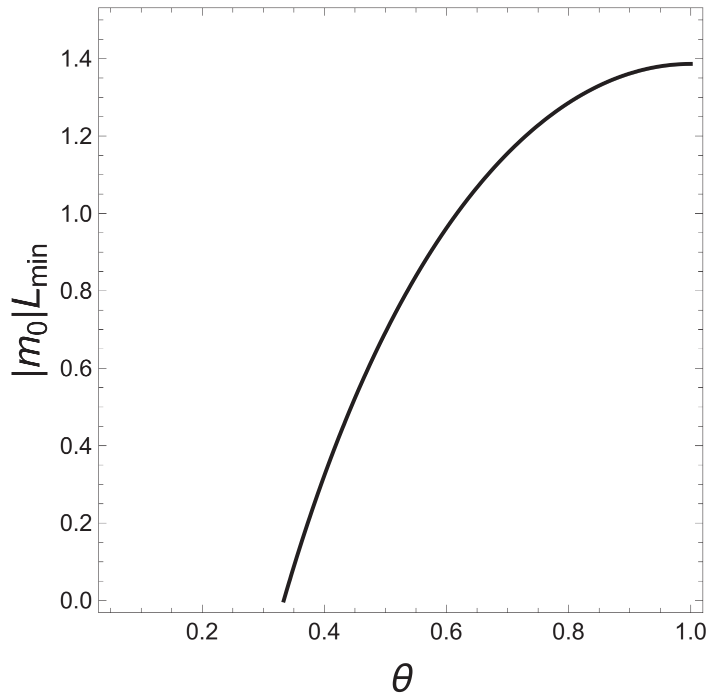

Fig. 7. Minimal length of the GN model for $D = 1 + 2$. Under the curve, the system is always in the symmetric phase.

4.2. $\mathbf{GN_{1+2}}$, *fermion on a tube*

As already stated, for $D = 3$, the GN model was shown to exist and was constructed[53] although it is not perturbatively renormalizable. Then, as a last example, we employ our mean-field nonperturbative approach to consider a fermion model on a tube ($D = 1 + 2$). The effective potential is

$$V_{\text{eff}}^{D=3} = \frac{m^2}{12\pi}(2|m| - 3|m_0|) + \sqrt{\frac{2}{\pi^3}} W_{\frac{3}{2}}[m^2; \beta, \mu, 1; L, \theta] \,. \tag{27}$$

The first derivative with respect to m exhibits two solutions: a symmetric solution corresponding to $\tilde{m} = 0$ and a broken one with $\tilde{m} \neq 0$ given by

$$|\tilde{m}| = |m_0| + \sqrt{\frac{8}{\pi}} W_{\frac{1}{2}}[\tilde{m}^2; \beta, \mu, 1; L, \theta] \,. \tag{28}$$

In the neighborhood of the symmetric case, $\tilde{m} = 0$ defines a critical temperature. As the critical temperature goes to zero, $T_c = 0$, a minimal length is defined,

$$|m_0|L_{\min} = \ln\bigl(1 - e^{i\pi\theta}\bigr) + \ln\bigl(1 - e^{-i\pi\theta}\bigr) \,. \tag{29}$$

For the antiperiodic boundary condition $\theta = 1$, we have the minimal length given by $|m_0|L_{\min}|_{a=1} = \ln 4$. Decreasing the value of the parameter θ which describes the quasiperiodic boundary condition, we find a critical contour parameter $\theta^\star = 1/3$ at which the minimal length turns out to be zero, see Fig. 7. This, again, is the same result we have obtained for the bosonic case when $D = 3$, indicating that the critical contour is only dimensional dependent.

5. Discussion

Along this paper, we have assumed a contour parameter θ defining quasiperiodic boundary conditions and studied its consequences using some bosonic and fermionic models. However, we did not take into account how these different boundary conditions arise. In fact, we have emphasized that we are dealing with a mathematical aspect of the formalism and are not directly concerned with the experimental comparison.

We propose that the contour parameter may arise as related to a constant gauge field component along the compactified dimension.[56,57] The action for a complex bosonic field minimally coupled to an external Abelian gauge field is

$$S = \int d^D x \big\{ (\partial_\mu \Phi + ieA_\mu \Phi)^\star (\partial^\mu \Phi + ieA^\mu \Phi) + m^2 \Phi^\star \Phi \big\} . \tag{30}$$

If we consider a constant gauge field only along the compactified dimension x_1 such that $A_\mu = (0, A_1, 0, \ldots, 0)$, where $A_1 = \text{const}$, we note that this contribution is given by the substitution $p_1 \to p_1 + eA_1$. Recalling the original identification that introduced the boundary parameter, see Eq. (2), we see that the relation between A_1 and θ is just

$$eA_1 = \frac{\theta\pi}{L} . \tag{31}$$

Therefore, the contour parameter can be thought of as a consequence of a constant gauge field that does not have any dependence on the Euclidean space variables. The value of A_1 allows interpolating between the perfect periodic and perfect antiperiodic conditions. Perhaps, this may be related to the well-known result that a constant gauge field generates an Aharonov–Bohm phase,[58] which induces a transmutation between fermions and bosons.[59] In another context, for which interpolation between bosons and fermions occurs in the imaginary-time variable, studies were made in which the Aharonov–Bohm phase is induced by a Chern–Simons term.[60,61] Furthermore, this topic has been the subject of a detailed study on how the relationship between the gauge field and the statistical phase emerges.[62] All these works[56,58–62] justify the introduction of the *contour parameter* θ whose consequences were studied along this paper.

It is not surprising that the contour condition (like a border effect) would influence the system even when its length is lowered to its minimal. We have exhibited, using some simple bosonic and fermionic models, that the boundary conditions directly influence the minimal length below which there is no thermally induced transition. Furthermore, there is a critical contour parameter at which the minimal length is zero.

We have found that the critical contour parameter depends only on the system dimensionality. For a bosonic system, we employ two models, one with a second-order phase transition and the other with a first-order phase transition; both show the same value for the critical parameter if the dimensions are equal. We have also tested a fermionic model and find that the parameter θ has the same value. The only difference between a bosonic and a fermionic system turns out to be that for a bosonic system, there is a minimal length for $\theta < \theta^{\star}$, while for a fermionic system, there is a minimal length for $\theta > \theta^{\star}$. The observed independence of $\theta^{\star}$ shows that there is a common substrate of models having quasiperiodic boundary conditions independent of its physical nature.

Acknowledgments

The authors thank the Brazilian agencies CAPES and CNPq for partial financial support. We also thank C. Farina for fruitful suggestions.

References

1. L. M. Abreu, A. P. C. Malbouisson, J. M. C. Malbouisson and A. E. Santana, *Phys. Rev. B* **67**, 212502 (2003).
2. L. M. Abreu, A. P. C. Malbouisson and I. Roditi, *Eur. Phys. J. B* **37**, 515 (2004).
3. C. A. Linhares, A. P. C. Malbouisson, Y. W. Milla and I. Roditi, *Phys. Rev. B* **73**, 214525 (2006).
4. C. A. Linhares, A. P. C. Malbouisson, Y. W. Milla and I. Roditi, *Eur. Phys. J. B* **60**, 353 (2007).
5. L. M. Abreu, A. P. C. Malbouisson, J. M. C. Malbouisson and A. E. Santana, *Nucl. Phys. B* **819**, 127 (2009).
6. L. M. Abreu, A. P. C. Malbouisson and J. M. C. Malbouisson, *Phys. Rev. D* **83**, 025001 (2011).
7. L. M. Abreu, A. P. C. Malbouisson and J. M. C. Malbouisson, *Phys. Rev. D* **84**, 065036 (2011).
8. C. A. Linhares, A. P. C. Malbouisson and M. L. Souza, *Eur. Phys. Lett.* **96**, 31002 (2011).
9. C. A. Linhares, A. P. C. Malbouisson, J. M. C. Malbouisson and I. Roditi, *Phys. Rev. D* **86**, 105022 (2012).
10. C. A. Linhares, A. P. C. Malbouisson and I. Roditi, *Eur. Phys. Lett.* **98**, 41001 (2012).
11. F. C. Khanna, A. P. C. Malbouisson, J. M. C. Malbouisson and A. E. Santana, *Eur. Phys. Lett.* **97**, 11002 (2012).
12. F. C. Khanna, A. P. C. Malbouisson, J. M. C. Malbouisson and A. E. Santana, *Phys. Rev. D* **85**, 085015 (2012).
13. L. M. Abreu, C. A. Linhares, A. P. C. Malbouisson and J. M. C. Malbouisson, *Phys. Rev. D* **88**, 107701 (2013).
14. E. B. S. Corrêa, C. A. Linhares and A. P. C. Malbouisson, *Phys. Lett. A* **377**, 1984 (2013).
15. F. C. Khanna, A. P. C. Malbouisson, J. M. C. Malbouisson and A. E. Santana, *Thermal Quantum Field Theory*: *Algebraic Aspects and Applications* (World Scientific, Singapore, 2009).
16. H. Boschi-Filho, C. Farina and A. de Souza Dutra, *J. Phys. A* **28**, L7 (1995).
17. S. Huang and B. Schreiber, *Nucl. Phys. B* **426**, 644 (1994).
18. W. Chen and Y. J. Ng, *Phys. Rev. B* **51**, 14479 (1995).
19. A. Khare, *Phys. Lett. A* **221**, 365 (1996).
20. A. Liguori, M. Mintchev and L. Pilo, *Nucl. Phys. B* **569**, 577 (2000).

21. A. LeClair, *J. High Energy Phys.* **2005**, 068 (2005).
22. E. Shech, *Found. Phys.* **45**, 1063 (2015).
23. A. Lerda, *Anyons — Quantum Mechanics of Particles with Fractional Statistics* (Springer-Verlag, Berlin, 1992).
24. M. Banados, T. Brotz and M. E. Ortiz, *Nucl. Phys. B* **545**, 340 (1999).
25. I. Antoniadis and C. Bachas, *Nucl. Phys. B* **298**, 586 (1988).
26. L. F. Alday, G. Arutyunov and S. Frolov, *J. High Energy Phys.* **06**, 018 (2006).
27. M. Billo, L. Ferro, M. Frau, F. Fucito, A. Lerda and J. F. Morales, *J. High Energy Phys.* **10**, 112 (2008).
28. C. Destri and H. J. De Vega, *Nucl. Phys. B* **438**, 413 (1995).
29. V. Bernard, M. Lage, U. G. Meissner and A. Rusetsky, *J. High Energy Phys.* **01**, 019 (2011).
30. C. T. Sachrajda and G. Villadoro, *Phys. Lett. B* **609**, 73 (2005).
31. UKQCD Collab. (J. M. Flynn, A. Juttner and C. T. Sachrajda), *Phys. Lett. B* **632**, 313 (2006).
32. T. Misumi and T. Kanazawa, *J. High Energy Phys.* **06**, 181 (2014).
33. V. B. Petkova and J. B. Zuber, *Phys. Lett. B* **504**, 157 (2001).
34. D. J. Toms, *Phys. Rev. D* **21**, 928 (1980).
35. A. Flachi and T. Tanaka, *Phys. Rev. D* **80**, 124022 (2009).
36. E. Elizalde, S. D. Odintsov and A. A. Saharian, *Phys. Rev. D* **87**, 084003 (2013).
37. D. Poilblanc, *Phys. Rev. B* **44**, 9562 (1991).
38. A. F. S. Ryu, C. Mudry and A. W. W. Ludwig, *Phys. Rev. B* **75**, 205344 (2007).
39. S. Bellucci, A. A. Saharian and V. M. Bardeghyan, *Phys. Rev. D* **82**, 065011 (2010).
40. T. Matsubara, *Prog. Theor. Phys.* **14**, 351 (1955).
41. N. P. Landsman and C. G. van Weert, *Phys. Rep.* **145**, 141 (1987).
42. F. C. Khanna, A. P. C. Malbouisson, J. M. C. Malbouisson and A. E. Santana, *Phys. Rep.* **539**, 135 (2014).
43. C. G. Bollini and J. J. Giambiagi, *Nuovo Cimento B* **12**, 20 (1972).
44. G. 't Hooft and M. J. G. Veltman, *Nucl. Phys. B* **44**, 189 (1972).
45. E. Elizalde, *Ten Physical Applications of Spectral Zeta Functions*, 2nd edn. (Springer-Verlag, Berlin, 2010).
46. J. M. Cornwall, R. Jackiw and E. Tomboulis, *Phys. Rev. D* **10**, 2428 (1974).
47. M. Le Bellac, *Quantum and Statistical Field Theory* (Clarendon Press, Oxford, 1991).
48. M. A. Continentino, *Quantum Scaling in Many-Body Systems* (World Scientific, Singapore, 2001).
49. D. J. Gross and A. Neveu, *Phys. Rev. D* **10**, 3235 (1974).
50. G. Parisi, *Nucl. Phys. B* **100**, 368 (1975).
51. K. Gawedzki and A. Kupiainen, *Phys. Rev. Lett.* **55**, 363 (1985).
52. K. Gawedzki and A. Kupiainen, *Nucl. Phys. B* **262**, 33 (1985).
53. C. de Calan, P. A. Faria da Veiga, J. Magnen and R. Seneor, *Phys. Rev. Lett.* **66**, 3233 (1991).
54. V. A. Miransky, *Dynamical Symmetry Breaking in Quantum Field Theories* (World Scientific, Singapore, 1993).
55. J. Zinn-Justin, *Quantum Field Theory and Critical Phenomena*, 4th edn. (Clarendon Press, Oxford, 2002).
56. P. Borges, H. Boschi-Filho and C. Farina, *Phys. Lett. B* **460**, 376 (1999).
57. C. Ccapa Ttira, C. D. Fosco, A. P. C. Malbouisson and I. Roditi, *Phys. Rev. A* **81**, 032116 (2010).
58. Y. Aharonov and D. Bohm, *Phys. Rev.* **115**, 485 (1959).

59. A. M. Polyakov, *Mod. Phys. Lett. A* **3**, 325 (1988).
60. E. H. Fradkin and F. A. Schaposnik, *Phys. Lett. B* **338**, 253 (1994).
61. G. V. Dunne, Aspects of Chern–Simons theory, in *Topological Aspects of Low-dimensional Systems*: *Proc., Les Houches Summer School of Theoretical Physics*, Session 69.
62. S. Forte, *Rev. Mod. Phys.* **64**, 193 (1992).

Chapter 3

Impact of unitarization on the J/ψ-light meson cross section

Published as:
L.M. Abreu, E. Cavalcanti, A.P.C. Malbouisson. Nuclear Physics A **978**, 107 (2018)
Impact of unitarization on the J/ψ-light meson cross section

Available online at www.sciencedirect.com

ScienceDirect

Nuclear Physics A 978 (2018) 107–122

NUCLEAR PHYSICS A

www.elsevier.com/locate/nuclphysa

Impact of unitarization on the J/ψ-light meson cross section

L.M. Abreu [a,*], E. Cavalcanti [b], A.P.C. Malbouisson [b]

[a] *Instituto de Física, Universidade Federal da Bahia, 40170-115, Salvador, BA, Brazil*
[b] *Centro Brasileiro de Pesquisas Físicas/MCTI, 22290-180, Rio de Janeiro, RJ, Brazil*

Received 2 July 2018; received in revised form 1 August 2018; accepted 1 August 2018
Available online 2 August 2018

Abstract

Hidden charm mesons continue playing an essential role as relevant probes to understand the evolution of partonic matter. It is expected that the charmonia that survived the quark-gluon plasma phase suffer collisions with other particles composing the hadronic matter. In this work, we intend to contribute on this subject by presenting an updated study about the interactions of J/ψ with surrounding hadronic medium. The meson-meson interactions are described with a $SU(4)$ effective Lagrangian, and within the framework of unitarized coupled channel amplitudes projected onto s-wave. The symmetry is explicitly broken to $SU(3)$ by suppression of the interactions driven by charmed mesons. We calculate the cross sections for J/ψ scattering by light pseudoscalar mesons (π, K, η) and vector mesons (ρ, K^*, ω), as well as their inverse processes. Keeping the validity of this present approach in the low CM energy range, the most relevant channels are evaluated and a comparison of the findings with existing literature is performed.

Keywords: Chiral Perturbation Theory; Charmonia states; Meson-meson interactions

* Corresponding author.
E-mail addresses: luciano.abreu@ufba.br (L.M. Abreu), erich@cbpf.br (E. Cavalcanti), adolfo@cbpf.br (A.P.C. Malbouisson).

https://doi.org/10.1016/j.nuclphysa.2018.08.001
0375-9474/

1. Introduction

Recent heavy-ion-collision experiments generated a prosperous era in particle and nuclear physics. Measurements that seemed hard to be performed two or three decades ago can now be done with unprecedent precision. Among them, those related to heavy-flavored hadrons have been proved to play an essential role. These states are of particular interest since they carry heavy quarks produced by hard gluons in the initial stages of collisions. Noticing that the hadronic medium is not hot enough to excite heavy-quark pairs, heavy hadrons are relevant probes to understand the evolution of partonic matter, in contrast to light hadrons, which can be yielded in the thermal medium at later stages.

In this scenario, the J/ψ reveals itself as a relevant probe of properties of quark-gluon plasma (QGP) phase produced in the collision. It relies on the suggestion done about three decades ago that this phase would screen the $c - \bar{c}$ interaction, leading to the drop of J/ψ multiplicity [1–3]. Indeed, several Collaborations have observed experimental evidences of J/ψ suppression [4–9]. However, at the highest energies reached today at the LHC, data on J/ψ production confirm that the QGP dynamics is richer and more complex. At low transverse momentum (p_T) range, the J/ψ drop is significantly smaller at LHC energy than at RHIC energy, which might be interpreted from regeneration mechanism due to larger total charm cross section at LHC; but at high p_T the dissociation increases as collision energy grows, indicating that the J/ψ yield is less sensitive to recombination and other effects [10–12].

On the other hand, alternative mechanisms have also been proposed to explain the drop of charmonium multiplicity, such as its absorption by comoving hadrons. It is worthy mentioning that between the chemical freeze-out (where the hadronization has already ended and there is a hadron gas) and the kinetical freeze-out (in which the interactions are expected to cease and the remaining particles go to the detectors), the charmonia that have survived the QGP phase are expected to collide with other particles composing the hadronic matter. Therefore, inelastic interactions of J/ψ with surrounding hadronic medium formed after QGP cooling and hadronization might have (at least partially) significance on the charmonium abundance analysis.

In this sense, a large amount of effort has been dedicated to estimate the charmonia interactions with light hadrons (mainly involving π and ρ mesons) using different approaches [13–37]. Most of these analyses explore the $J/\psi - \pi$ reactions with reasonable results, and can be classified in the following sort: interactions based on effective hadron Lagrangians [15–20,22,27,28, 34,36,37] and constituent quark-model framework [13,14,17,21,24,25,33,35].

Concerning those works involving J/ψ absorption by light hadrons (and their inverse reactions) derived from chiral Lagrangians, we believe that there is still enough room for other contributions on this issue. First, due to the fact that the charmonium-hadron cross sections are dependent of the effective couplings that control the reactions considered [15–20,22,27,28,34, 36,37]. Secondly, the majority of these mentioned calculations make use of form factors with different functional forms and cutoff values which could not be justified a priori. It should be also mentioned that appropriate choice for the form factors is essential to obtain reliable predictions, since the range of heavy meson exchange is much smaller than the sizes of the initial hadrons [22]. Third, the older calculations are deficient of the methods that have been developed subsequently, as well as lack the novel data of heavy-ion-collision experiments at RHIC and LHC, which requires a new round of updated predictions.

Thus, in the present work we will contribute on calculations about the interactions of J/ψ with surrounding hadronic medium compared to previous studies in the following way. We consider the medium composed of the lightest pseudoscalar mesons (π, K, η) and the lightest vector mesons (ρ, K^*, ω), and calculate the cross sections for $J/\psi X$ scattering and their inverse processes (in which X stands for light pseudoscalar and vector mesons), within the framework of unitarized coupled channel amplitudes projected onto s-wave [36,38–41]. We analyze the magnitude of unitarized cross sections of the different channels, and perform a comparison of our results with other reported ones.

This work is structured as follows. In Section 2 we will give an overview of the effective $SU(4)$ model and calculate the unitarized coupled channel amplitudes. Results will be presented in Section 3. We summarize the results and conclusions in Section 4. Some relevant tables are given in Appendix A.

2. Formalism

The main purpose here is the discussion of J/ψ interaction with the hadronic medium. We intend to calculate and analyze the cross sections for the $J/\psi - X$ interactions, where X denotes a pseudoscalar or vector meson. On that subject, we work within the framework of effective field theories whose hadrons are the relevant degrees of freedom. The effective Lagrangian used in the present study is based on $SU(4)$ lowest order Chiral Perturbation Theory [36,38,39],

$$\mathcal{L}_{\text{int}} = -\frac{1}{4f^2}\text{Tr}\left(J^\mu \mathcal{J}_\mu\right) - \frac{1}{4f^2}\text{Tr}\left(\mathcal{J}^\mu \mathcal{J}_\mu\right), \tag{1}$$

where $Tr(...)$ denotes the trace over flavor indices, $J^\mu = [P, \partial^\mu P]$ and $\mathcal{J}^\mu = [V^\nu, \partial^\mu V_\nu]$ are the pseudoscalar and vector currents, respectively, with P and V being 4×4 matrices carrying 15-plets of pseudoscalar and vector fields as show below in an unmixed representation,

$$\begin{aligned}
P &= \sum_{i=1}^{15} \frac{\varphi_i}{\sqrt{2}}\lambda_i = \\
&\begin{pmatrix}
\frac{\pi^0}{\sqrt{2}} + \frac{\eta}{\sqrt{6}} + \frac{\eta_c}{\sqrt{12}} & \pi^+ & K^+ & \bar{D}^0 \\
\pi^- & -\frac{\pi^0}{\sqrt{2}} + \frac{\eta}{\sqrt{6}} + \frac{\eta_c}{\sqrt{12}} & K^0 & D^- \\
K^- & \bar{K}^0 & -2\frac{\eta}{\sqrt{6}} + \frac{\eta_c}{\sqrt{12}} & D_s^- \\
D^0 & D^+ & D_s^+ & -\frac{\sqrt{3}}{2}\eta_c
\end{pmatrix}; \\
V_\mu &= \sum_{i=1}^{15} \frac{v_{\nu i}}{\sqrt{2}}\lambda_i = \\
&\begin{pmatrix}
\frac{\rho^0}{\sqrt{2}} + \frac{\omega}{\sqrt{6}} + \frac{J/\psi}{\sqrt{12}} & \rho^+ & K^{*+} & \bar{D}^{*0} \\
\rho^- & -\frac{\rho^0}{\sqrt{2}} + \frac{\omega}{\sqrt{6}} + \frac{J/\psi}{\sqrt{12}} & K^{*0} & D^{*-} \\
K^{*-} & \bar{K}^{*0} & -2\frac{\omega}{\sqrt{6}} + \frac{J/\psi}{\sqrt{12}} & D_s^{*-} \\
D^{*0} & D^{*+} & D_s^{*+} & -\frac{\sqrt{3}}{2}J/\psi
\end{pmatrix}_\mu ;
\end{aligned} \tag{2}$$

λ_a being the Gell-Mann matrices for $SU(4)$. The parameter f is the meson decay constant, which is the pion decay constant in the usual $SU(3)$ symmetry. But here f^2 which will appear in the amplitudes must be replaced by $\sqrt{f}$ for each meson leg in the corresponding vertex, with $\sqrt{f_\pi}$ for light mesons and $\sqrt{f_D}$ for heavy ones.

The couplings given by the effective Lagrangian in Eq. (1) allows us to obtain the scattering amplitudes for the following $J/\psi X$ absorption processes:

$$\begin{aligned}
&(1)\ \ J/\psi(p_1)P(p_2) \to V(p_3)P(p_4),\\
&(2)\ \ J/\psi(p_1)V(p_2) \to P(p_3)P(p_4),\\
&(3)\ \ J/\psi(p_1)V(p_2) \to V(p_3)V(p_4),
\end{aligned} \tag{3}$$

where P and V in the initial and final states stand for pseudoscalar and vector mesons, and p_j denotes the momentum of particle j, with particles 1 and 2 standing for initial state mesons, and particles 3 and 4 for final state mesons.

Thus, the invariant amplitudes engendered by effective Lagrangian in Eq. (1) for processes of type $VP \to VP$ in Eq. (3) are given by

$$\mathcal{M}_{1;ij}(s,t,u) = \frac{\xi_{ij}}{2f^2}(s-u)\varepsilon_1 \cdot \varepsilon_3^*, \tag{4}$$

for processes $VV \to PP$ they are

$$\mathcal{M}_{2;ij}(s,t,u) = \frac{\chi_{ij}}{2f^2}(t-u)\varepsilon_1 \cdot \varepsilon_2, \tag{5}$$

and finally for processes $VV \to VV$,

$$\begin{aligned}
\mathcal{M}_{3;ij}(s,t,u) = &\frac{\zeta_{ij}^{(s)}}{f^2}(t-u)\varepsilon_1 \cdot \varepsilon_2\varepsilon_3^* \cdot \varepsilon_4^* \\
&+\frac{\zeta_{ij}^{(t)}}{f^2}(s-u)\varepsilon_1 \cdot \varepsilon_3^*\varepsilon_2 \cdot \varepsilon_4^* \\
&+\frac{\zeta_{ij}^{(u)}}{f^2}(s-t)\varepsilon_1 \cdot \varepsilon_4^*\varepsilon_2 \cdot \varepsilon_3^*,
\end{aligned} \tag{6}$$

where the labels i and j refer to the initial and final channels; s, t and u to the Mandelstam variables; ε_a to the polarization vector related to the respective vector particle a. The coefficients ξ_{ij}, χ_{ij} and ζ_{ij} will depend on the initial and final channels of each process, and are given in Appendix A in an isospin basis.

The processes above are assumed to have conservation of the quantum numbers for the incoming and outcoming meson pairs; they are $I^G(J^{PC})$, charm (C) and strangeness (S). Therefore, relating to s-wave reactions, we deal with the channels involving pairs of vector mesons in Eq. (6) by making use of spin-projectors that distinguish the allowed values of spin [38,42]. Explicitly, suppose a given generic amplitude,

$$\begin{aligned}
\mathcal{A} = &\alpha\, \varepsilon_1 \cdot \varepsilon_2\varepsilon_3^* \cdot \varepsilon_4^* + \beta\, \varepsilon_1 \cdot \varepsilon_3^*\varepsilon_2 \cdot \varepsilon_4^* \\
&+\gamma\, \varepsilon_1 \cdot \varepsilon_4^*\varepsilon_2 \cdot \varepsilon_3^*.
\end{aligned} \tag{7}$$

We can decompose the polarization vectors of each incoming/outgoing pair of vector mesons into the following representations: scalar ($S=0$), antisymmetric tensor ($S=1$) and symmetric tensor ($S=2$), namely

$$\varepsilon_a^i\varepsilon_b^j = \mathcal{P}_{ab}^{(S=0)ij} + \mathcal{P}_{ab}^{(S=1)ij} + \mathcal{P}_{ab}^{(S=2)ij} \tag{8}$$

where

$$\mathcal{P}_{ab}^{(S=0)ij} = \frac{\delta^{ij}}{3}\varepsilon_a^k\varepsilon_b^k,$$
$$\mathcal{P}_{ab}^{(S=1)ij} = \frac{1}{2}\left(\varepsilon_a^i\varepsilon_b^j - \varepsilon_a^j\varepsilon_b^i\right)$$
$$\mathcal{P}_{ab}^{(S=2)ij} = \frac{1}{2}\left(\varepsilon_a^i\varepsilon_b^j + \varepsilon_a^j\varepsilon_b^i\right) - \frac{\delta^{ij}}{3}\varepsilon_a^k\varepsilon_b^k. \tag{9}$$

Then, using this decomposition in Eq. (7), the generic amplitude can be written as

$$\mathcal{A} = (3\alpha+\beta+\gamma)\mathcal{A}^{(S=0)} + (\beta-\gamma)\mathcal{A}^{(S=1)} + (\beta+\gamma)\mathcal{A}^{(S=2)}, \tag{10}$$

where

$$\mathcal{A}^{(S=0)} \equiv \mathcal{P}_{ab}^{(S=0)ii}\mathcal{P}_{cd}^{(S=0)jj},$$
$$\mathcal{A}^{(S=1)} \equiv \mathcal{P}_{ab}^{(S=1)ij}\mathcal{P}_{cd}^{(S=1)ij},$$
$$\mathcal{A}^{(S=2)} \equiv \mathcal{P}_{ab}^{(S=2)ij}\mathcal{P}_{cd}^{(S=2)ij}. \tag{11}$$

Hence, the coefficients in the amplitude depends on the total angular momentum. We also remark that for $VV \to PP$ reactions in Eq. (5), the only relevant contribution comes from $\mathcal{P}_{ab}^{(S=0)}$.

In order to have the correct behavior of the amplitudes at high energies, we need to implement a control procedure of the energy-dependence of cross sections. As mentioned before, most calculations found in literature for some reactions of our interest make use of form factors with different functional forms and cutoff values which could not be justified a priori [15–20,22,27,28,34,36,37].

We adopt another scheme in the present approach: we work within the framework of unitarized coupled channel amplitudes. It ensures the validity of the optical theorem and enhances the range of applicability of the effective model controlling the behavior of the amplitudes at large energies, and has properly described hadronic resonances and meson-meson scattering [36,38–41,43–46].

The matrix representing unitarized coupled channel transitions can be derived by a Bethe–Salpeter equation whose kernel is the s-wave projection of a given amplitude by Eqs. (4), (5) or (6), and can be diagrammatically viewed as the sum over processes showed in Fig. 1. In this way, the unitarized amplitude reads [36,38–41,43–46],

$$\mathcal{T}(s) = \frac{V(s)}{1+V(s)G(s)}, \tag{12}$$

where $V(s)$ is the s-wave projected scattering amplitude,

$$V_{r;ij}(s) = \frac{1}{2}\int_{-1}^{1} d(\cos\theta)\mathcal{M}_{r;ij}\left(s, t(s,\cos\theta), u(s,\cos\theta)\right), \tag{13}$$

with $r = 1, 2, 3$, and $G(s)$ stands for the two-meson loop integral. In the case of two pseudoscalars mesons (PP), $G_{PP}(s)$ is given by

$$G_{PP}(s) = i\int \frac{d^4q}{(2\pi)^4}\frac{1}{\left(q^2-m_1^2+i\epsilon\right)\left[(P-q)^2-m_2^2+i\epsilon\right]}. \tag{14}$$

$P^2 = s$ and m_1 and m_2 are pseudoscalar mesons masses. Employing dimensional regularization, this integral is rewritten as

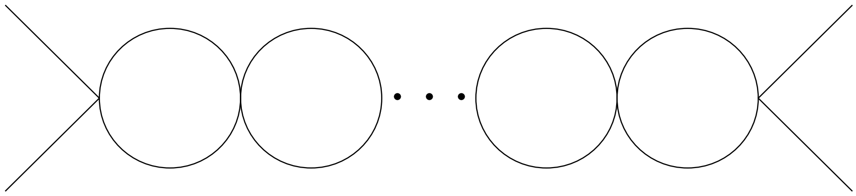

Fig. 1. Feynman Diagrams representing the Bethe–Salpeter equation for the scattering amplitudes. Each loop denotes a two-meson loop integral G.

$$
\begin{aligned}
G_{PP}(s) = \frac{1}{16\pi^2}\Bigg\{ & a(\mu) + \ln\frac{m_1^2}{\mu^2} + \frac{m_2^2 - m_1^2 + s}{2s}\ln\frac{m_2^2}{m_1^2} \\
& + \frac{p}{\sqrt{s}}\Big[\ln(s - (m_1^2 - m_2^2) + 2p\sqrt{s}) \\
& + \ln(s + (m_1^2 - m_2^2) + 2p\sqrt{s}) \\
& - \ln(s - (m_1^2 - m_2^2) - 2p\sqrt{s}) \\
& - \ln(s + (m_1^2 - m_2^2) - 2p\sqrt{s}) - 2\pi i\Big]\Bigg\} ,
\end{aligned}
\tag{15}
$$

where μ is the regularization energy scale, $a(\mu)$ is a subtraction constant which absorbs the scale dependence of the integral, and p is the three-momentum in the center of mass frame of the two mesons in channel PP,

$$
p = \frac{1}{2\sqrt{s}}\sqrt{\left[s - (m_1 + m_2)^2\right]\left[s - (m_1 - m_2)^2\right]}. \tag{16}
$$

When the two-meson loop integral involves a pseudoscalar and a vector meson (PV) and two vector mesons (VV), we perform standard approximation as in previous studies [38,39], resulting in the expressions

$$
\begin{aligned}
G_{VP}(s) &= \left(1 + \frac{p^2}{3M_1^2}\right) G_{PP}(s), \\
G_{VV}(s) &= \left(1 + \frac{p^2}{3M_1^2}\right)\left(1 + \frac{p^2}{3M_2^2}\right) G_{PP}(s),
\end{aligned}
\tag{17}
$$

where M_1 and M_2 represent the masses of vector mesons in the loop. Notice that the masses in $G_{PP}(s)$ that appear in Eq. (17) must be replaced by the masses of the mesons in the loop according to each case.

Once the unitarized transition amplitudes are obtained, we can determine the isospin-spin-averaged cross section for the processes in Eq. (3), which in the center of mass (CM) frame is defined as

$$
\sigma(s) = \frac{\chi}{32\pi s}\overline{\sum_{\text{Isospin}}}\left|\frac{p_f}{p_i}\right| |\mathcal{T}(s)|^2, \tag{18}
$$

where p_f and p_i are, respectively the momentum of the outcoming and incoming particles in the CM frame; χ is a constant whose value depends on the total angular momentum of the channel considered:

Table 1
Channel content in each sector. It is shown only relevant channels for S-wave processes.

$\mathbf{I^G(J^{PC})}$	$\mathbf{C = S = 0}$
$0^+(0^{++}), 0^-(1^{+-})$	$J/\psi J/\psi, \omega J/\psi, \omega\omega, \rho\rho, D_s^*\bar{D}_s^*$
$0^+(2^{++})$	
$0^-(1^{+-})$	$\pi\rho, \eta\omega, \eta J/\psi, \eta_c\omega, K\bar{K}^* - c.c.,$
	$\eta_c J/\psi, D\bar{D}^* - c.c., D_s\bar{D}_s^* + c.c.$
$1^-(0^{++})$	$\rho\omega, K^*\bar{K}^*, \eta\pi, \bar{K}K$
	$\rho J/\psi, D^*\bar{D}^*, \eta_c\pi, \bar{D}D$
$1^+(1^{+-}), 1^-(2^{++})$	$\rho J/\psi, \rho\omega, K^*\bar{K}^*, D^*\bar{D}^*$
$1^+(1^{+-})$	$\pi\omega, \eta\rho, K\bar{K}^* + c.c.$
	$\pi J/\psi, \eta_c\rho, D\bar{D}^* + c.c.$

$\mathbf{I^G(J^{PC})}$	$\mathbf{C = 0, S = 1}$
$\frac{1}{2}(0^+)$	$K\eta, K\pi, K^*\omega, K^*\rho$
	$K\eta_c, D_s\bar{D}, K^*J/\psi, D_s^*\bar{D}^*$
$\frac{1}{2}(1^+), \frac{1}{2}(2^+)$	$K^*J/\psi, K^*\omega,$
	$K^*\rho, D_s^*\bar{D}^*$
$\frac{1}{2}(1^+)$	$\pi K^*, \eta K^*, K\rho, K\omega$
	$\eta_c K^*, J/\psi K, \bar{D}D_s^*, \bar{D}^*D_s$

$$
\begin{aligned}
\chi &= 2 \qquad (PP \to PP, VP \to VP) \\
\chi &= 6 \qquad (PP \to VV) \\
\chi &= 2/3 \qquad (VV \to PP) \\
\chi &= 2/9 \qquad (VV \to VV; S = 0) \\
\chi &= 2/3 \qquad (VV \to VV; S = 1) \\
\chi &= 10/9 \qquad (VV \to VV; S = 2).
\end{aligned}
$$

Next, we use the formalism developed above to compute the cross sections of reactions involving charmonium.

3. Results

Now we are able to calculate the cross sections for elastic and inelastic J/ψ scattering by pseudoscalar and vector mesons using the framework of unitarized coupled channel amplitudes obtained in previous section. In particular, the channels considered are the $J/\psi X$, with X being the mesons associated to the fields introduced in the P and V matrices in Eq. (2), i.e. the $\pi, K, \eta, \rho, K^*, \omega$ mesons. In this context, we use an enlarged coupled channel basis by taking into account the quantum numbers $I^G(J^{PC})$, charm (C) and strangeness (S) of each channel. Thus, remembering that in present work our interest is only on s-wave processes, in Table 1 it is displayed the channel content in each sector, determined by analyzing the meson pairs with same quantum numbers and with possible transitions among them. Accordingly, the decomposition of these channels involving light and heavy mesons allows us to obtain the coefficients ξ_{ij}, χ_{ij} and ζ_{ij} given in Eqs. (4)–(6); they are given in Appendix A in an isospin basis.

We have employed in the computations of the present work the following values for the masses: $m_\pi = 138$ MeV, $m_\rho = 771$ MeV, $m_K = 495$ MeV, $m_\eta = 548$ MeV, $m_\omega = 782$ MeV,

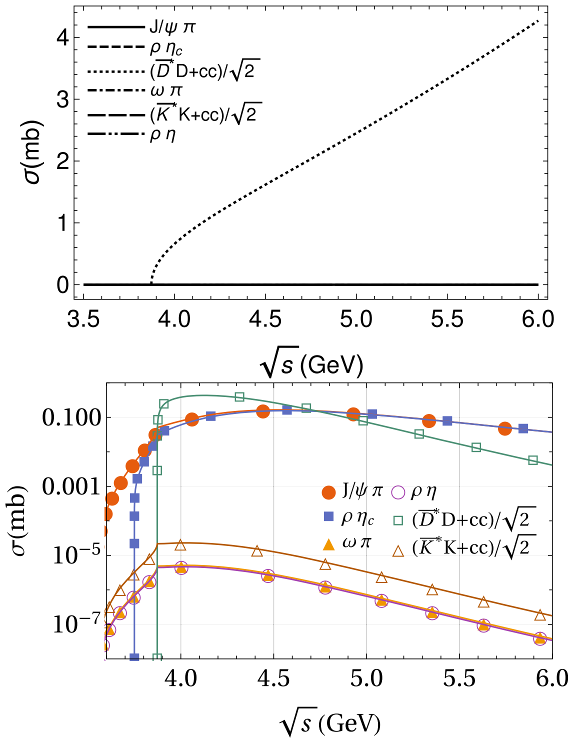

Fig. 2. Cross sections for $J/\psi\pi$ scattering into allowed final states as a function of the CM energy $\sqrt{s}$. Top panel: use of tree-level amplitudes. Bottom panel: use of unitary amplitudes.

$m_{K^*} = 892$ MeV, $m_D = 1865$ MeV, $m_{D^*} = 2008$ MeV, $m_{D_s} = 1968$ MeV, $m_{D_s^*} = 2008$ MeV, $m_{\eta_c} = 2979$ MeV, $m_{J/\psi} = 3097$ MeV, $m_L = 800$ MeV, $m_H = 2050$ MeV and $m'_H = 3000$ MeV; for the decay constants: $f_\pi = 93$ MeV and $f_D = 165$ MeV. We have fixed the free parameters in the loop function, Eq. (15), as in Ref. [39]: setting the scale μ to 1.5 GeV, the subtraction constant is adjusted to data taking $a_H(\mu) = -1.55$ for channels involving at least one heavy meson, and $a_L(\mu) = -0.8$ for channels involving only light mesons.

In what follows we present and discuss the cross sections for the J/ψ-meson interactions regarding the channel content in each sector, as reproduced Table 1. We start by showing in Fig. 2 the most investigated scattering in literature: the cross sections for $J/\psi\pi$ scattering into allowed final states. Particularly, beyond the reactions $J/\psi\pi \to J/\psi\pi, \rho\eta_c, (D\bar{D}^* + c.c.)$, which are also present in Ref. [36], we examine $J/\psi\pi \to \omega\pi, \rho\eta, (\bar{K}^* K + c.c.)$ as well. Some remarks are worthy of mention when compare them. First, we must take care of the validity of the present treatment: it is valid at low-energy range, since it is employed the lowest order Lagrangian filtered out projecting it onto s-wave. Keeping this in mind, we see that at three level only the reaction with final state $(D\bar{D}^* + c.c.)$ has non-zero cross section. Once the amplitude is unitarized, the meson loops engender non-vanishing cross sections for all reactions, with an universal behavior: they have a peak shortly after the respective threshold, and decrease rapidly or slowly as energy increases, depending on the reaction. In addition, it can be observed that the most relevant processes are those whose final state carries charmed quarks. The contributions with final states $J/\psi\pi, \rho\eta_c, (\bar{D}^* D + c.c.)$ can be regarded as approximately with the same order of magnitude in the energy range under consideration. On the other hand, they are greater than cross sections for $J/\psi\pi \to \omega\pi, \rho\eta, (\bar{K}^* K + c.c.)$ by about a factor 10^5, which justifies the neglect of these last reactions for practical purposes.

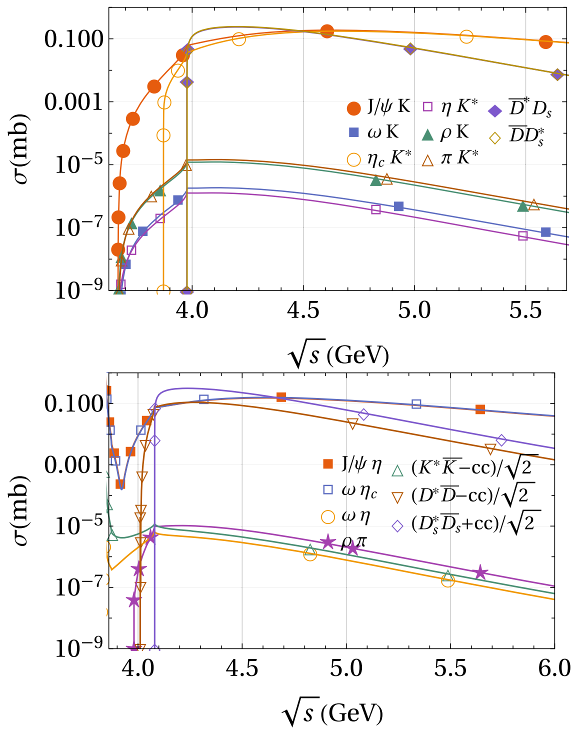

Fig. 3. Unitarized cross sections for $J/\psi K$ (top panel) and $J/\psi\eta$ (bottom panel) scatterings into allowed final states as a function of the CM energy $\sqrt{s}$.

Another point we would like to observe is on the comparison of our results with existing literature. In general, the cross section we have obtained for $J/\psi\pi \to (D\bar{D}^* + c.c.)$ reaction has a comparable or smaller magnitude at low CM energies than other ones [13–37]. As CM energy grows, the high-energy behavior of the presented findings show a more pronounced decrease of magnitude of cross section than those with any kind of control of high-energy behavior. Possible discrepancies can be attributed to the different energy dependence of the adopted formalism describing the interactions; contributions of higher partial waves; distinct approach employed to control the high-energy behavior, as in the cases of form-factors; and differing values of coupling constants, masses, cutoffs, ... Notwithstanding, it is worthy noticing that a faster decreasing for higher CM energies qualitatively similar to our findings in Ref. [22], which makes use of covariant form-factors.

For completeness, In Figs. 3 and 4 are also plotted the unitarized cross sections for $J/\psi X$ scatterings into allowed final states, with X being the pseudoscalar and vector mesons K, η, ρ, K^*, ω. In view of these results, we remark the points below:

- At tree level, before unitarization procedure, only reactions with open charmed mesons in final states (i.e. $J/\psi X \to \bar{D}^{(*)}_{(s)} D^{(*)}_{(s)} + c.c.$) have non-vanishing cross sections, with an uncontrolled behavior with energy.
- The unitarized coupled channel amplitudes via the meson loops generate non-vanishing and controlled cross sections, with a peak shortly after the threshold and a decrease with increasing energy.
- In general, reactions with charmed final state are the most relevant contributions for the cross sections, while the other ones have a very small magnitude and are highly suppressed as

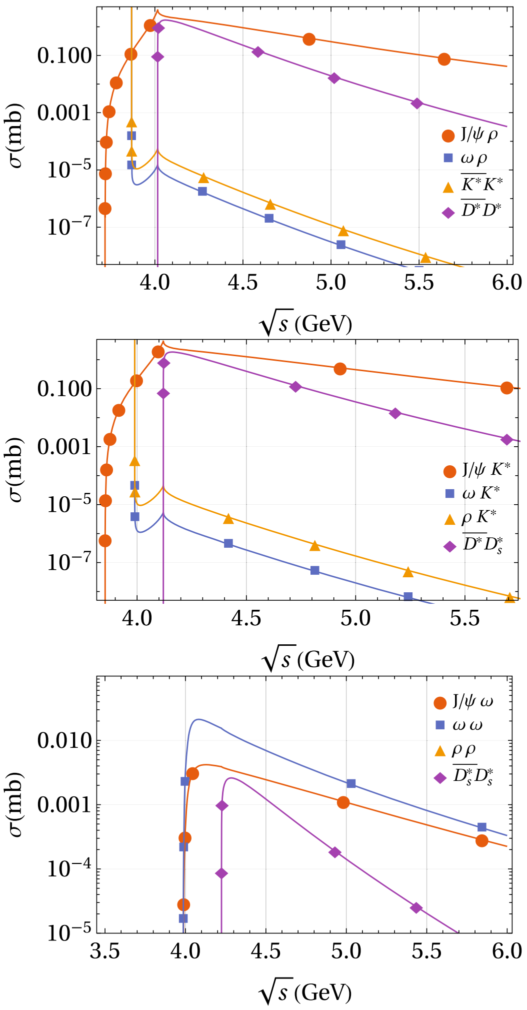

Fig. 4. Unitarized cross sections for $J/\psi\rho$ (top panel), $J/\psi K^*$ (center panel), and $J/\psi\omega$ (bottom panel) scatterings into allowed final states as a function of the CM energy $\sqrt{s}$.

energy increases. Precisely, most relevant processes are the elastic ones, $J/\psi X \to J/\psi X$, as well as the inelastic ones with η_c and open charmed mesons in final states ($(J/\psi X \to \eta_c Y)$ and $J/\psi X \leftrightarrow \bar{D}^{(*)}_{(s)} D^{(*)}_{(s)} + c.c.$).

- In the case of $J/\psi\omega$ scattering the final state $\rho\rho$ does not appear in the plot, since it is vanishing. The reason is due to the fact that meson loops do not generate allowed combinations for this channel.
- In the plots of the cross sections for J/ψ scattering by vector mesons, we have considered the sum of the situations with different spin contributions ($J = 0, 1, 2$). However, we have restricted ourselves to the $VV \to VV$ processes, because of the negligible contributions of $VV \to PP$ ones (see comment below). In this sense, we have not taken into account these latter channels both in the mesonic loops and in the final states.
- We have employed the lowest order Lagrangian in chiral expansion, with their contributions projected onto s-wave. In this sense, higher partial waves would dominate the cross section at greater CM energies above threshold, which would modify the faster decreasing of cross sections.

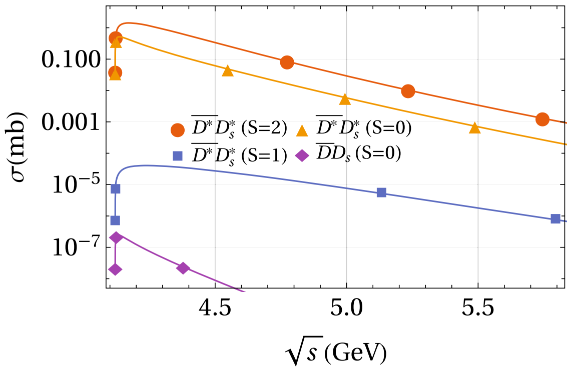

Fig. 5. Cross section of J/ψ scattering by the vector meson K^* using the unitarized coupled channel approach. It is shown only final states with open charmed mesons. For $\bar{D}^* D^*$ there are three combinations of total spin that are exhibited.

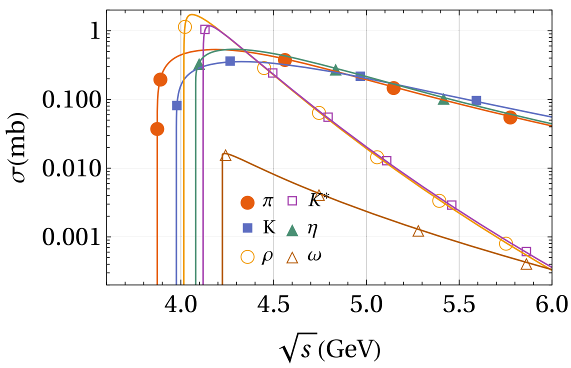

Fig. 6. Cross-sections as function of center-of-mass energy $\sqrt{s}$ for $J/\psi X$ scattering into all allowed final states; X denotes π, K, η, ρ, K^*, ω mesons.

Furthermore, we should add some comments concerning the large suppression of magnitude for the processes $VV \to PP$. Due to the nature of this interaction, the only way to obtain one reaction of this type is through s-channel in Eq. (6), which is proportional to the term $(t-u)$. In particular, if the s-channel is zero, as for the $J/\psi\omega$ scattering, $VV \to PP$ reactions are forbidden. Nevertheless, the $J/\psi\rho$ and $J/\psi K^*$ scatterings have not all s-channels being null. Notwithstanding, notice that at s-wave, $(t-u)$ is $(m_1^2 - m_2^2)(m_1'^2 - m_2'^2)$, where m_i are the masses of the incoming particles and m_i' the masses of the outgoing particles. Consequently, when the incoming or outgoing particles have close masses, the s-channel becomes highly suppressed. This effect can be illustrated from the cross sections of the reaction $J/\psi K^*$ taking as final states open charmed mesons, as shown in Fig. 5. As it can be seen, the contribution of reaction with final state being $(\bar{D}D_{(s)} + c.c.)$ is largely suppressed with respect to the other ones. This result is relatively reproduced in the findings of Ref. [37], in which the processes $\sigma(J/\psi K^* \to \bar{D}^* D_s^* + c.c.)$ and $\sigma(J/\psi K^* \to \bar{D}D_s + c.c.)$ have cross sections with amplitudes that differ by about a factor 10^2.

We summarize the results above by estimating the cross sections for the J/ψ with each meson resulting in all possible channels; they are plotted in Fig. 6. It is clear that the cross sections involving pseudoscalars $J/\psi P \to$ All (where *All* means the coupled channels to each of the initial state according to Table 1) have magnitudes larger than those with vector mesons ($J/\psi V \to$ All).

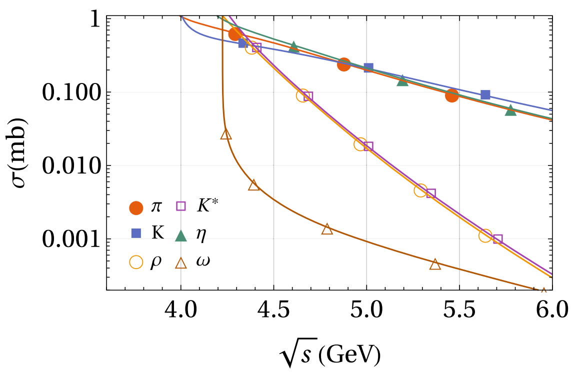

Fig. 7. Cross-sections as function of center-of-mass energy $\sqrt{s}$ for inverse reactions discussed in Fig. 6.

This result is qualitatively in accordance with Ref. [37] as well as other works, always taking care of the validity of the present approach.

Finally, in Fig. 7 is shown the cross sections for inverse reactions discussed in Fig. 6, i.e. All $\to J/\psi X$. We notice that the cross sections for direct and inverse processes can be considered to be approximately of the same order of magnitude: they are between 0.1 and 1 mbarn in the range 4 GeV $< \sqrt{s} <$ 5 GeV, and are suppressed at high energies.

Hence, the findings reported above allow us to evaluate the most relevant interactions between the J/ψ resonance and the hadronic medium composed of the lightest mesons, and will be useful for the determination of evolution of J/ψ abundance in high energy collisions, even as for correspondence among other procedures.

4. Concluding remarks

In this work we have evaluated the interactions of J/ψ with surrounding hadronic medium. We have considered the medium composed of light pseudoscalar mesons (π, K, η) and vector mesons (ρ, K^*, ω), and calculated the cross sections for J/ψ scattering by light mesons, as well as their inverse processes. Within the framework of unitarized coupled channel amplitudes, we have analyzed the magnitude of unitarized cross sections of the different channels, and performed a comparison of our results with existing literature.

The employment of unitarized coupled channel amplitudes via the meson loops have generated non-vanishing and controlled cross sections, including reactions without open charmed mesons in final states which have zero-amplitudes at tree level. Also, from the results it can be inferred that reactions with charmed final state are the most relevant contributions for the cross sections, while the other ones have a very small magnitude and are highly suppressed as energy increases. Another feature is the negligible contribution of $VV \to PP$ processes both in the mesonic loops and in the final states.

Moreover, concerning the estimates of the cross sections for the J/ψ with each meson resulting in all possible channels, they suggest that the scattering $J/\psi P \to$ All have magnitudes larger than those with vector mesons ($J/\psi V \to$ All) in the most range of center-of-mass energy $\sqrt{s}$.

It is relevant to notice the limitations of the present treatment. Since it has been employed the lowest-order Lagrangian in chiral expansion, with their contributions projected onto s-wave, therefore in principle the investigation of low-energy range near threshold is valid, despite there are outcomes reported in literature whose higher-energy behavior is qualitatively similar to ours.

Further work is needed to improve these results, in order to perform more precise comparison with predictions made by other phenomenological models. In particular, the analysis of higher partial waves would modify the decreasing of cross sections at greater energies, and will be useful in the determination of evolution of J/ψ abundance in high energy collisions.

Acknowledgements

We are grateful to F. S. Navarra and M. Nielsen for reading our manuscript and for fruitful discussions. The authors thank CNPq (Brazilian Agency) for financial support. L.M.A. would like to thank the funding agencies CNPq (contracts 308088/2017-4 and 400546/2016-7) and FAPESB (contract INT0007/2016) for financial support.

Appendix A. ξ_{ij}, χ_{ij} and ζ_{ij} coefficients

The decomposition of the channels involving light and heavy mesons allows us to obtain the coefficients ξ_{ij}, χ_{ij} and ζ_{ij} given in Eqs. (4)–(6). Here we summarize the values that they must assume with the choice of a proper isospin basis, and according to the type of mesons involved in relevant channels ($VP \to VP$, $VV \to PP$, and $VV \to VV$). Here, we denote

$$\gamma = \left(\frac{m_L}{m_H}\right)^2,$$

$$\psi = -\frac{1}{3} + \frac{4}{3}\left(\frac{m_L}{m'_H}\right)^2, \tag{A.1}$$

where the values of these quantities are given in Section 3.

A.1. $VP \to VP$ $(S = 1)$

The non-vanishing $VP \to VP$ scatterings in Eq. (4) are only s-wave processes. The coefficients ξ_{ij} are shown in the tables below.

$\mathbf{C = S = 0, I^G(J^{PC}) = 0^-(1^{+-})}$								
Channel	$J/\psi\eta_c$	$J/\psi\eta$	$\omega\eta_c$	$\omega\eta$	$\rho\pi$	$\bar{K}^*K - c.c.$	$\bar{D}^*D - c.c.$	$\bar{D}_s^*D_s + c.c.$
$J/\psi\eta_c$	0	0	0	0	0	0	$\frac{4\gamma}{3}$	$\frac{\sqrt{8}\gamma}{3}$
$J/\psi\eta$	0	0	0	0	0	0	$\frac{\sqrt{2}\gamma}{3}$	$\frac{-2\gamma}{3}$
$\omega\eta_c$	0	0	0	0	0	0	$\frac{\sqrt{2}\gamma}{3}$	$\frac{-2\gamma}{3}$
$\omega\eta$	0	0	0	0	0	$\frac{-3}{2}$	$\frac{\gamma}{6}$	$\frac{\sqrt{2}\gamma}{3}$
$\rho\pi$	0	0	0	0	2	$\frac{\sqrt{3}}{2}$	$\frac{-\sqrt{3}\gamma}{2}$	0
$\bar{K}^*K - c.c.$	0	0	0	$\frac{-3}{2}$	$\frac{\sqrt{3}}{2}$	$\frac{3}{2}$	$\frac{-\gamma}{2}$	$\frac{-\gamma}{\sqrt{2}}$
$\bar{D}^*D - c.c.$	$\frac{4\gamma}{3}$	$\frac{\sqrt{2}\gamma}{3}$	$\frac{\sqrt{2}\gamma}{3}$	$\frac{\gamma}{6}$	$\frac{-\sqrt{3}\gamma}{2}$	$\frac{-\gamma}{2}$	$\frac{(\psi+2)}{2}$	$\frac{1}{\sqrt{2}}$
$\bar{D}_s^*D_s + c.c.$	$\frac{\sqrt{8}\gamma}{3}$	$\frac{-2\gamma}{3}$	$\frac{-2\gamma}{3}$	$\frac{\sqrt{2}\gamma}{3}$	0	$\frac{-\gamma}{\sqrt{2}}$	$\frac{1}{\sqrt{2}}$	$\frac{(\psi+1)}{2}$

$\mathbf{C=S=0, I^G(J^{PC})=1^+(1^{+-})}$						
Channels	$J/\psi\pi$	$\omega\pi$	$\rho\eta_c$	$\rho\eta$	$\bar{K}^*K+c.c.$	$\bar{D}^*D+c.c.$
$J/\psi\pi$	0	0	0	0	0	$-\sqrt{\frac{2}{3}}\gamma$
$\omega\pi$	0	0	0	0	$-\frac{\sqrt{3}}{2}$	$-\frac{\gamma}{2\sqrt{3}}$
$\rho\eta_c$	0	0	0	0	0	$-\sqrt{\frac{2}{3}}\gamma$
$\rho\eta$	0	0	0	0	$-\frac{\sqrt{3}}{2}$	$-\frac{\gamma}{2\sqrt{3}}$
$\bar{K}^*K+c.c.$	0	$-\frac{\sqrt{3}}{2}$	0	$-\frac{\sqrt{3}}{2}$	$\frac{1}{2}$	$\frac{\gamma}{2}$
$\bar{D}^*D+c.c.$	$-\sqrt{\frac{2}{3}}\gamma$	$-\frac{\gamma}{2\sqrt{3}}$	$-\sqrt{\frac{2}{3}}\gamma$	$-\frac{\gamma}{2\sqrt{3}}$	$\frac{\gamma}{2}$	$\frac{\psi}{2}$

$\mathbf{C=0, S=1, I^G(J^{PC})=1/2(1^+)}$								
Channels	$J/\psi K$	ωK	$K^*\eta_c$	$K^*\eta$	ρK	$K^*\pi$	$\bar{D}^*D_s$	$\bar{D}D_s^*$
$J/\psi K$	0	0	0	0	0	0	$\frac{\gamma}{\sqrt{3}}$	$\frac{\gamma}{\sqrt{3}}$
ωK	0	0	0	$-\frac{3}{4}$	0	$\frac{3}{4}$	$\frac{\gamma}{2\sqrt{6}}$	$\frac{-\gamma}{\sqrt{6}}$
$K^*\eta_c$	0	0	0	0	0	0	$\frac{\gamma}{\sqrt{3}}$	$\frac{\gamma}{\sqrt{3}}$
$K^*\eta$	0	$\frac{-3}{4}$	0	0	$\frac{3}{4}$	0	$\frac{-\gamma}{\sqrt{6}}$	$\frac{\gamma}{2\sqrt{6}}$
ρK	0	0	0	$\frac{3}{4}$	1	$\frac{1}{4}$	$\frac{-\sqrt{3}\gamma}{\sqrt{8}}$	0
$K^*\pi$	0	$\frac{3}{4}$	0	0	$\frac{1}{4}$	1	0	$\frac{-\sqrt{3}\gamma}{\sqrt{8}}$
$\bar{D}^*D_s$	$\frac{\gamma}{\sqrt{3}}$	$\frac{\gamma}{2\sqrt{6}}$	$\frac{\gamma}{\sqrt{3}}$	$\frac{-\gamma}{\sqrt{6}}$	$\frac{-\sqrt{3}\gamma}{\sqrt{8}}$	0	$\frac{\psi}{2}$	0
$\bar{D}D_s^*$	$\frac{\gamma}{\sqrt{3}}$	$\frac{-\gamma}{\sqrt{6}}$	$\frac{\gamma}{\sqrt{3}}$	$\frac{\gamma}{2\sqrt{6}}$	0	$\frac{-\sqrt{3}\gamma}{\sqrt{8}}$	0	$\frac{\psi}{2}$

A.2. $VV \to VV$ and $VV \to PP$

As it is shown in Eq. (6), the $VV \to VV$ reactions can occur via (s,t,u)-processes. Therefore, we exhibit in the tables below the coefficients $(\zeta_{ij}^{(s)}, \zeta_{ij}^{(t)}, \zeta_{ij}^{(u)})$.

For processes $VV \to PP$ the coefficients are obtained just by replacing the vector pair in final state of $VV \to VV$ by the respective pseudoscalar pair PP in $SU(4)$ basis (i.e. $J/\psi K^*$ by $\eta_c K$, and so on). Notice, however, that $VV \to PP$ scatterings are proportional to $t-u$, see Eq. (5). Hence, the coefficients χ_{ij} are equal to $\zeta_{ij}^{(s)}$, i.e. they are the first coefficients in the tables below.

$\mathbf{C=S=0, I^G(J^{PC})}=1^+(1^{+-}), 1^-(2^{++}); I_z=+1$				
Channel	$J/\psi\rho$	$\omega\rho$	$\bar{K}^*K^*$	$\bar{D}^*D^*$
$J/\psi\rho$	$0, 0, 0$	$0, 0, 0$	$0, 0, 0$	$0, \frac{-\gamma}{\sqrt{3}}, \frac{-\gamma}{\sqrt{3}}$
$\omega\rho$	$0, 0, 0$	$0, 0, 0$	$0, \frac{-\sqrt{3}}{\sqrt{8}}, \frac{-\sqrt{3}}{\sqrt{8}}$	$0, \frac{-\gamma}{2\sqrt{6}}, \frac{-\gamma}{2\sqrt{6}}$
$\bar{K}^*K^*$	$0, 0, 0$	$0, \frac{-\sqrt{3}}{\sqrt{8}}, \frac{-\sqrt{3}}{\sqrt{8}}$	$\frac{1}{2}, \frac{1}{2}, 0$	$\frac{-1}{4}, \frac{\gamma}{8}, \frac{3\gamma}{8}$
$\bar{D}^*D^*$	$0, \frac{-\gamma}{\sqrt{3}}, \frac{-\gamma}{\sqrt{3}}$	$0, \frac{-\gamma}{2\sqrt{6}}, \frac{-\gamma}{2\sqrt{6}}$	$\frac{-1}{4}, \frac{\gamma}{8}, \frac{3\gamma}{8}$	$\frac{1}{4}, \frac{(2\psi+1)}{8}, \frac{(2\psi-1)}{8}$

$\mathbf{C = S = 0, I^G(J^{PC})} = 1^+(1^{+-}), 1^-(2^{++}); I_z = 0$

Channel	$J/\psi\rho$	$\omega\rho$	$\bar{K}^*K^*$	$\bar{D}^*D^*$
$J/\psi\rho$	$0, 0, 0$	$0, 0, 0$	$0, 0, 0$	$0, \frac{-\gamma}{\sqrt{3}}, \frac{-\gamma}{\sqrt{3}}$
$\omega\rho$	$0, 0, 0$	$0, 0, 0$	$0, \frac{-\sqrt{3}}{\sqrt{8}}, \frac{-\sqrt{3}}{\sqrt{8}}$	$0, \frac{-\gamma}{2\sqrt{6}}, \frac{-\gamma}{2\sqrt{6}}$
$\bar{K}^*K^*$	$0, 0, 0$	$0, \frac{-\sqrt{3}}{\sqrt{8}}, \frac{-\sqrt{3}}{\sqrt{8}}$	$\frac{1}{4}, \frac{1}{4}, 0$	$0, \frac{\gamma}{4}, \frac{\gamma}{4}$
$\bar{D}^*D^*$	$0, \frac{-\gamma}{\sqrt{3}}, \frac{-\gamma}{\sqrt{3}}$	$0, \frac{-\gamma}{2\sqrt{6}}, \frac{-\gamma}{2\sqrt{6}}$	$0, \frac{\gamma}{4}, \frac{\gamma}{4}$	$0, \frac{\psi}{4}, \frac{\psi}{4}$

$\mathbf{C = S = 0, I^G(J^{PC})} = 1^+(1^{+-}), 1^-(2^{++}); I_z = -1$

Channel	$J/\psi\rho$	$\omega\rho$	$\bar{K}^*K^*$	$\bar{D}^*D^*$
$J/\psi\rho$	$0, 0, 0$	$0, 0, 0$	$0, 0, 0$	$0, \frac{-\gamma}{\sqrt{3}}, \frac{-\gamma}{\sqrt{3}}$
$\omega\rho$	$0, 0, 0$	$0, 0, 0$	$0, \frac{-\sqrt{3}}{\sqrt{8}}, \frac{-\sqrt{3}}{\sqrt{8}}$	$0, \frac{-\gamma}{2\sqrt{6}}, \frac{-\gamma}{2\sqrt{6}}$
$\bar{K}^*K^*$	$0, 0, 0$	$0, \frac{-\sqrt{3}}{\sqrt{8}}, \frac{-\sqrt{3}}{\sqrt{8}}$	$\frac{1}{2}, \frac{1}{2}, 0$	$\frac{-1}{2}, 0, \frac{\gamma}{2}$
$\bar{D}^*D^*$	$0, \frac{-\gamma}{\sqrt{3}}, \frac{-\gamma}{\sqrt{3}}$	$0, \frac{-\gamma}{2\sqrt{6}}, \frac{-\gamma}{2\sqrt{6}}$	$\frac{-1}{2}, 0, \frac{\gamma}{2}$	$\frac{1}{2}, \frac{\psi}{2}, 0$

$\mathbf{C = S = 0, I^G(J^{PC})} = 0^+(0^{++}), 0^-(1^{+-}), 0^+(2^{++})$

Channels	$J/\psi J/\psi$	$J/\psi\omega$	$\omega\omega$	$\rho\rho$	$\bar{D}_s^*D_s^*$
$J/\psi J/\psi$	$0, 0, 0$	$0, 0, 0$	$0, 0, 0$	$0, 0, 0$	$0, \frac{2\gamma}{3}, \frac{2\gamma}{3}$
$J/\psi\omega$	$0, 0, 0$	$0, 0, 0$	$0, 0, 0$	$0, 0, 0$	$0, -\frac{\sqrt{2}\gamma}{3}, -\frac{\sqrt{2}\gamma}{3}$
$\omega\omega$	$0, 0, 0$	$0, 0, 0$	$0, 0, 0$	$0, 0, 0$	$0, \frac{\gamma}{3}, \frac{\gamma}{3}$
$\rho\rho$	$0, 0, 0$	$0, 0, 0$	$0, 0, 0$	$0, 2, 2$	$0, 0, 0$
$\bar{D}_s^*D_s^*$	$0, \frac{2\gamma}{3}, \frac{2\gamma}{3}$	$0, -\frac{\sqrt{2}\gamma}{3}, -\frac{\sqrt{2}\gamma}{3}$	$0, \frac{\gamma}{3}, \frac{\gamma}{3}$	$0, 0, 0$	$0, \frac{(\psi+1)}{4}, \frac{(\psi+1)}{4}$

$\mathbf{C = 0, S = 1, I^G(J^{PC})} = 1/2(0^+), 1/2(1^+), 1/2(2^+); I_z = +1/2$

Channels	$J/\psi K^*$	ωK^*	ρK^*	$\bar{D}^*D_s^*$
$J/\psi K^*$	$0, 0, 0$	$0, 0, 0$	$0, 0, 0$	$0, \frac{\gamma}{\sqrt{3}}, \frac{\gamma}{\sqrt{3}}$
ωK^*	$0, 0, 0$	$\frac{3}{4}, 0, \frac{-3}{4}$	$\frac{-1}{4}, 0, \frac{1}{4}$	$\sqrt{\frac{3}{8}}, \frac{\gamma}{2\sqrt{6}}, \frac{-\gamma}{\sqrt{6}}$
ρK^*	$0, 0, 0$	$\frac{-1}{4}, 0, \frac{1}{4}$	$\frac{1}{12}, -\frac{1}{3}, -\frac{5}{12}$	$\frac{-1}{2\sqrt{6}}, \frac{-\gamma}{2\sqrt{6}}, 0$
$\bar{D}^*D_s^*$	$0, \frac{\gamma}{\sqrt{3}}, \frac{\gamma}{\sqrt{3}}$	$\sqrt{\frac{3}{8}}, \frac{\gamma}{2\sqrt{6}}, \frac{-\gamma}{\sqrt{6}}$	$\frac{-1}{2\sqrt{6}}, \frac{-\gamma}{2\sqrt{6}}, 0$	$\frac{1}{2}, \frac{\psi}{2}, 0$

$\mathbf{C = 0, S = 1, I^G(J^{PC})} = 1/2(0^+), 1/2(1^+), 1/2(2^+); I_z = -1/2$

Channels	$J/\psi K^*$	ωK^*	ρK^*	$\bar{D}^*D_s^*$
$J/\psi K^*$	$0, 0, 0$	$0, 0, 0$	$0, 0, 0$	$0, \frac{\gamma}{\sqrt{3}}, \frac{\gamma}{\sqrt{3}}$
ωK^*	$0, 0, 0$	$\frac{3}{4}, 0, \frac{-3}{4}$	$\frac{3}{4}, 0, \frac{-3}{4}$	$\sqrt{\frac{3}{8}}, \frac{\gamma}{2\sqrt{6}}, \frac{-\gamma}{\sqrt{6}}$
ρK^*	$0, 0, 0$	$\frac{3}{4}, 0, \frac{-3}{4}$	$\frac{3}{4}, 1, \frac{1}{4}$	$\frac{\sqrt{3}}{\sqrt{8}}, \frac{\sqrt{3}\gamma}{\sqrt{8}}, 0$
$\bar{D}^*D_s^*$	$0, \frac{\gamma}{\sqrt{3}}, \frac{\gamma}{\sqrt{3}}$	$\sqrt{\frac{3}{8}}, \frac{\gamma}{2\sqrt{6}}, \frac{-\gamma}{\sqrt{6}}$	$\frac{\sqrt{3}}{\sqrt{8}}, \frac{\sqrt{3}\gamma}{\sqrt{8}}, 0$	$\frac{1}{2}, \frac{\psi}{2}, 0$

References

[1] T. Matsui, H. Satz, Phys. Lett. B 178 (1986) 416.
[2] R. Rapp, D. Blaschke, P. Crochet, Prog. Part. Nucl. Phys. 65 (2010) 209.
[3] P. Braun-Munzinger, V. Koch, T. Schäfer, J. Stachel, Phys. Rep. 621 (2016) 76.

[4] M. Gonin, et al., NA50, Nucl. Phys. A 610 (1996) 404C.
[5] M.C. Abreu, et al., NA50, Phys. Lett. B 410 (1997) 337.
[6] B. Alessandro, et al., NA50, Eur. Phys. J. C 39 (2005) 335.
[7] R. Arnaldi, et al., NA60, Nucl. Phys. A 774 (2006) 711.
[8] R. Arnaldi, et al., NA60, Phys. Rev. Lett. 99 (2007) 132302.
[9] A. Adare, et al., PHENIX, Phys. Rev. Lett. 98 (2007) 172301.
[10] B.B. Abelev, et al., ALICE, Phys. Lett. B 734 (2014) 314.
[11] J. Adam, et al., ALICE, Phys. Lett. B 766 (2017) 212.
[12] W. Zha, Z. Tang, Nucl. Part. Phys. Proc. 289 (2017) 83.
[13] C.-Y. Wong, E.S. Swanson, T. Barnes, Phys. Rev. C 62 (2000) 045201.
[14] C.-Y. Wong, E.S. Swanson, T. Barnes, Phys. Rev. C 65 (2001) 014903; Erratum: Phys. Rev. C 66 (2002) 029901.
[15] S.G. Matinyan, B. Muller, Phys. Rev. C 58 (1998) 2994.
[16] K.L. Haglin, Phys. Rev. C 61 (2000) 031902.
[17] P. Braun-Munzinger, K. Redlich, Eur. Phys. J. C 16 (2000) 519.
[18] Z. Lin, C.M. Ko, Phys. Rev. C 62 (2000) 034903.
[19] K.L. Haglin, C. Gale, Phys. Rev. C 63 (2001) 065201.
[20] Y. Oh, T. Song, S.H. Lee, Phys. Rev. C 63 (2001) 034901.
[21] T. Barnes, E.S. Swanson, C.-Y. Wong, X.-M. Xu, Phys. Rev. C 68 (2003) 014903.
[22] Y.-s. Oh, T.-s. Song, S.H. Lee, C.-Y. Wong, J. Korean Phys. Soc. 43 (2003) 1003.
[23] F.O. Duraes, H. Kim, S.H. Lee, F.S. Navarra, M. Nielsen, Phys. Rev. C 68 (2003) 035208.
[24] L. Maiani, F. Piccinini, A.D. Polosa, V. Riquer, Nucl. Phys. A 741 (2004) 273.
[25] L. Maiani, F. Piccinini, A.D. Polosa, V. Riquer, Nucl. Phys. A 748 (2005) 209.
[26] F.O. Dures, S.H. Lee, F.S. Navarra, M. Nielsen, Phys. Lett. B 564 (2003) 97.
[27] A. Bourque, C. Gale, K.L. Haglin, Phys. Rev. C 70 (2004) 055203.
[28] F. Carvalho, F.O. Duraes, F.S. Navarra, M. Nielsen, Phys. Rev. C 72 (2005) 024902.
[29] T. Song, S.H. Lee, Phys. Rev. D 72 (2005) 034002.
[30] A. Capella, L. Bravina, E.G. Ferreiro, A.B. Kaidalov, K. Tywoniuk, E. Zabrodin, Eur. Phys. J. C 58 (2008) 437.
[31] W. Cassing, L. Kondratyuk, G. Lykasov, M. Rz janin, Phys. Lett. B 513 (2001) 1.
[32] O. Linnyk, E.L. Bratkovskaya, W. Cassing, Int. J. Mod. Phys. E 17 (2008) 1367.
[33] J. Zhou, X.-M. Xu, Phys. Rev. C 85 (2012) 064904.
[34] S. Mitra, S. Ghosh, S.K. Das, S. Sarkar, J. e Alam, Nucl. Phys. A 951 (2016) 75.
[35] F.-R. Liu, S.-T. Ji, X.-M. Xu, J. Korean Phys. Soc. 69 (2016) 472.
[36] M. Cleven, V.K. Magas, A. Ramos, Phys. Rev. C 96 (2017) 045201.
[37] L.M. Abreu, K.P. Khemchandani, A.M. Torres, F.S. Navarra, M. Nielsen, Phys. Rev. C 97 (2018) 044902.
[38] L. Roca, E. Oset, J. Singh, Phys. Rev. D 72 (2005) 014002.
[39] D. Gamermann, E. Oset, Eur. Phys. J. A 33 (2007) 119.
[40] L.M. Abreu, D. Cabrera, F.J. Llanes-Estrada, J.M. Torres-Rincon, Ann. Phys. (N. Y.) 326 (2011) 2737.
[41] L.M. Abreu, D. Cabrera, J.M. Torres-Rincon, Phys. Rev. D 87 (2013) 034019.
[42] R. Molina, D. Nicmorus, E. Oset, Phys. Rev. D 78 (2008) 114018.
[43] J. Weinstein, N. Isgur, Phys. Rev. D 41 (1990) 2236.
[44] G. Janssen, B.C. Pearce, K. Holinde, J. Speth, Phys. Rev. D 52 (1995) 2690.
[45] J. Oller, E. Oset, Nucl. Phys. A 620 (1997) 438.
[46] J.A. Oller, E. Oset, J.R. Pelaez, Phys. Rev. D 59 (1999) 074001.

Chapter 4

Appearance and disappearance of thermal renormalons

Published as:
E. Cavalcanti, J.A. Lourenço, C.A. Linhares, and A.P.C. Malbouisson. Physical Review D **98**, 045013 (2018) *Appearance and Disappearance of thermal renormalons*

PHYSICAL REVIEW D **98,** 045013 (2018)

Appearance and disappearance of thermal renormalons

E. Cavalcanti,[1,*] J. A. Lourenço,[2,†] C. A. Linhares,[3,‡] and A. P. C. Malbouisson[1,§]

[1] *Centro Brasileiro de Pesquisas Físicas/MCTI, 22290-180 Rio de Janeiro, RJ, Brazil*
[2] *Departamento de Ciências Naturais, Universidade Federal do Espírito Santo, 29932-540 Campus São Mateus, ES, Brazil*
[3] *Instituto de Física, Universidade do Estado do Rio de Janeiro, 20559-900 Rio de Janeiro, RJ, Brazil*

(Received 27 April 2018; published 15 August 2018)

We consider a scalar field model with a $g\phi_4^4$ interaction and compute the mass correction at next-to-leading order in a large-N expansion to study the summability of the perturbative series. It is already known that at zero temperature this model has a singularity in the Borel plane (a "renormalon"). We find that a small increase in temperature adds two countable sets both with an infinite number of renormalons. For one of the sets the position of the poles is thermal independent and the residue is thermal dependent. In the other one both the position of poles and the residues are thermal dependent. However, if we consider the model at extremely high temperatures, such that a dimensional reduction takes place, one observes that all the renormalons disappear and the model becomes Borel summable.

DOI: 10.1103/PhysRevD.98.045013

I. INTRODUCTION

The understanding of strongly coupled systems remains one of the major challenges in particle physics and requires the knowledge of the nonperturbative regime of quantum chromodynamics (QCD), the currently accepted theory of strong interactions.

Also, in the realm of condensed matter physics, systems involving strongly coupled particles (fermions, for instance) fall, in principle, outside the scope of perturbation theory. However, apart from some simple models, nonperturbative solutions are very hard to be found, which led along the years to attempts to rely in some way on perturbative methods (valid in general for weak couplings) to get some results in strong-coupling regimes [1–6].

It is broadly discussed in the literature whether nonperturbative solutions in field theory can or cannot be recovered from a perturbative expansion. In any case, a procedure is needed to make sense out of the perturbative series. In fact, often the perturbative expansions are asymptotic rather than convergent. Actually, we remember that the perturbative series can be viewed just as a representation of the exact solution and if we want to obtain information about the nonperturbative solution from its perturbative representation some summation technique must be implemented. [1–6]

One of the most employed of these procedures is to investigate, after perturbative renormalization has been performed, the so-called *Borel summability* of a theory, for a brief introduction see Refs. [7,8] and for a complete review on the subject see Ref. [9]. If we start with an asymptotic series, its Borel transform defines a new series that can be convergent. The representation of the nonperturbative result can be obtained by an inverse Borel transform, essentially a Laplace transform, which requires a contour integration in the complex Borel plane in order to be properly defined. This procedure allows one to gain access to the correct nonperturbative solution in many situations [3]. More precisely: if we take a theory characterized by an already perturbatively renormalized coupling constant g and consider a given quantity $F(g)$ given by a formal series (perhaps asymptotically divergent) in g, $F(g) = \sum_n a_n g^n$; define its Borel transform $\mathcal{B}(F;b)$ as $\mathcal{B}(F;b) = \sum_n a_n b^n/n!$ and the inverse Borel transform as $\tilde{F}(g) = 1/g \int_0^\infty db e^{-b/g}\mathcal{B}(F;b)$. It can be easily verified that $\tilde{F}(g)$ reproduces formally the original series $F(g)$. The interesting point is that even if $F(g)$ is divergent the series $\mathcal{B}(F;b)$ may converge and in this case the inverse Borel transform $\tilde{F}(g)$ defines a function of g which can be considered in some sense as the sum of the original divergent series $F(g)$. This "mathematical phenomenon" is named *Borel summability* and is a way of giving a meaning to divergent perturbative series. However, for the inverse Borel transform to be well defined, the absence of singularities at least on the positive real axis of the Borel plane b is required.

* erich@cbpf.br
† jose.lourenco@ufes.br
‡ linharescesar@gmail.com
§ adolfo@cbpf.br

We emphasize that we are working with a model in which the perturbative renormalization of the coupling constant has already been performed, in the spirit of Ref. [10,11]. In the above quoted references, by starting with a perturbatively renormalized QFT there can be singularities on the positive real axis of the Borel plane that obstruct the Borel resummation of the perturbation theory. These singularities, in the case of non-asymptotically free theories like $\lambda\phi_4^4$ and QED_4 are called ultraviolet (UV) *renormalons*.

The study of renormalons is also important from a phenomenological perspective, as one needs, for instance, to know the solution at the nonperturbative level to obtain an estimate of the heavy-quark mass [12,13].

In the context of IR renormalons that arise in the context of asymptotically free theories, it has been a subject of recent investigation to consider compactified theories such as non-Abelian SU(N) gauge theories on $\mathbb{R}^3 \times \mathbb{S}^1$ [14] and the $\mathbb{C}P^{N-1}$ nonlinear sigma model on $\mathbb{R}^1 \times \mathbb{S}^1$ [4,15]. The interest of considering a finite spatial extent L or thermal dependence $\beta = 1/T$ arises from the fact that for small L or large T a weakly coupled regime is observed due to asymptotic freedom [16,17]. A careful study of renormalons for an $SU(N)$ gauge theory has been made in Ref. [14]. In it the absence of renormalons is discussed when one introduces a finite small length L. However, in the context of non-asymptotically free theories, it is not yet clear how the renormalon phenomenon is influenced by the presence of a finite temperature or finite extension.

In the present article, we investigate the behavior of a scalar field model with $O(N)$ symmetry in four dimensions. Our main concern is the careful investigation of the renormalon poles and residues at next-to-leading order in the large-N expansion, as presented in Sec. II. This $1/N$-expansion allows to resum a class of diagrams (usually called *ring* diagrams or *necklaces*) that generates the renormalon contribution. Following recent literature, we investigate the role of a compactification parameter, here taken as introducing a temperature dependence. First, we review in Sec. III the behavior at zero temperature and find the existence of two renormalons. In Sec. IV, we observe that at small temperatures the system develops a countable set with an infinite number of renormalons that can be separated into two classes: renormalons without thermal poles but that can have thermal residues and renormalons with thermal poles. In Sec. V we consider an extreme increase in temperature, which is related to a dimensional reduction, and obtain that it implies the disappearance of renormalons. We summarize our conclusions in Sec. VI.

II. SCALAR FIELD MODEL AND RESUMMATION

We are mainly interested in computing corrections to the field mass in a scalar theory with coupling $(g/N)(\phi_i\phi_i)^2$, at which $i = 1, \ldots, N$. The full propagator G is given by

$$G = G_0 \sum_{k=0}^{\infty} (\Sigma G_0)^k \equiv \frac{G_0}{1 - \Sigma G_0}, \tag{1}$$

where Σ is the sum of all 1PI (one-particle irreducible) diagrams built with the free propagator G_0. Or, if we establish Σ using the full propagator G (a recurrence relation) then, to avoid double counting, it is necessary to consider just the 2PI diagrams. We use a set of 2PI diagrams known as *necklace* or *ring* diagrams as illustrated in Fig. 1. This set is the leading order contribution in the $1/N$ expansion, any other diagram will contribute only at next to leading order in $1/N$ [18] and is then consistently ignored as a subdominant behavior at this order.

Therefore, at an unspecified spacetime dimension D a necklace with $(k-1)$-*pearls* is given by $R_k(p)$,

$$R_k(p) = -\frac{g}{N} \int \frac{d^D \ell}{(2\pi)^D} \frac{1}{(p-l)^2 + M^2} \left[-\frac{g}{2N} (NB(\ell)) \right]^{k-1}, \tag{2}$$

where

$$B(\ell) = \int \frac{d^D q}{(2\pi)^D} \frac{1}{q^2 + M^2} \frac{1}{(q+l)^2 + M^2} \tag{3}$$

stands for each *pearl* [1,18].

Thus, by taking into account necklaces with all numbers of pearls we obtain the full correction

$$\Sigma = \sum_{k=1}^{\infty} R_k(p). \tag{4}$$

The subsequent analysis of this expression intends to verify whether the series representation is or is not Borel summable. This is entirely dependent on the behavior of $R_k(p)$ with respect to the summation index k.

Now that we have introduced the general idea, let us investigate the thermal dependence in detail. By making a compactification in imaginary time we introduce the inverse temperature $\beta = 1/T$. With this, the expression for each pearl is modified to

$$B(\ell, \omega_m) = \frac{1}{\beta} \sum_{n \in \mathbb{Z}} \int \frac{d^{D-1} q}{(2\pi)^{D-1}} \frac{1}{q^2 + \omega_n^2 + M^2} \times \frac{1}{(q+l)^2 + (\omega_n - \omega_m)^2 + M^2}, \tag{5}$$

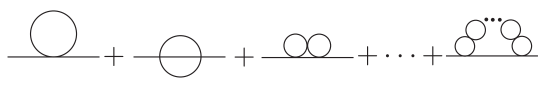

FIG. 1. Sum over the class of necklace diagrams. The case without any pearl is the usual "tadpole" (first diagram), the special case with just one pearl is the usual "sunset" diagram (second diagram). Each vertex contributes a factor g/N and each "pearl" a factor N; therefore the whole series has the same order in the $1/N$ expansion.

where $\omega_n = 2\pi nT$ is the frequency related to the $(D-1)$-dimensional momentum q, while the necklaces become

$$R_k(p,\omega_o) = \frac{(-g)^k}{2^{k-1}N\beta}\sum_{m\in\mathbb{Z}}\int\frac{d^{D-1}\ell}{(2\pi)^{D-1}} \times \frac{B^{k-1}(\ell,\omega_m)}{(p-l)^2+(\omega_o-\omega_m)^2+M^2}, \tag{6}$$

where ω_m and ω_o are the frequencies related, respectively, to the loop momentum ℓ and the external momentum p.

Then, Eq. (5) can be treated by using the Feynman parametrization, integrating over the momenta q and identifying the infinite sum as an Epstein-Hurwitz zeta function $Z^{X^2}(\beta;\nu)$ defined by

$$Z^{X^2}(\beta;\nu) = \sum_{m\in\mathbb{Z}}\frac{1}{(\omega_m^2+X^2)^\nu}. \tag{7}$$

We now perform the analytic expansion of the Epstein-Hurwitz zeta function to whole complex ν plane [19], which allows us to rewrite Eq. (5) as

$$\begin{aligned} B(\ell,\omega_m) =& \frac{\Gamma(2-\frac{D}{2})}{(4\pi)^{\frac{D}{2}}}\int_0^1 dz[M^2+(\ell^2+\omega_m^2)z(1-z)]^{-2+\frac{D}{2}} \\ &+\frac{1}{(2\pi)^{\frac{D}{2}}}\sum_{n\in\mathbb{N}^\star}\int_0^1 dz\frac{(n\beta)^{2-\frac{D}{2}}\cos[2\pi nm(1-z)]}{[M^2+(\ell^2+\omega_m^2)z(1-z)]^{\frac{2-\frac{D}{2}}{2}}} \\ &\times K_{2-\frac{D}{2}}\left[n\beta\sqrt{M^2+(\ell^2+\omega_m^2)z(1-z)}\right], \end{aligned} \tag{8}$$

where $K_\nu(x)$ is the modified Bessel function of the second kind.

Considering the case where $D = 4-2\varepsilon$, we get

$$\begin{aligned} B(\ell,\omega_m) =& B_0(\ell,\omega_m)+B_\beta(\ell,\omega_m) \\ =& \frac{\Gamma(\varepsilon)}{(4\pi)^2}\int_0^1 dz\{1-\varepsilon\ln[M^2+(\ell^2+\omega_m^2)z(1-z)]\} \\ &+\frac{1}{(2\pi)^2}\sum_{n\in\mathbb{N}^\star}\int_0^1 dz\cos[2\pi nm(1-z)] \\ &\times K_0\left[n\beta\sqrt{M^2+(\ell^2+\omega_m^2)z(1-z)}\right]. \end{aligned} \tag{9}$$

The temperature-independent component B_0 is standard and well known [18],

$$\begin{aligned} B_0(\ell,\omega_m) =& -\frac{1}{(4\pi^2)}\left\{\ln\frac{M^2}{\Lambda^2}-2+\sqrt{1+\frac{4M^2}{\ell^2+\omega_m^2}}\right. \\ &\left.\times\ln\left[\frac{1+\sqrt{1+4\frac{M^2}{\ell^2+\omega_m^2}}}{1-\sqrt{1+4\frac{M^2}{\ell^2+\omega_m^2}}}\right]\right\}. \end{aligned} \tag{10}$$

For high values of the momentum ℓ we have the asymptotic expression

$$B_0(\ell,\omega_m) \sim -\frac{1}{(4\pi^2)}\ln\frac{\ell^2+\omega_m^2+M^2}{M^2}. \tag{11}$$

However, we do not have a solution for the term B_β for all temperatures. In Secs. IV and V we respectively investigate the regimes of low temperatures and extremely high temperatures.

III. A FIRST GLANCE: RENORMALON AT $T=0$

In this section we consider the special case of zero temperature. In this situation the only contribution to the pearl diagram comes from the B_0 component. To obtain a treatable expression to the necklace diagrams, we consider the expansion for high values of the momentum ℓ, Eq. (11), at zero temperature

$$B(\ell,\omega_m) \overset{T=0}{\sim} -\frac{1}{(4\pi)^2}\ln\frac{\ell^2+M^2}{M^2}. \tag{12}$$

At this point we recall that the standard approximation is to consider the leading behavior in the momentum ℓ, that is, $\ln(\ell^2+M^2)\approx\ln\ell^2$. Here, we avoid this particular approximation and explore the consequences of keeping the exact term $\ln(\ell^2+M^2)$. Let us return to the necklace diagrams. To render the theory finite, we employ the well-established Bogoliubov-Parasiuk-Hepp-Zimmerman (BPHZ) procedure [20] to renormalize the amplitude. Therefore, the renormalized necklace $\hat{R}_k(p)$ is

$$\hat{R}_k(p) = R_k(p)-R_k(0)-p^2\frac{\partial}{\partial p^2}R_k(p)\Big|_{p=0}. \tag{13}$$

We shall drop the hat unless it becomes important to distinguish between the renormalized $\hat{R}_k(p)$ and non-renormalized $R_k(p)$ necklaces.

As can be noted, this affects only the p-dependent propagator in the zero-temperature version of Eq. (6). Regarding the expression of $R_k(p)$ given by Eq. (6), the procedure of Eq. (13) is equivalent to perform the substitution on the denominator

$$\frac{1}{p^2+\ell^2+M^2} \to \frac{p^4}{(\ell^2+M^2)^2(p^2+\ell^2+M^2)}$$
$$\approx \begin{cases} \frac{p^4}{(\ell^2+M^2)^3}, & \text{low } p; \\ \frac{p^2}{(\ell^2+M^2)^2}, & \text{high } p, \end{cases} \tag{14}$$

where the standard *naive* expansion $(p-l)^2 \approx p^2 + l^2$ is assumed.

In a low-p expansion, then, for $T=0$ and small values of p, the integral to be solved to obtain the necklace expression is

$$R_k(p) \sim -\frac{gp^4}{N}\left(\frac{g}{2(4\pi)^2}\right)^{k-1}\int \frac{d^4\ell}{(2\pi)^4}\frac{(\ln\frac{\ell^2+M^2}{M^2})^{k-1}}{(\ell^2+M^2)^3}. \tag{15}$$

To solve it we first perform the integral over the solid angle ($\Omega_4 = 2\pi^2$) and then reorganize the result by making the change of variables $\ell^2 + M^2 = M^2 e^t$, that is,

$$R_k(p) \sim -\frac{gp^4}{16\pi^2 NM^2}\left(\frac{g}{2(4\pi)^2}\right)^{k-1}\int_0^\infty dt(e^{-t}-e^{-2t})t^{k-1}. \tag{16}$$

At this point we can clearly identify the presence of two gamma functions, so that

$$R_k(p) \sim -\frac{gp^4}{16\pi^2 NM^2}\left\{(k-1)!\left(\frac{g}{2(4\pi)^2}\right)^{k-1} - (k-1)!\left(\frac{g}{4(4\pi)^2}\right)^{k-1}\right\}. \tag{17}$$

We can finally return to the sum over all contributions Eq. (4),

$$\Sigma \sim -\frac{2\tilde{g}p^2}{NM^2}\left\{\sum_{k=1}^{\infty}(k-1)!\tilde{g}^{k-1} - \sum_{k=1}^{\infty}(k-1)!\left(\frac{\tilde{g}}{2}\right)^{k-1}\right\}, \tag{18}$$

where we have defined $\tilde{g} = g/(2(4\pi)^2)$. Both sums are divergent, but we can try to make sense of them by defining a Borel transform,

$$\mathcal{B}(\Sigma; y) \sim -\frac{2\tilde{g}p^2}{NM^2}\left\{\sum_{k=1}^{\infty}(\tilde{g}y)^{k-1} - \sum_{k=1}^{\infty}\left(\frac{\tilde{g}y}{2}\right)^{k-1}\right\}$$
$$= -\frac{2\tilde{g}p^2}{NM^2}\left\{\frac{1}{1-\tilde{g}y} - \frac{1}{1-\tilde{g}y/2}\right\} \tag{19}$$

We then obtain two poles on the real positive axis of the Borel plane at $y = 1/\tilde{g}$, $2/\tilde{g}$. These poles (renormalons) introduce problems to compute the inverse Borel transform.

In the standard procedure, see Ref. [18], Eq. (15) is solved for very large ℓ, which is justified as this is the relevant region to get the asymptotic behavior for the k index. This means that the approximation $[\ln(\ell^2+M^2)/M^2]^{k-1}/(\ell^2+M^2)^3 \approx (\ln \ell^2)^{k-1}/\ell^6$ is employed. Therefore, only the first pole is found (at $y = 1/\tilde{g}$) while the second pole is hidden. When $\tilde{g}$ is very small this could be justified as $2/\tilde{g}$ being very far from the origin.

IV. APPEARANCE OF THERMAL RENORMALONS (LOW TEMPERATURES)

For low but finite temperatures, we can use the asymptotic representation of the modified Bessel function of the second kind $K_0(z) \sim e^{-z} f(z)$, so that the thermal component of the pearl (9) becomes

$$B_\beta(\ell, \omega_m) \sim \frac{1}{(4\pi)^2}\sum_{n\in\mathbb{N}^*}\frac{8K_0(n\beta M)}{n\beta}\frac{1}{\ell^2+\omega_m^2}. \tag{20}$$

Using the above equation for B_β and the expression for the $T=0$ component, B_0 [see Eq. (11)], the quantity $B = B_0 + B_\beta$ can be written in the low-temperature regime as

$$B(\ell,\omega_m) \sim -\frac{1}{(4\pi)^2}\left[\ln\frac{\ell^2+\omega_m^2+M^2}{M^2} - \frac{A(\beta)}{\ell^2+\omega_m^2}\right], \tag{21}$$

where

$$A(\beta) = \frac{1}{(4\pi)^2}\sum_{n\in\mathbb{N}^*}\frac{8K_0(n\beta M)}{n\beta} \tag{22}$$

stores information about the dependence on the temperature.

We then replace the expression in Eq. (21) into Eq. (6), employ the BPHZ procedure and use a low-p expansion as in Eq. (14),

$$R_k(p,\omega_o) = -\frac{g}{N}(p^2+\omega_o^2)^2\left(\frac{g}{2(4\pi)^2}\right)^{k-1}\frac{1}{\beta} \times \sum_{m\in\mathbb{Z}}\int\frac{d^3\ell}{(2\pi)^3}\frac{\left(\ln\frac{\ell^2+\omega_m^2+M^2}{M^2} - \frac{A(\beta)}{\ell^2+\omega_m^2}\right)^{k-1}}{(\ell^2+\omega_m^2+M^2)^3}. \tag{23}$$

So, integrating over the solid angle and expanding the binomial, we get

$$R_k(p,\omega_o) = -\frac{g(p^2+\omega_o^2)^2}{2\pi^2 N}\left(\frac{g}{2(4\pi)^2}\right)^{k-1}\frac{1}{\beta}\sum_{m\in\mathbb{Z}}\sum_{i=0}^{k-1}\binom{k-1}{i}(-A(\beta))^i \times \int_0^\infty d\ell\ell^2 \frac{\ln^{k-1-i}[(\ell^2+\omega_m^2+M^2)/M^2]}{(\ell^2+\omega_m^2+M^2)^3}\left(\frac{1}{\ell^2+\omega_m^2}\right)^i. \tag{24}$$

We reorganize the above expression in a more convenient way to compute the sum over the Matsubara frequencies. The denominator is treated by employing a Feynman parametrization and the logarithm in the numerator is expanded in powers of $\omega_m^2/(\ell^2+M^2)$, which is justified by an asymptotic behavior in ℓ assuring that $m/\ell < 1$. This allows us to rewrite the above equation in the form

$$R_k(p,\omega_o) = -\frac{g(p^2+\omega_o^2)^2}{2\pi^2 N}\left(\frac{g}{2(4\pi)^2}\right)^{k-1}\sum_{i=0}^{k-1}\binom{k-1}{i}(-A(\beta))^i\int_0^1 dz\frac{\Gamma(3+i)z^2z^{i-1}}{\Gamma(3)\Gamma(i)} \times\left\{\int_0^\infty d\ell\ell^2\ln^{k-i-1}\frac{\ell^2+M^2}{M^2}\frac{1}{\beta}\sum_{m\in\mathbb{Z}}\frac{1}{(\ell^2+\omega_m^2+M^2z)^{3+i}} + \int_0^\infty d\ell\ell^2\frac{\ln^{k-i-2}\frac{\ell^2+M^2}{M^2}}{\ell^2+M^2}\frac{1}{\beta}\sum_{m\in\mathbb{Z}}\frac{(k-i-1)\omega_m^2}{(\ell^2+\omega_m^2+M^2z)^{3+i}} + \mathcal{O}(\omega_m^4)\right\}. \tag{25}$$

Although we could use this complete expression, this is unnecessary. It can be shown, after a lengthy computation, that the relevant information (poles in the Borel plane) can already be obtained by using the following approximation,

$$R_k(p,\omega_o) \approx -\frac{g(p^2+\omega_o^2)^2}{2\pi^2 N}\left(\frac{g}{2(4\pi)^2}\right)^{k-1}\sum_{i=0}^{k-1}\binom{k-1}{i}(-A(\beta))^i\left\{\int_0^\infty d\ell\ell^2\ln^{k-1-i}\frac{\ell^2+M^2}{M^2}\frac{1}{\beta}Z^{\ell^2+M^2}(\beta;3+i)\right\}, \tag{26}$$

where $Z^{X^2}(\beta;\nu)$ is the Epstein-Hurwitz zeta function defined in Eq. (7). The contributions of order $\mathcal{O}(\omega_m^2)$ do not modify the position of the poles and only change their residues. Moreover, for large values of k the integration of the expression over the Feynman parameter z is asymptotically equal to the expression without the Feynman parameters. To avoid a tedious calculation we do not exhibit in this article the step-by-step of this process.

Taking the approximation in Eq. (26) and considering again the analytic expansion of the Epstein-Hurwitz zeta function to the whole complex ν plane, we get

$$R_k(p,\omega_o) \approx -\frac{g(p^2+\omega_o^2)^2}{2\pi^2 N}\left(\frac{g}{2(4\pi)^2}\right)^{k-1}\sum_{i=0}^{k-1}\binom{k-1}{i}(-A(\beta))^i\int_0^\infty d\ell\ell^2\ln^{k-1-i}\frac{\ell^2+M^2}{M^2} \times\frac{1}{\sqrt{4\pi}\Gamma(3+i)}\left\{\frac{\Gamma(\frac{5}{2}+i)}{(\ell^2+M^2)^{\frac{5}{2}+i}}+\frac{4}{2^{\frac{5}{2}+i}}\sum_{n\in\mathbb{N}^*}\left(\frac{n\beta}{\sqrt{\ell^2+M^2}}\right)^{\frac{5}{2}+i}K_{\frac{5}{2}+i}\left(n\beta\sqrt{\ell^2+M^2}\right)\right\}. \tag{27}$$

Since i is an integer, the modified Bessel function of the second kind has a half-integer order, which has the series representation [21]

$$K_{\frac{5}{2}+i}(n\beta\sqrt{\ell^2+M^2}) = \sqrt{\frac{\pi}{2}}\sum_{j=0}^{i+2}\frac{(j+i+2)!}{j!(i+2-j)!}\frac{1}{2^j(n\beta)^{j+\frac{1}{2}}}\frac{e^{-n\beta\sqrt{\ell^2+M^2}}}{(\ell^2+M^2)^{j+\frac{1}{2}}}. \tag{28}$$

So, the remaining integrals are given by

$$R_k(p,\omega_o) = -\frac{g(p^2+\omega_o^2)^2}{4\pi^{5/2}N}\left(\frac{g}{2(4\pi)^2}\right)^{k-1}\sum_{i=0}^{k-1}\binom{k-1}{i} \times\frac{(-A(\beta))^i}{(2+i)!}\left\{\Gamma\left(\frac{5}{2}+i\right)\int_0^\infty d\ell\ell^2\frac{\ln^{k-1-i}\frac{\ell^2+M^2}{M^2}}{(\ell^2+M^2)^{\frac{5}{2}+i}} + \frac{\sqrt{\pi}}{2^{1+i}}\sum_{n\in\mathbb{N}^\star}\sum_{j=0}^{i+2}\frac{(j+i+2)!}{j!(i+2-j)!}\frac{1}{2^j(n\beta)^{j-i-2}} \times\int_0^\infty d\ell\ell^2\frac{e^{-n\beta\sqrt{\ell^2+M^2}}}{(\sqrt{\ell^2+M^2})^{2j+i+\frac{7}{2}}}\ln^{k-1-i}\frac{\ell^2+M^2}{M^2}\right\}. \tag{29}$$

The first integral in the preceding equation can be solved as in the zero-temperature case (see Sec. III) by the change of variables $\ell^2+M^2=M^2e^t$. One must note that $\sqrt{e^t-1}$ has an upper bound $\sqrt{e^t}$ that is also its asymptotic value for large values of the momentum t (which means also large values of the index k). Then, we can use that $\sqrt{e^t-1}\lesssim\sqrt{e^t}$ to simplify the integral

$$\begin{aligned}\mathcal{I}_1 &= \int_0^\infty d\ell\ell^2\frac{\ln^{k-1-i}\frac{\ell^2+M^2}{M^2}}{(\ell^2+M^2)^{\frac{5}{2}+i}}\\ &= \frac{1}{2M^{2+2i}}\int_0^\infty dt t^{k-i-1}\sqrt{e^t-1}e^{-t(\frac{3}{2}+i)}\\ &\lesssim \frac{1}{2M^{2+2i}}\int_0^\infty dt t^{k-i-1}e^{-t(1+i)}\\ &= \frac{(k-i-1)!}{2M^{2+2i}}\frac{1}{(1+i)^{k-i}}.\end{aligned} \tag{30}$$

For the second integral in Eq. (29) we make the change of variables $\ell^2+M^2=M^2r^2$ so that we obtain

$$\begin{aligned}\mathcal{I}_2 &= \int_0^\infty d\ell\ell^2\frac{e^{-n\beta\sqrt{\ell^2+M^2}}}{(\sqrt{\ell^2+M^2})^{2j+i+\frac{7}{2}}}\ln^{k-1-i}\frac{\ell^2+M^2}{M^2}\\ &= 2^{k-i-1}M^{3-2(j+i/2+7/4)}\int_1^\infty dr\sqrt{r^2-1}\frac{e^{-n\beta r}\ln^{k-i-1}r}{r^{2(j+i/2+7/4)-1}}\\ &\lesssim 2^{k-i-1}M^{3-2(j+i/2+7/4)}\int_1^\infty dr\frac{e^{-n\beta r}\ln^{k-i-1}r}{r^{2(j+i/2+7/4)-2}}.\end{aligned} \tag{31}$$

Once more, we used that $\sqrt{r^2-1}\lesssim r$, which considerably simplifies the integral and allows it to be identified as the Milgram generalization of the integroexponential function whose asymptotic behavior is known [22]

$$E_s^\alpha(z) = \frac{1}{\Gamma(\alpha+1)}\int_1^\infty dt\frac{(\ln t)^\alpha e^{-zt}}{t^s} \overset{\mathrm{Re}z\to\infty}{\sim} \frac{e^{-z}}{z^{\alpha+1}}\left[1-\frac{(\alpha+1)(\alpha+2s)}{2z}+\cdots\right]. \tag{32}$$

Hence, after substituting Eqs. (30) and (31) into Eq. (29), and using the asymptotic behavior of the generalized integroexponential, Eq. (32), we have

$$R_k(p,\omega_o) \lesssim -\frac{g(p^2+\omega_o^2)^2}{4\pi^{5/2}N}\left(\frac{g}{2(4\pi)^2}\right)^{k-1}\sum_{i=0}^{k-1}\binom{k-1}{i} \times\frac{(-A(\beta))^i(k-i-1)!}{(2+i)!}\left\{\Gamma\left(\frac{5}{2}+i\right)\frac{1}{2M^{2+2i}} \times\frac{1}{(1+i)^{k-i}}+\sqrt{\pi}\sum_{n\in\mathbb{N}^\star}\sum_{j=0}^{i+2}\frac{(j+i+2)!}{j!(i+2-j)!} \times\frac{2^{k-2i-j-2}}{(n\beta)^{k+j-2i-2}}\frac{e^{-n\beta}}{M^{2j+i+1/2}}\right\}. \tag{33}$$

Now, let us focus attention on the k-dependence. The previous equation can then be rewritten as

$$R_k \lesssim \gamma_1\tilde{g}^{k-1}(k-1)!\sum_{i=0}^{k-1}\left[\frac{\gamma_{2,i}(\beta,M)}{(1+i)^{k-1}}+\sum_{n\in\mathbb{N}^\star}\frac{2^{k-1}\gamma_{3,i,n}(\beta,M)}{(n\beta)^{k-1}}\right], \tag{34}$$

where we have defined,

$$\gamma_1 = -\frac{g(p^2+\omega_o^2)^2}{4\pi^{5/2}N}, \tag{35a}$$

$$\tilde{g} = \frac{g}{2(4\pi)^2}, \tag{35b}$$

$$\gamma_{2,i}(\beta,M) = \frac{(-A(\beta))^i}{(2+i)!i!}\Gamma\left(\frac{5}{2}+i\right)\frac{(1+i)^{i-1}}{2M^{2+2i}}, \tag{35c}$$

$$\gamma_{3,i,n}(\beta,M) = \sum_{j=0}^{i+2}\frac{(-A(\beta))^i}{(2+i)!i!}\sqrt{\pi}\frac{(j+i+2)!}{j!(i+2-j)!} \times\frac{e^{-n\beta}}{M^{2j+i+1/2}}\frac{2^{-2i-j-1}}{(n\beta)^{j-2i-1}}. \tag{35d}$$

The sum over all necklaces is then

$$\mathcal{R} = \sum_{k\in\mathbb{N}^\star}R_k \lesssim \sum_{k\in\mathbb{N}^\star}\gamma_1\tilde{g}^{k-1}(k-1)!\sum_{i=0}^{k-1}\left[\frac{\gamma_{2,i}(\beta,M)}{(1+i)^{k-1}} + \sum_{n\in\mathbb{N}^\star}\frac{2^{k-1}}{(n\beta)^{k-1}}\gamma_{3,i,n}(\beta,M)\right].$$

The range of summation for the double sum is $0 \le i < k < \infty$; we can change the sum ordering and then split the sum over the index k in the form

$$\sum_{k\in\mathbb{N}^+}\sum_{i=0}^{k-1} f_{i,k} = \sum_{i=0}^{\infty}\sum_{k=i+1}^{\infty} f_{i,k} = \sum_{i=0}^{\infty}\left(\sum_{k=1}^{\infty} f_{i,k} - \sum_{k=1}^{i+1} f_{i,k}\right).$$

The first double sum has the dominant contribution; this can be seen by checking for each value of i. Therefore, the relevant contribution is

$$\begin{aligned}\mathcal{R} \sim \gamma_1 \sum_{i=0}^{\infty}\Bigg[&\gamma_{2,i}\sum_{k=1}^{\infty}\frac{\tilde{g}^{k-1}(k-1)!}{(1+i)^{k-1}} \\ &+ \sum_{n\in\mathbb{N}^\star}\gamma_{3,i,n}\sum_{k=1}^{\infty}\frac{\tilde{g}^{k-1}(k-1)!}{(n\beta/2)^{k-1}}\Bigg]. \end{aligned} \tag{36}$$

However, this is not summable due to the presence of the $(k-1)!$. To overcome this difficulty we can employ a Borel transform,

$$\begin{aligned}\mathcal{B}(\mathcal{R};y) \sim \gamma_1 \sum_{i=0}^{\infty}\Bigg[&\gamma_{2,i}\sum_{k=1}^{\infty}\frac{\tilde{g}^{k-1}y^{k-1}}{(1+i)^{k-1}} \\ &+ \sum_{n\in\mathbb{N}^\star}\gamma_{3,i,n}\sum_{k=1}^{\infty}\frac{\tilde{g}^{k-1}y^{k-1}}{(n\beta/2)^{k-1}}\Bigg] \\ = \gamma_1\sum_{i=0}^{\infty}\Bigg[&\frac{\gamma_{2,i}(\beta,M)}{1-\frac{\tilde{g}y}{1+i}} + \sum_{n\in\mathbb{N}^\star}\frac{\gamma_{3,i,n}(\beta,M)}{1-\frac{2\tilde{g}y}{n\beta}}\Bigg]. \end{aligned} \tag{37}$$

Finally, we see in Eq. (37) the renormalons that appear at low temperatures. There are two different sets of renormalons both with residues that are thermal dependent, respectively $\gamma_{2,i}(\beta,M)$ and $\gamma_{3,i,n}(\beta,M)$. The first set of renormalons was already found in previous works [23]; it is characterized by poles whose position are thermal-independent and they are located along the real axis at positions $(1+i)/\tilde{g}$ for $i\in\mathbb{N}$. However, the second set of poles, as far as we know, has not yet been reported. These poles are also in the real axis but they are thermal-dependent as they are located at $n\beta/2\tilde{g}$ for $n\in\mathbb{N}^\star$. The existence of this new set seems to be a remarkable enrichment for the model.

We remark that in the limit of extremely small temperatures these new renormalons are all very far from the origin and this may justify why they are usually hidden. Therefore, our result can be viewed as a first correction to the standard approach. Furthermore, as we pointed out before, we claim that our approximation in Eq. (26) is the sufficient one (at least to describe the poles) and any further corrections shall only change the residues. This means that we have mapped *all* the renormalons that appear at low temperatures.

As a further comment, we remember that in Sec. III we show that at zero temperature there is a hidden second pole located at $2/\tilde{g}$. This does not add any new poles at low temperatures because, as can be easily noted, we already have an infinite set of poles located at $i/\tilde{g}$ for $i\in\mathbb{N}^\star$.

V. DISAPPEARANCE OF THERMAL RENORMALONS (EXTREMELY HIGH TEMPERATURES)

In this section we explore the regime of extremely high temperatures. In fact, we consider the regime of temperatures $T\to\infty$ which is equivalent to a dimensional reduction of one unit. In this case, it is well-known that if the original theory was UV divergent the resulting theory is not anymore UV divergent; which means that UV renormalons should disappear. In this work, we recover this fact using our formalism. In this situation, to treat Eq. (9) we can use the following series expansion of the modified Bessel function of the second kind [21],

$$K_0(z) = -\ln\frac{ze^{\gamma}}{2} - \frac{z^2}{4}\ln\frac{ze^{\gamma-1}}{2} + \mathcal{O}(z^4). \tag{38}$$

The result is easier to get by assuming from the beginning that $m=0$ (which means that this is the only relevant mode) and recalling the following properties of the Riemann zeta function, $\zeta(s) = \sum_{n\in\mathbb{N}^\star} n^{-s}$,

$$\zeta'(s) = -\sum_{n\in\mathbb{N}^+}\frac{\ln n}{n^s}, \tag{39a}$$

$$\zeta(0) = -1/2, \tag{39b}$$

$$\zeta'(0) = \ln\sqrt{2\pi}, \tag{39c}$$

$$\zeta(-2k) = 0, \quad \forall\ k\in\mathbb{N}^\star, \tag{39d}$$

$$\zeta'(-2k) = \frac{(-1)^k\zeta(2k+1)(2k)!}{2^{2k+1}\pi^{2k}}, \quad \forall\ k\in\mathbb{N}^\star. \tag{39e}$$

Remembering Eq. (9), we then obtain the result

$$\begin{aligned}B_\beta(\ell,\omega_m) \sim -B_0(\ell,\omega_m) - \frac{1}{8\pi^2}\ln\frac{4\pi T}{Me^{\gamma}} \\ - \frac{\zeta(3)}{2^7\pi^4}\left(M^2+\frac{\ell^2}{6}\right)\frac{1}{T^2},\end{aligned} \tag{40}$$

revealing that at extremely high temperatures the original contribution from zero temperature is not present anymore. This has a major impact and is responsible for the disappearance of the renormalons. Therefore, we may write

$$B(\ell,\omega_m)\overset{T\to\infty}{\sim} -\frac{1}{8\pi^2}\ln\frac{4\pi T}{Me^\gamma}-\frac{\zeta(3)}{2^7\pi^4}\left(M^2+\frac{\ell^2}{6}\right)\frac{1}{T^2}. \quad (41)$$

If we replace this back into the necklace expression $R_k(p,o)$, in Eq. (23), we get

$$R_k(p,\omega_o) = -g(p^2+\omega_o)^2\left(\frac{g}{2(4\pi)^2N}\right)^{k-1}\frac{1}{\beta} \times \sum_{n\in\mathbb{Z}}\int\frac{d^3\ell}{(2\pi)^3}\frac{\ln^{k-1}(\frac{4\pi T}{Me^\gamma})}{(\ell^2+\omega_n^2+M^2)^3}. \quad (42)$$

Since the integration over the internal loop is independent of k we find that

$$R_k \propto \left(2\tilde{g}\ln\left(\frac{4\pi T}{Me^\gamma}\right)\right)^{k-1}, \quad (43)$$

and, therefore, there is no renormalon in this case.

The function $\Sigma(g)=\sum_{k=1}^{\infty}R_k(p)$ is Borel summable,

$$\Sigma\sim\frac{1}{1-2\tilde{g}\ln(\frac{4\pi T}{Me^\gamma})};$$

it is a meromorphic function of the coupling constant $\tilde{g}$ having a simple pole at $\tilde{g}=[2\ln(4\pi T/(Me^\gamma))]^{-1}$.

VI. CONCLUSION

In this article we study the existence of renormalons in a scalar field theory with a $g\phi_4^4$ coupling at next-to-leading order in a large-N expansion. The results in the literature report that there is one renormalon pole at zero temperature (located at $y=1/\tilde{g}$) and there is an appearance of a countable infinite set of renormalons at low temperatures with the property that the poles are thermal-independent (located at $y=i/\tilde{g}$, for $i\in\mathbb{N}^\star$). Although, in this article, the standard behavior is reproduced, we also manage to identify the existence of hidden poles, both at zero temperature and at low temperatures. As far as we know, it seems that this fact has not been noted in the literature. Perhaps, these poles were hidden by the approximations used. The extra pole at zero temperature is slightly shifted on the real axis ($y=2/\tilde{g}$) and can be ignored, as it is done currently in the literature, if the coupling is small enough. At low temperatures, however, there is an entirely new set of renormalons on the real axis that are located at $y=n\beta/2\tilde{g}$ for $n\in\mathbb{N}^\star$. The appearance of renormalons with a small increase in temperature is a remarkable feature of the theory. In this paper we claim that we have mapped all the poles that occur at low temperatures, therefore identifying completely the thermal renormalons that appear. Any further approximation would only improve the value of the residues, but would not modify the number nor the position of the poles in the Borel plane.

Furthermore, we obtain that at extremely high temperatures, which is related to a dimensional reduction from $D=4$ to $D=3$, as expected, no renormalon singularities occur and the series becomes Borel summable. This seems to indicate that we could speculate about the existence of a "critical temperature" at which renormalons appear/disappear. This will be the subject of investigation in future work.

ACKNOWLEDGMENTS

The authors thank the Brazilian agency Conselho Nacional de Desenvolvimento Científico e Tecnológico (CNPq) for partial financial support.

[1] *Large Order Behavior of Perturbation Theory*, edited by J. C. Le Guillou and J. Zinn-Justin (North Holland, Amsterdam, 2013), p. 580.
[2] I. Aniceto and R. Schiappa, Commun. Math. Phys. **335**, 183 (2015).
[3] A. Grassi, M. Marino, and S. Zakany, J. High Energy Phys. 05 (2015) 038.
[4] A. Cherman, D. Dorigoni, and M. Ünsal, J. High Energy Phys. 10 (2015) 056.
[5] D. Dorigoni, arXiv:1411.3585.
[6] C. M. Bender and S. A. Orszag, *Advanced Mathematical Methods for Scientists and Engineers I* (Springer, New York, 1999).
[7] V. Rivasseau, *From Perturbative to Constructive Renormalization* (Princeton University Press, Princeton, NJ, 1991).
[8] F. C. Khanna, A. P. C. Malbouisson, J. M. C. Malbouisson, and A. R. Santana, *Thermal Quantum Field Theory—Algebraic Aspects and Applications* (World Scientific Publishing, Singapore, 2009).
[9] B. Hirsbrunner, La sommabilité selon Borel et son application en théorie des champs, Ph.D. thesis, Université de Lausanne—Faculté des Sciences, 1981.
[10] F. David, J. Feldman, and V. Rivasseau, Commun. Math. Phys. **116**, 215 (1988).
[11] G. 't Hooft, *The Whys of Subnuclear Physics*, The Subnuclear Series Vol. 15, edited by A. L. Zichichi (Springer, New York, 1979), p. 943.
[12] M. Shifman, Int. J. Mod. Phys. A **30**, 1543001 (2015).
[13] M. Beneke and V. M. Braun, Nucl. Phys. **B426**, 301 (1994).
[14] M. M. Anber and T. Sulejmanpasic, J. High Energy Phys. 01 (2015) 139.
[15] M. Shifman and M. Ünsal, Phys. Rev. D **78**, 065004 (2008).
[16] A. P. C. Malbouisson, J. M. C. Malbouisson, A. E. Santana, and J. C. da Silva, Phys. Lett. B **583**, 373 (2004).

[17] F. C. Khanna, A. P. C. Malbouisson, J. M. C. Malbouisson, and A. E. Santana, Phys. Rev. D **85**, 085015 (2012).
[18] J. Zinn-Justin, *Quantum Field Theory and Critical Phenomena*, 4th ed. (Clarendon Press, Oxford, 2002).
[19] E. Elizalde, *Ten Physical Applications of Spectral Zeta Functions*, 2nd ed. (Springer-Verlag, Berlin Heidelberg, 1995).
[20] C. Itzykson and J. B. Zuber, *Physics* (McGraw-Hill, New York, 1980).
[21] I. S. Gradshteyn and I. M. Ryzhik, *Table of Integrals, Series, and Products*, 7th ed. (Academic Press, New York, 2007).
[22] M. S. Milgram, Math. Comput. **44**, 443 (1985).
[23] M. Loewe and C. Valenzuela, Mod. Phys. Lett. A **15**, 1181 (2000).

Chapter 5

Dimensional reduction of a finite-size scalar field model at finite temperature

Published as:
E. Cavalcanti, J.A. Lourenço, C.A. Linhares, and A.P.C. Malbouisson. Physical Review D **99**, 025007 (2019) *Dimensional reduction of a finite-size scalar field model at finite temperature*

PHYSICAL REVIEW D **99,** 025007 (2019)

Dimensional reduction of a finite-size scalar field model at finite temperature

E. Cavalcanti,[1,*] J. A. Lourenço,[2,†] C. A. Linhares,[3,‡] and A. P. C. Malbouisson[1,§]
[1]*Centro Brasileiro de Pesquisas Físicas/MCTI, Rio de Janeiro, RJ 22290-180, Brazil*
[2]*Departamento de Ciências Naturais, Universidade Federal do Espírito Santo, Campus São Mateus, ES 29932-540, Brazil*
[3]*Instituto de Física, Universidade do Estado do Rio de Janeiro, Rio de Janeiro, RJ 20559-900, Brazil*

(Received 30 November 2018; published 8 January 2019)

We investigate the process of dimensional reduction of one spatial dimension in a thermal scalar field model defined in D dimensions (inverse temperature and $D-1$ spatial dimensions). We obtain that a thermal model in D dimensions with one of the spatial dimensions having a finite size L is related to the finite-temperature model with just $D-1$ spatial dimensions and no finite size. Our results are obtained for one-loop calculations and for any dimension D. For example, in $D=4$ we have a relationship between a thin film with thickness L at finite temperature and a surface at finite temperature. We show that, although a strict dimensional reduction is not allowed, it is possible to define a valid prescription for this procedure.

DOI: 10.1103/PhysRevD.99.025007

I. INTRODUCTION

Dimensional reduction states that by considering a model in D dimensions we can obtain—following some prescription—a theory with fewer dimensions. One approach is to take a model with a compactified dimension and investigate its behavior when the size of the compactified dimension is reduced to zero.

Let us consider the case of a finite-temperature field theory using the imaginary-time formalism. Temperature is introduced by compactifying the imaginary-time variable using periodic or antiperiodic boundary conditions, respectively, for bosons or fermions. In this context, dimensional reduction would be equivalent to a high-temperature limit. This idea was proposed long ago by Appelquist and Pisarski [1] and later formulated in more detail by Landsman [2]. This idea is currently accepted and understood [3,4]. However, up to now, we think that there is a lack of investigation on this topic when one is interested in a greater number of compactifications.

We might ask how a system in arbitrary D dimensions with two compactified dimensions—one corresponding to the inverse temperature $\beta = 1/T$ and the other with a finite size L—behave when $L \to 0$. However, strictly speaking, in the context of both first-order and second-order phase transitions, it can be shown that the limit of $L \to 0$ cannot be fully attained [5]. There have been many works in the context of phase transitions in thin films using different models (Ginzburg-Landau, Nambu-Jona-Lasinio, Gross-Neveu, and others; see Refs. [6–16]) that indicate the existence of a minimal thickness below which no phase transitions occur. Reference [6] also strengthened this indication by comparing a phenomenological model for superconducting thin films using a Ginzburg-Landau model with experimental results. Therefore, this is a direct indication that the physics of surfaces and thin films are different and one cannot achieve a surface from a thin film.

In this article, we investigate the problem of dimensional reduction from a mathematical physics perspective, e.g., to investigate the relationship between systems in the form of "films" and "surfaces." Here this is generalized so that we investigate the relation between D-dimensional and $D-1$-dimensional scenarios.

To study a quantum field theory at finite temperature and finite size, we use the formalism of quantum field theory in spaces with toroidal topologies [5,17]. As a first investigation, we consider a scalar field model at the one-loop level. We obtain a remarkably simple relationship between the following situations:

(1) Starting with a space in D dimensions, we consider two compactifications: one of the dimensions corresponds to the inverse temperature $1/T$ and another corresponds to a finite size L, while the other $D-2$ dimensions are of infinite size.

(2) Another possibility is to eliminate one spatial dimension from the beginning; starting in a space with $D-1$ dimensions, we consider one compactification corresponding to the inverse temperature $1/T$.

*erich@cbpf.br
†jose.lourenco@ufes.br
‡linharescesar@gmail.com
§adolfo@cbpf.br

This should, e.g., provide us with a relation between surfaces and thin films for $D = 4$. Furthermore, from a mathematical physics perspective, we also investigate the possibility of fractal dimensions.

II. THE MODEL

In this article, we take a scalar field theory with a quartic interaction in D dimensions with Euclidean action,

$$S_E = \int d^D x \left\{ \frac{1}{2}(\partial\phi)^2 + \frac{M^2}{2}\phi^2 + \frac{\lambda}{4!}\phi^4 \right\}. \tag{1}$$

We shall only discuss the one-loop Feynman amplitude $\mathcal{I}$ with ρ propagators and zero external momenta,

$$\mathcal{I}_\rho^D(M^2) = \int \frac{d^D p}{(2\pi)^D} \frac{1}{(p^2 + M^2)^\rho}. \tag{2}$$

In particular, $\rho = 1$ corresponds to the tadpole contribution to the effective mass and $\rho = 2$ corresponds to the first-order correction to the coupling constant. We introduce periodic boundary conditions on $d < D$ coordinates. The compactification of the imaginary time introduces the inverse temperature $\beta = 1/T \equiv L_0$ and the compactification of the spatial coordinates introduces the characteristic lengths L_i. Thus, the amplitude becomes

$$\mathcal{I}_\rho^{D,d}(M^2; L_\alpha) = \frac{1}{\prod_{\alpha=0}^{d-1} L_\alpha} \sum_{n_0,\ldots,n_{d-1}=-\infty}^{\infty} \int \frac{d^{D-d} q}{(2\pi)^{D-d}} \frac{1}{[q^2 + M^2 + \sum_{\alpha=0}^{d-1} (\frac{2\pi n_\alpha}{L_\alpha})^2]^\rho}. \tag{3}$$

We compute the remaining integrals on the $(D - d)$-dimensional subspace using dimensional regularization. The remaining infinite sum can be identified as an Epstein-Hurwitz zeta function [18] and leads—after an analytic continuation—to the sum over modified Bessel functions of the second kind $K_\nu(x)$; see Refs. [5,19] for further details. The function $\mathcal{I}_\rho^{D,d}(M^2; L_\alpha)$ in the case of $d = 2$ reads

$$\mathcal{I}_\rho^{D,2}(M^2; \beta, L) = \frac{(M^2)^{-\rho+\frac{D}{2}}\Gamma[\rho - \frac{D}{2}]}{(4\pi)^{\frac{D}{2}}\Gamma[\rho]} + \frac{\mathcal{W}_{\frac{D}{2}-\rho}(M^2; \beta, L)}{(2\pi)^{\frac{D}{2}} 2^{\rho-2}\Gamma[\rho]}, \tag{4}$$

where

$$\mathcal{W}_\nu(M^2; \beta, L) = \sum_{n=1}^{\infty} \left(\frac{M}{n\beta}\right)^\nu K_\nu(n\beta M) + \sum_{n=1}^{\infty} \left(\frac{M}{nL}\right)^\nu K_\nu(nLM) + 2 \sum_{n_0,n_1=1}^{\infty} \left(\frac{M}{\sqrt{n_0^2\beta^2 + n_1^2 L^2}}\right)^\nu K_\nu\left(M\sqrt{n_0^2\beta^2 + n_1^2 L^2}\right), \tag{5}$$

with $\nu = \frac{D}{2} - \rho$.

As in Ref. [20], we investigate these infinite sums using a representation of the modified Bessel function in the complex plane,

$$K_\nu(X) = \frac{1}{4\pi i} \int_{c-i\infty}^{c+i\infty} dt\, \Gamma(t)\Gamma(t-\nu) \left(\frac{X}{2}\right)^{-2t+\nu}. \tag{6}$$

We remark that c is a point located on the positive real axis that has a greater value than all of the poles of the gamma function. With this definition, it is clear that $c > \max[0, \nu]$. However, we extend this definition so that we are allowed to interchange the integral over t and the summation over n. Therefore, c must be chosen in such a way that there is no pole located to the right of it. Substituting Eq. (6) into Eq. (5), we obtain

$$\begin{aligned} \mathcal{W}_\nu(M^2; \beta, L) = {} & \frac{1}{4\pi i} \int_{c-i\infty}^{c+i\infty} dt\, \Gamma(t)\Gamma(t-\nu)\zeta(2t) \left(\frac{M^2}{2}\right)^\nu \left[\left(\frac{M\beta}{2}\right)^{-2t} + \left(\frac{ML}{2}\right)^{-2t} \right] \\ & + \frac{1}{2\pi i} \int_{c-i\infty}^{c+i\infty} dt\, \Gamma(t)\Gamma(t-\nu) \left(\frac{M^2}{2}\right)^\nu \left(\frac{M}{2}\right)^{-2t} \sum_{n_0,n_1=1}^{\infty} (n_0^2\beta^2 + n_1^2 L^2)^{-t}. \end{aligned} \tag{7}$$

The double sum in Eq. (7) is known and has the analytical extension [18]

$$\sum_{n_0,n_1=1}^{\infty}(n_0^2\beta^2+n_1^2L^2)^{-t}=-\frac{\zeta(2t)}{2L^{2t}}+\frac{\sqrt{\pi}L}{2\beta}\frac{\Gamma(t-\frac{1}{2})\zeta(2t-1)}{\Gamma(t)L^{2t}}+\frac{2\pi^t}{\Gamma(t)}\sum_{n_0,n_1=1}^{\infty}\left(\frac{n_0}{n_1}\right)^{t-\frac{1}{2}}\sqrt{\frac{L}{\beta}}\frac{1}{(\beta L)^t}K_{t-\frac{1}{2}}\left(2\pi n_0 n_1\frac{L}{\beta}\right). \quad (8)$$

After substituting Eq. (8) into Eq. (7) and taking into account Eq. (6), we finally obtain the integral representation in the complex plane for the function $\mathcal{W}_\nu$ as the sum of these terms:

$$\left(\frac{2}{M^2}\right)^{\nu}\mathcal{W}_\nu=\mathcal{W}_\nu^{(1)}+\mathcal{W}_\nu^{(2)}+\mathcal{W}_\nu^{(3)},\quad \text{where}$$

$$\mathcal{W}_\nu^{(1)}=\frac{1}{4\pi i}\int_{c-i\infty}^{c+i\infty}dt\,\Gamma(t)\Gamma(t-\nu)\zeta(2t)\left(\frac{M\beta}{2}\right)^{-2t},$$

$$\mathcal{W}_\nu^{(2)}=\frac{\sqrt{\pi}L}{4\pi i\beta}\int_{c-i\infty}^{c+i\infty}dt\,\Gamma(t-\nu)\Gamma\left(t-\frac{1}{2}\right)\zeta(2t-1)\left(\frac{ML}{2}\right)^{-2t},$$

$$\mathcal{W}_\nu^{(3)}=\frac{1}{2\pi i}\sum_{k=0}^{\infty}\frac{(-1)^k}{\Gamma(k+1)}\left(\frac{M\beta}{2\pi}\right)^{2k-2\nu}\int_{c-i\infty}^{c+i\infty}\frac{dt}{\sqrt{\pi}}\Gamma(t)\zeta(2t)\Gamma\left(t-\nu+k+\frac{1}{2}\right)\zeta(2t-2\nu+2k+1)\left(\frac{\pi L}{\beta}\right)^{-2t}. \quad (9)$$

The next step is to determine the positions of the poles of the functions in the complex-plane integrals and compute their residues. We see that the positions of the poles depend on the value of ν. We compute the integrals for the following specific cases:

(1) Integer ν, related to an even number of dimensions D.
(2) Half-integer ν, related to an odd number of dimensions D.
(3) Other real values of ν (for completeness), which can be thought of as related to fractal dimensions D.

In this article we consider two different scenarios. The first scenario involves a model in D dimensions with two compactified dimensions: one related to the inverse temperature $\beta=1/T$ and the other with a finite size L. For this case we need the function $\mathcal{W}_\nu$ [as defined in Eq. (9)] and Eq. (4). The second scenario involves a model in $D-1$ dimensions with just one compactified dimension which is related to the inverse temperature. We see that the amplitude only requires the knowledge of $\mathcal{W}_\nu^{(1)}$,

$$\mathcal{I}_\rho^{D-1,1}(M^2;\beta)=\frac{(\frac{M^2}{2})^{\frac{D}{2}-\rho}}{(2\pi)^{\frac{D}{2}}2^{\rho-2}\Gamma[\rho]}\left\{\frac{\sqrt{\pi}}{2M}\Gamma\left(\rho-\frac{D}{2}+\frac{1}{2}\right)+\frac{2\sqrt{\pi}}{M}\mathcal{W}^{(1)}_{\frac{D}{2}-\frac{1}{2}-\rho}(M^2;\beta)\right\}. \quad (10)$$

To avoid a lengthy exposition, we only show the final expressions for each case. For integer ν the function $\mathcal{W}_\nu^{(1)}$ reads

$$\mathcal{W}_\nu^{(1)}=\frac{\sqrt{\pi}}{2M\beta}\Gamma\left(\frac{1}{2}-\nu\right)+\frac{1}{2}\mathcal{S}_0^{(3)}\left(\nu;\frac{M\beta}{2}\right)+\frac{1}{2}\mathcal{S}^{(2)}\left(\nu;\frac{M\beta}{4\pi}\right)+\begin{cases}-\frac{1}{4}\Gamma(-\nu) & \nu<0,\\ -\frac{(-1)^\nu}{4\Gamma(\nu+1)^2}\begin{bmatrix}\nu+1\\2\end{bmatrix}+\frac{(-1)^\nu}{2\Gamma(\nu+1)}\left(\gamma+\ln\frac{M\beta}{4\pi}\right) & \nu\geq 0,\end{cases} \quad (11)$$

and $\mathcal{W}_\nu$ reads

$$\left(\frac{2}{M^2}\right)^\nu \mathcal{W}_\nu = +\frac{1}{2}\mathcal{S}^{(2)}\left(\nu;\frac{ML}{4\pi}\right) + \frac{1}{2}\mathcal{S}_1^{(3)}\left(\nu;\frac{ML}{2}\right) - \frac{2\pi}{M^2\beta L}\left\{\mathcal{S}^{(1)}\left(\nu;\frac{M\beta}{2\pi}\right) + \mathcal{S}^{(4)}(\nu;M\beta)\right\}$$
$$+\begin{cases} -\frac{1}{4}\Gamma(-\nu) & \nu < 0, \\ +\frac{(-1)^\nu}{2\Gamma(\nu+1)}\left\{-\frac{1}{2\Gamma(\nu+1)}\begin{bmatrix}\nu+1\\2\end{bmatrix} + \gamma + \ln\frac{ML}{4\pi} + \frac{\pi}{6}\frac{\beta}{L}\right\} & \nu \geq 0, \\ +\frac{\pi}{M^2\beta L}\Gamma(-\nu+1) & \nu < 1, \\ +\frac{\pi}{M^2\beta L}\frac{(-1)^\nu}{\Gamma(\nu)}\left\{-\frac{1}{\Gamma(\nu)}\begin{bmatrix}\nu\\2\end{bmatrix} + 2\ln M\beta - \frac{\pi}{3}\frac{\beta}{L}\right\} & \nu \geq 1. \end{cases} \tag{12}$$

Here the notation $\begin{bmatrix}a\\2\end{bmatrix}$ indicates the unsigned Stirling number of the first kind:

$$\begin{bmatrix}1\\2\end{bmatrix} = 0, \qquad \begin{bmatrix}2\\2\end{bmatrix} = 1, \qquad \begin{bmatrix}3\\2\end{bmatrix} = 3, \qquad \begin{bmatrix}4\\2\end{bmatrix} = 11, \qquad \begin{bmatrix}5\\2\end{bmatrix} = 50.$$

In the above expressions, the functions $\mathcal{S}^{(1)}$, $\mathcal{S}^{(2)}$, $\mathcal{S}^{(3)}$, and $\mathcal{S}^{(4)}$ are defined by

$$\mathcal{S}_i^{(1)}(\nu;\alpha) = \sum_{k=1+i}^{\infty}(-1)^{k+\nu}\frac{\Gamma(k)\zeta(2k)}{\Gamma(k+\nu)}\alpha^{2k}, \tag{13}$$

$$\mathcal{S}^{(2)}(\nu;\alpha) = \sum_{k=1}^{\infty}(-1)^{k+\nu}\frac{\Gamma(2k+1)\zeta(2k+1)}{\Gamma(k+1)\Gamma(k+\nu+1)}\alpha^{2k}, \tag{14}$$

$$\mathcal{S}_i^{(3)}(\nu;\alpha) = \sum_{k=1+i}^{\nu}(-1)^{\nu-k}\frac{\Gamma(k)\zeta(2k)}{\Gamma(\nu-k+1)}\alpha^{-2k}, \tag{15}$$

$$\mathcal{S}^{(4)}(\nu;\alpha) = \sum_{k=1}^{\nu-1}(-1)^{\nu-k}\frac{\Gamma(2k+1)\zeta(2k+1)}{\Gamma(k+1)\Gamma(\nu-k)}\alpha^{-2k}. \tag{16}$$

For half-integer values of ν ($\nu = \mu + 1/2$, for integer μ), we obtain

$$\mathcal{W}_\nu^{(1)} = -\frac{1}{4}\Gamma\left(-\frac{1}{2}-\mu\right) - \frac{\sqrt{\pi}}{M\beta}\mathcal{S}^{(4)}(\mu+1;M\beta) - \frac{\sqrt{\pi}}{M\beta}\mathcal{S}_0^{(1)}\left(\mu+1;\frac{M\beta}{2\pi}\right)$$
$$+\begin{cases} +\frac{\sqrt{\pi}}{2M\beta}\Gamma(-\mu) & \mu < 0, \\ +\frac{\sqrt{\pi}}{2M\beta}\frac{(-1)^\mu}{\Gamma(\mu+1)}\left(\begin{bmatrix}1+\mu\\2\end{bmatrix}\frac{1}{\Gamma(\mu+1)} - \ln M\beta\right) & \mu \geq 0, \end{cases} \tag{17}$$

and

$$\mathcal{W}_\nu\left(\frac{2}{M^2}\right)^\nu = -\frac{1}{4}\Gamma\left(-\frac{1}{2}-\mu\right) + \frac{\pi}{M^2\beta L}\Gamma\left(\frac{1}{2}-\mu\right) + \frac{\sqrt{\pi}}{ML}\frac{(-1)^\mu}{\Gamma(\mu+1)}\left(\gamma + \ln\frac{\beta}{4\pi L}\right)$$
$$-\frac{\sqrt{\pi}}{ML}\mathcal{S}_0^{(1)}\left(\mu+1;\frac{ML}{2\pi}\right) + \frac{\sqrt{\pi}}{ML}\mathcal{S}^{(2)}\left(\mu;\frac{M\beta}{4\pi}\right) - \frac{\sqrt{\pi}}{ML}\mathcal{S}^{(4)}(\mu+1;ML) + \frac{\sqrt{\pi}}{ML}\mathcal{S}_0^{(3)}\left(\mu;\frac{M\beta}{2}\right). \tag{18}$$

Finally, for other real values of the index ν that are neither integer nor half-integer, we have

$$\mathcal{W}_\nu^{(1)} = \frac{1}{2}\left[\frac{\sqrt{\pi}}{M\beta}\Gamma\left(\frac{1}{2}-\nu\right) - \frac{1}{2}\Gamma(-\nu) + \sum_{k=0}^{\infty}\frac{(-1)^k}{\Gamma(k+1)}\Gamma(\nu-k)\zeta(2\nu-2k)\left(\frac{M\beta}{2}\right)^{-2\nu+2k}\right] \tag{19}$$

and

$$\mathcal{W}_\nu\left(\frac{2}{M^2}\right)^\nu = -\frac{1}{4}\Gamma(-\nu) + \frac{\pi}{M^2\beta L}\Gamma(1-\nu) + \frac{1}{2}\sum_{k=0}^{\infty}\frac{(-1)^k}{\Gamma(k+1)}\Gamma(\nu-k)\zeta(2\nu-2k)\left[\left(\frac{M\beta}{2}\right)^{-2\nu+2k} + \left(\frac{ML}{2}\right)^{-2\nu+2k}\right]$$
$$+ \frac{\sqrt{\pi}L}{2\beta}\sum_{k=0}^{\infty}\frac{(-1)^k}{\Gamma(k+1)}\Gamma\left(\nu-k-\frac{1}{2}\right)\zeta(2\nu-2k-1)\left[\left(\frac{M\beta}{2}\right)^{2k-2\nu} - \left(\frac{ML}{2}\right)^{2k-2\nu}\right]$$
$$+ \sum_{k=0}^{\infty}\frac{(-1)^k}{\Gamma(k+1)}\left(\frac{M\beta}{2\pi}\right)^{2k-2\nu}\left[\frac{\beta}{2\pi L}\Gamma(1-\nu+k)\zeta(2-2\nu+2k) - \frac{1}{2\sqrt{\pi}}\Gamma\left(\frac{1}{2}-\nu+k\right)\zeta(1-2\nu+2k)\right]. \quad (20)$$

So far we have managed to take both situations into account, i.e., one or two compactified dimensions. Let us remember that we are interested in the one-loop Feynman diagram with ρ internal lines and at zero external momentum. The amplitude in the scenario with two compactifications (one related to the inverse temperature $\beta = 1/T$ and another to a finite size L) is given by Eq. (4), and the amplitude in the scenario in which there are $D-1$ dimensions and just one compactification related to the inverse temperature β is given by Eq. (10).

In the following, we investigate, for any value of ν, the relationship between both scenarios. The contribution from $\Gamma(-\nu)$ in the amplitude is divergent for integer values of $\nu \geq 0$. To avoid the presence of poles in physical quantities we employ the modified minimal subtraction scheme [21], and the function $\Gamma(-\nu)$ is replaced by $\bar{\Gamma}(-\nu)$ such that

$$\bar{\Gamma}(-\nu) = -\frac{(-1)^{\nu+1}}{\Gamma(\nu+1)^2}\begin{bmatrix}\nu+1\\2\end{bmatrix}, \qquad \nu \geq 0. \quad (21)$$

III. DIMENSIONAL REDUCTION

We have considered a class of one-loop Feynman diagrams with ρ internal lines in D dimensions. Their contributions involve the above-defined functions $\mathcal{W}_\nu$, where the index ν is given by $\nu = D/2 - \rho$. In the previous section we managed to obtain the final version of $\mathcal{W}_\nu$ in terms of some analytical functions and sums over the Riemann zeta function in the argument. This was done for the specific cases of integer values of ν (useful for even dimensions), half-integer values of ν (for odd dimensions), and other real values of ν (for completeness, and which can be considered for models with fractal dimensions).

Taking the situation with D dimensions and letting two of them be compactified, which introduces the temperature $1/\beta$ and a finite length L, one might ask how the function behaves as one takes the limit $L \to 0$. This can be interpreted as a "dimensional reduction." In general, what happens is that the function $\mathcal{W}_\nu(\beta, L)$ diverges as $L \to 0$. However, if we interpret the procedure of "dimensional reduction" as taking the dominant contribution[1] in β in the limit $L \to 0$ and ignore the remaining dependence on the finite length, we obtain the relation

$$L\mathcal{I}_\rho^{D,2}(M^2;\beta,L)|_{L\to 0} = \mathcal{I}_\rho^{D-1,1}(M^2;\beta) + \text{divergent terms}. \quad (22)$$

This relation holds for any real value of D, which will be shown in the following subsections. The divergent behavior of $\mathcal{I}$ in Eq. (22) as L goes to zero depends on the quantity $D/2 - \rho$.

A. Integer ν, even D

To investigate the so-called dimensional reduction we first consider the case with integer values of ν, which corresponds to even dimensions D. The amplitude of a one-loop Feynman diagram in a scenario with both finite temperature and finite size is given by Eq. (4). To study its behavior we substitute Eq. (12) into Eq. (4) and split its contributions coming from the three functions $\mathcal{F}_1$, $\mathcal{G}_1$, and $\mathcal{H}_1$, such that

$$L\mathcal{I}_\rho^{D,2}(M^2;\beta,L) = \frac{L}{(2\pi)^{\frac{D}{2}}2^{\rho-2}\Gamma(\rho)} \times \left[\left(\frac{M^2}{2}\right)^{\frac{D}{2}-\rho}\frac{\Gamma(\rho-\frac{D}{2})}{4} + \mathcal{W}_{\frac{D}{2}-\rho}\right]$$
$$= \left(\frac{M^2}{2}\right)^{\frac{D}{2}-\rho}\frac{\mathcal{F}_1+\mathcal{G}_1+\mathcal{H}_1}{(2\pi)^{\frac{D}{2}}2^{\rho-2}\Gamma(\rho)}. \quad (23)$$

The function $\mathcal{H}_1$ is the contribution that vanishes in the $L \to 0$ limit:

$$\mathcal{H}_1 = \frac{L}{2}\mathcal{S}^{(2)}\left(\frac{D}{2}-\rho;\frac{ML}{4\pi}\right) + \frac{(-1)^{\frac{D}{2}-\rho}L}{2\Gamma(\frac{D}{2}-\rho+1)}\left(\gamma + \ln\frac{ML}{4\pi}\right). \quad (24)$$

[1]This is a stronger result for integer dimension D as the divergent terms do not depend on β. However, this is not the case for a noninteger dimension D as it can depend on the temperature.

Note that the zero-temperature contribution was consistently subtracted. The divergent behavior as L goes to zero is given by $\mathcal{G}_1$,

$$\mathcal{G}_1 = -\frac{(-1)^{\frac{D}{2}-\rho}}{\Gamma(\frac{D}{2}-\rho)}\frac{\pi^2}{3M^2L} + \frac{L}{2}\mathcal{S}_1^{(3)}\left(\frac{D}{2}-\rho;\frac{ML}{2}\right). \tag{25}$$

Finally, the function $\mathcal{F}_1$ is the contribution that survives during the *dimensional reduction* and does not diverge,

$$\begin{aligned}\mathcal{F}_1 = &-\frac{2\pi}{M^2\beta}\left[\mathcal{S}_1^{(1)}\left(\frac{D}{2}-\rho;\frac{M\beta}{2\pi}\right) + \mathcal{S}^{(4)}\left(\frac{D}{2}-\rho;M\beta\right)\right] + \frac{\pi\beta}{12}\frac{(-1)^{\frac{D}{2}-\rho}}{\Gamma(\frac{D}{2}-\rho+1)} \\ &+ \begin{cases} \frac{\pi}{M^2\beta}\Gamma\left(1-\frac{D}{2}+\rho\right), & \frac{D}{2}\leq\rho, \\ \frac{\pi}{M^2\beta}\frac{(-1)^{\frac{D}{2}-\rho}}{\Gamma(\frac{D}{2}-\rho)}\left(-\frac{1}{\Gamma(\frac{D}{2}-\rho)}\begin{bmatrix}\frac{D}{2}-\rho \\ 2\end{bmatrix} + 2\ln M\beta\right), & \frac{D}{2}>\rho. \end{cases}\end{aligned} \tag{26}$$

Therefore, as the $L\to 0$ limit is taken the contribution $\mathcal{H}_1$ vanishes and the divergent behavior in L is given by the function $\mathcal{G}_1$:

$$L\mathcal{I}_\rho^{D,2}(M^2;\beta,L)|_{L\to 0} = \frac{1}{(2\pi)^{\frac{D}{2}}2^{\rho-2}\Gamma(\rho)}L\mathcal{W}_{\frac{D}{2}-\rho}|_{L\to 0} = \left(\frac{M^2}{2}\right)^{\frac{D}{2}-\rho}\frac{\mathcal{F}_1+\mathcal{G}_1}{(2\pi)^{\frac{D}{2}}2^{\rho-2}\Gamma(\rho)}. \tag{27}$$

On the other hand, let us consider the second case in which we start from a scenario with one less dimension, $D-1$. The amplitude of the one-loop Feynman diagram is simply Eq. (10), written here as

$$\mathcal{I}_\rho^{D-1,1}(M^2;\beta) = \frac{(\frac{M^2}{2})^{\frac{D}{2}-\rho}}{(2\pi)^{\frac{D}{2}}2^{\rho-2}\Gamma[\rho]}\left\{\frac{\sqrt{\pi}}{2M}\Gamma\left(\rho-\frac{D}{2}+\frac{1}{2}\right) + \frac{2\sqrt{\pi}}{M}\mathcal{W}^{(1)}_{\frac{D}{2}-\frac{1}{2}-\rho}(M^2;\beta)\right\}. \tag{28}$$

And, for even dimensions D, we get that $\frac{D}{2}-\frac{1}{2}-\rho$ is a half-integer. So, we use Eq. (17) with $\mu=\frac{D}{2}-\rho-1$ and obtain

$$\begin{aligned}\mathcal{W}^{(1)}_{\frac{D}{2}-\frac{1}{2}-\rho} = &-\frac{1}{4}\Gamma\left(\frac{1}{2}-\frac{D}{2}+\rho\right) + \frac{\sqrt{\pi}}{2M\beta}\Gamma\left(-\frac{D}{2}+\rho+1\right) + \frac{\sqrt{\pi}}{2M\beta}\frac{(-1)^{\frac{D}{2}-\rho-1}}{\Gamma(\frac{D}{2}-\rho)}\left(\begin{bmatrix}\frac{D}{2}-\rho \\ 2\end{bmatrix}\frac{1}{\Gamma(\frac{D}{2}-\rho)} - 2\ln M\beta\right) \\ &-\frac{\sqrt{\pi}}{M\beta}\mathcal{S}^{(4)}\left(\frac{D}{2}-\rho;M\beta\right) - \frac{\sqrt{\pi}}{M\beta}\mathcal{S}_0^{(1)}\left(\frac{D}{2}-\rho;\frac{M\beta}{2\pi}\right).\end{aligned} \tag{29}$$

Therefore, Eq. (28) becomes

$$\begin{aligned}\mathcal{I}_\rho^{D-1,1}(M^2;\beta) = \frac{(\frac{M^2}{2})^{\frac{D}{2}-\rho}}{(2\pi)^{\frac{D}{2}}2^{\rho-2}\Gamma[\rho]}&\left\{\frac{\pi}{M^2\beta}\Gamma\left(\rho-\frac{D}{2}+1\right) + \frac{\pi}{M^2\beta}\frac{(-1)^{\frac{D}{2}-\rho-1}}{\Gamma(\frac{D}{2}-\rho)}\left(\begin{bmatrix}\frac{D}{2}-\rho \\ 2\end{bmatrix}\frac{1}{\Gamma(\frac{D}{2}-\rho)} - 2\ln M\beta\right)\right. \\ &\left.-\frac{2\pi}{M^2\beta}\mathcal{S}^{(4)}\left(\frac{D}{2}-\rho;M\beta\right) - \frac{2\pi}{M^2\beta}\mathcal{S}_0^{(1)}\left(\frac{D}{2}-\rho;\frac{M\beta}{2\pi}\right)\right\}.\end{aligned} \tag{30}$$

Furthermore, since $\frac{2\pi}{M^2\beta}\mathcal{S}_0^{(1)}(\frac{D}{2}-\rho;\frac{M\beta}{2\pi}) = \frac{2\pi}{M^2\beta}\mathcal{S}_1^{(1)}(\frac{D}{2}-\rho;\frac{M\beta}{2\pi}) - \frac{\pi\beta}{12}\frac{(-1)^{\frac{D}{2}-\rho}}{\Gamma(\frac{D}{2}-\rho+1)}$, by direct comparison with $\mathcal{F}_1$ we get

$$\mathcal{I}_\rho^{D-1,1}(M^2;\beta) = \frac{(\frac{M^2}{2})^{\frac{D}{2}-\rho}}{(2\pi)^{\frac{D}{2}}2^{\rho-2}\Gamma[\rho]}\mathcal{F}_1. \tag{31}$$

Then we find the relation

$$L\mathcal{I}_\rho^{D,2}(M^2;\beta,L)|_{L\to 0} = \mathcal{I}_\rho^{D-1,1}(M^2;\beta) + \left(\frac{M^2}{2}\right)^{\frac{D}{2}-\rho}\frac{\mathcal{G}_1}{(2\pi)^{\frac{D}{2}}2^{\rho-2}\Gamma(\rho)} = \mathcal{I}_\rho^{D-1,1}(M^2;\beta) + \mathcal{O}(L^{-1}). \tag{32}$$

The asymptotic behavior of the function $\mathcal{G}_1$ as $L \to 0$ is

$$\mathcal{G}_1 \sim \begin{cases} L^{-1}, & D-2\rho < 4, \\ L^{-(D-2\rho-1)}, & D-2\rho \geq 4. \end{cases}$$

B. Half-integer ν, odd D

Now we consider odd dimensions D, which implies half-integer values of $\nu = \mu + 1/2$. For reference, $\mu = \frac{D-1}{2} - \rho$. Again, we split the contributions into three functions $\mathcal{F}_2$, $\mathcal{G}_2$, and $\mathcal{H}_2$, and after substituting Eq. (18) into Eq. (4) the amplitude is given by

$$L\mathcal{I}_\rho^{D,2}(M^2;\beta,L) = \left(\frac{M^2}{2}\right)^{\frac{D}{2}-\rho} \frac{1}{(2\pi)^{\frac{D}{2}} 2^{\rho-2}\Gamma(\rho)}(\mathcal{F}_2+\mathcal{G}_2+\mathcal{H}_2), \tag{33}$$

with

$$\mathcal{F}_2 = \frac{\pi}{M^2\beta}\Gamma\left(1-\frac{D}{2}+\rho\right) + \frac{\sqrt{\pi}}{M}\frac{(-1)^{\frac{D-1}{2}-\rho}}{\Gamma(\frac{D+1}{2}-\rho)}\left(\gamma+\ln\frac{M\beta}{4\pi}\right) + \frac{\sqrt{\pi}}{M}\mathcal{S}^{(2)}\left(\frac{D-1}{2}-\rho;\frac{M\beta}{4\pi}\right) + \frac{\sqrt{\pi}}{M}\mathcal{S}_0^{(3)}\left(\frac{D-1}{2}-\rho;\frac{M\beta}{2}\right), \tag{34}$$

$$\mathcal{G}_2 = -\frac{\sqrt{\pi}}{M}\frac{(-1)^{\frac{D-1}{2}-\rho}}{\Gamma(\frac{D+1}{2}-\rho)}\ln ML - \frac{\sqrt{\pi}}{M}\mathcal{S}^{(4)}\left(\frac{D+1}{2}-\rho;ML\right), \tag{35}$$

$$\mathcal{H}_2 = -\frac{\sqrt{\pi}}{M}\mathcal{S}_0^{(1)}\left(\frac{D+1}{2}-\rho;\frac{ML}{2\pi}\right). \tag{36}$$

The second scenario, with a reduced number of dimensions, is given by Eq. (10):

$$\mathcal{I}_\rho^{D-1,1}(M^2;\beta) = \frac{(\frac{M^2}{2})^{\frac{D}{2}-\rho}}{(2\pi)^{\frac{D}{2}}2^{\rho-2}\Gamma[\rho]}\left\{\frac{\sqrt{\pi}}{2M}\Gamma\left(\rho+\frac{1-D}{2}\right) + \frac{2\sqrt{\pi}}{M}\mathcal{W}^{(1)}_{\frac{D-1}{2}-\rho}(M^2;\beta)\right\}, \tag{37}$$

with $\mathcal{W}^{(1)}$ given by Eq. (11), that is,

$$\mathcal{W}^{(1)}_{\frac{D-1}{2}-\rho} = -\frac{1}{4}\Gamma\left(\rho+\frac{1-D}{2}\right) - \frac{(-1)^{\frac{D-1}{2}-\rho}}{4\Gamma(\frac{D+1}{2}-\rho)^2}\left[\begin{matrix}\frac{D+1}{2}-\rho \\ 2\end{matrix}\right] + \frac{\sqrt{\pi}}{2M\beta}\Gamma\left(1+\rho-\frac{D}{2}\right) + \frac{(-1)^{\frac{D-1}{2}-\rho}}{2\Gamma(\frac{D+1}{2}-\rho)}\left(\gamma+\ln\frac{M\beta}{4\pi}\right) + \frac{1}{2}\mathcal{S}_0^{(3)}\left(\frac{D-1}{2}-\rho;\frac{M\beta}{2}\right) + \frac{1}{2}\mathcal{S}^{(2)}\left(\frac{D-1}{2}-\rho;\frac{M\beta}{4\pi}\right). \tag{38}$$

Once again, we must be careful with the zero-temperature contribution, as a modified minimal subtraction scheme is assumed [see Eq. (21)]. We obtain, after the cancellation with the zero-temperature contribution,

$$\mathcal{I}_\rho^{D-1,1}(M^2;\beta) = \frac{(\frac{M^2}{2})^{\frac{D}{2}-\rho}}{(2\pi)^{\frac{D}{2}}2^{\rho-2}\Gamma[\rho]}\mathcal{F}_2. \tag{39}$$

Therefore, we get the relation

$$L\mathcal{I}_\rho^{D,2}(M^2;\beta,L)|_{L\to 0} = \mathcal{I}_\rho^{D-1,1}(M^2;\beta) + \left(\frac{M^2}{2}\right)^{\frac{D}{2}-\rho}\frac{\mathcal{G}_2}{(2\pi)^{\frac{D}{2}}2^{\rho-2}\Gamma(\rho)} = \mathcal{I}_\rho^{D-1,1}(M^2;\beta) + \mathcal{O}(\ln L). \tag{40}$$

The only difference compared to the scenario with integer values of ν is the divergent behavior of $\mathcal{G}_2$; in this case, we have

$$\mathcal{G}_2 \sim \begin{cases} \ln L, & D-2\rho < 3, \\ L^{-(D-2\rho-1)}, & D-2\rho \geq 3. \end{cases}$$

C. Other real ν, noninteger D

To complete the analysis, we consider other real values of ν that allow to take into account noninteger values of the dimension D. We follow the same procedure and define three functions $\mathcal{F}_3$, $\mathcal{G}_3$, and $\mathcal{H}_3$; after substituting Eq. (20) into Eq. (4), we get

$$L\mathcal{I}_\rho^{D,2}(M^2;\beta,L) = \left(\frac{M^2}{2}\right)^{\frac{D}{2}-\rho} \frac{1}{(2\pi)^{\frac{D}{2}} 2^{\rho-2}\Gamma(\rho)} (\mathcal{F}_3 + \mathcal{G}_3 + \mathcal{H}_3), \tag{41}$$

$$\mathcal{F}_3 = \frac{\pi}{M^2\beta}\Gamma(1-\nu) + \sum_{k=0}^{\infty} \frac{(-1)^k}{\Gamma(k+1)} \left(\frac{M\beta}{2\pi}\right)^{2k-2\nu} \frac{\beta}{2\pi}\Gamma(1-\nu+k)\zeta(2-2\nu+2k), \tag{42}$$

$$\begin{aligned}\mathcal{G}_3 = {} & \frac{L}{2}\sum_{k=0}^{\lfloor\frac{\nu-1}{2}\rfloor} \frac{(-1)^k}{\Gamma(k+1)}\Gamma(\nu-k)\zeta(2\nu-2k)\left(\frac{ML}{2}\right)^{-2\nu+2k} \\ & - \frac{\sqrt{\pi}L^2}{2\beta}\sum_{k=0}^{\lfloor\nu-1\rfloor} \frac{(-1)^k}{\Gamma(k+1)}\Gamma\left(\nu-k-\frac{1}{2}\right)\zeta(2\nu-2k-1)\left(\frac{ML}{2}\right)^{2k-2\nu},\end{aligned} \tag{43}$$

$$\begin{aligned}\mathcal{H}_3 = {} & \frac{L}{2}\sum_{k=0}^{\infty} \frac{(-1)^k}{\Gamma(k+1)}\Gamma(\nu-k)\zeta(2\nu-2k)\left(\frac{M\beta}{2}\right)^{-2\nu+2k} \\ & + \frac{L}{2}\sum_{k=\max(0,\lfloor\frac{\nu-1}{2}\rfloor)}^{\infty} \frac{(-1)^k}{\Gamma(k+1)}\Gamma(\nu-k)\zeta(2\nu-2k)\left(\frac{ML}{2}\right)^{-2\nu+2k} \\ & + \frac{\sqrt{\pi}L^2}{2\beta}\sum_{k=0}^{\infty} \frac{(-1)^k}{\Gamma(k+1)}\Gamma\left(\nu-k-\frac{1}{2}\right)\zeta(2\nu-2k-1)\left(\frac{M\beta}{2}\right)^{2k-2\nu} \\ & - \frac{\sqrt{\pi}L^2}{2\beta}\sum_{k=\max(0,\lfloor\nu-1\rfloor)}^{\infty} \frac{(-1)^k}{\Gamma(k+1)}\Gamma\left(\nu-k-\frac{1}{2}\right)\zeta(2\nu-2k-1)\left(\frac{ML}{2}\right)^{2k-2\nu} \\ & - \frac{L}{2\sqrt{\pi}}\sum_{k=0}^{\infty} \frac{(-1)^k}{\Gamma(k+1)}\left(\frac{M\beta}{2\pi}\right)^{2k-2\nu}\Gamma\left(\frac{1}{2}-\nu+k\right)\zeta(1-2\nu+2k).\end{aligned} \tag{44}$$

In this case, the second scenario is obtained after substituting Eq. (19) into Eq. (10),

$$\mathcal{I}_\rho^{D-1,1}(M^2;\beta) = \frac{(\frac{M^2}{2})^{\frac{D}{2}-\rho}}{(2\pi)^{\frac{D}{2}} 2^{\rho-2}\Gamma(\rho)} \left[\frac{\pi}{M^2\beta}\Gamma(1-\nu) + \frac{\sqrt{\pi}}{M}\sum_{k=0}^{\infty} \frac{(-1)^k}{\Gamma(k+1)}\Gamma\left(\nu-k-\frac{1}{2}\right)\zeta(2\nu-2k-1)\left(\frac{M\beta}{2}\right)^{-2\nu+2k+1}\right].$$

The product of the gamma and zeta functions can be rewritten, and we obtain

$$\mathcal{I}_\rho^{D-1,1}(M^2;\beta) = \left(\frac{M^2}{2}\right)^{\frac{D}{2}-\rho} \frac{1}{(2\pi)^{\frac{D}{2}} 2^{\rho-2}\Gamma(\rho)} \mathcal{F}_3. \tag{45}$$

Finally, we obtain the simple relation

$$L\mathcal{I}_\rho^{D,2}(M^2;\beta,L)|_{L\to 0} = \mathcal{I}_\rho^{D-1,1}(M^2;\beta) + \left(\frac{M^2}{2}\right)^{\frac{D}{2}-\rho} \frac{\mathcal{G}_3}{(2\pi)^{\frac{D}{2}} 2^{\rho-2}\Gamma(\rho)} = \mathcal{I}_\rho^{D-1,1}(M^2;\beta) + \mathcal{O}(L). \tag{46}$$

The leading-L behavior depends on the structure of $\mathcal{G}_3$ which has the asymptotic behavior $\mathcal{G}_3 \sim L^{-(D-2\rho-1)}$, $D-2\rho \geq 2$ as $L \to 0$.

IV. CONCLUSIONS

We obtained that, at least for the class of one-loop diagrams, it is possible to consistently reduce the dimension of the system if one proceeds carefully.

We are not allowed to perform a strict dimensional reduction by taking a model with a finite length L and suppressing it continuously to zero. The first obstruction is the function $\mathcal{G}$, which carries the divergent behavior as L goes to zero. Of course, strictly speaking, $\mathcal{I}_\rho^{D,2}(M^2;\beta,L)$ cannot be evaluated at $L=0$ due to this divergence. However, we can also obtain some specific possibilities where $\mathcal{G}=0$, which occurs for $D=1$, 2 or any noninteger dimension $D<4$. Of course, $D=1$ is inconsistent (as there are two compactified dimensions) and must be discarded, and $D=2$ is the case where all dimensions are compactified. Anyway, assuming $\mathcal{G}=0$, the procedure of dimensional reduction for $L\to 0$ is

$$L\mathcal{I}_\rho^{D,2}(M^2;\beta,L)|_{L\to 0}=\mathcal{I}_\rho^{D-1,1}(M^2;\beta) \qquad \left(\text{for } \frac{D}{2}-\rho<1\right). \tag{47}$$

The identification in Eq. (47) is also valid for any D if we choose the prescription to ignore the divergent function $\mathcal{G}$. This prescription is what we defined as "dimensional reduction": we take the limit of a function as the length L goes to zero and remove its divergent components.

We remark that the L on the right-hand side of the above equation simply indicates that $\mathcal{I}_\rho^{D,2}$ also diverges as L goes to zero despite the existence of $\mathcal{G}$. The result that a continuous approach to the dimensional reduction is not possible is not a surprise. Indeed, in previous articles (in the context of phase transitions) a *minimal length* has been found below which the phase transition does not occur. Moreover, this result agrees with experimental observations about the existence of a minimal length.

However, now that we have made it clear that a strictly dimensional reduction is not attainable, we are allowed to discuss the existence of a prescription to do so. The idea is that there is a relationship between both situations: one with a small system length L and another where this dimension is ignored from the beginning.

Moreover, we could consider an N-component scalar model with a quartic interaction in $D=3$ with a tree-level coupling λ and mass m: this describes a heated surface. Taking the large-N limit and using a formal resummation, the one-loop corrections to the coupling constant g and squared mass M^2 are

$$g_3=\frac{\lambda_3}{1-\lambda_3\mathcal{I}_2^{3,1}(M^2;\beta)}, \tag{48a}$$

$$M^2=m^2+\lambda_3\mathcal{I}_1^{3,1}(M^2;\beta). \tag{48b}$$

Assuming that the surface is indeed a "dimensionally reduced" case of a heated film with thickness L, we can ignore the divergent component $\mathcal{G}$ and use the identification in Eq. (47) to write Eqs. (48a)–(48b) as

$$g_3=\frac{\lambda_3}{1-(\lambda_3 L)\mathcal{I}_2^{4,2}(M^2;\beta,L)}, \tag{49a}$$

$$M^2=m^2+(\lambda_3 L)\mathcal{I}_1^{4,2}(M^2;\beta,L). \tag{49b}$$

On the other hand, if we simply consider a heated film in $D=4$ with N scalar fields and explore its behavior for very small thickness, we get

$$g_4=\frac{\lambda_4}{1-\lambda_4\mathcal{I}_2^{4,2}(M^2;\beta,L)}, \tag{50a}$$

$$M^2=m^2+\lambda_4\mathcal{I}_1^{4,2}(M^2;\beta,L). \tag{50b}$$

Comparing both scenarios in Eqs. (49a)–(49b) and (50a)–(50b), we see that the coupling constant from the planar scenario (both the free λ_3 and corrected g_3) is related to the coupling constant from the thin film scenario by

$$\lambda_3 L=\lambda_4. \tag{51}$$

We can extract from this simple relation some important conclusions:

(1) A strict dimensional reduction, once again, is not allowed. It would require that the coupling constant for the reduced scenario goes to infinity.
(2) This is a direct indication that both scenarios are physically different.
(3) In the context of phase transitions or some other situation where the existence of a minimal thickness $L_{\rm min}$ can be observed, we can consider that the effective coupling constant in the planar scenario is $\lambda_3=\lambda_4/L_{\rm min}$.

ACKNOWLEDGMENTS

The authors thank the Brazilian agency Conselho Nacional de Desenvolvimento Científico e Tecnológico (CNPq) for partial financial support.

[1] T. Appelquist and R. Pisarski, High-temperature Yang-Mills theories and three-dimensional quantum chromodynamics, Phys. Rev. D **23**, 2305 (1981).

[2] N. P. Landsman, Limitations to dimensional reduction at high temperature, Nucl. Phys. **B322**, 498 (1989).

[3] J. Zinn-Justin, *Quantum Field Theory and Critical Phenomena*, 4th ed. (Clarendon Press, Oxford, 2002).

[4] H. Meyer-Ortmanns and T. Reisz, *Principles of Phase Structures in Particle Physics* (World Scientific Publishing Company, Singapore, 2007).

[5] F. C. Khanna, A. P. C. Malbouisson, J. M. C. Malbouisson, and A. E. Santana, Quantum field theory on toroidal topology: Algebraic structure and applications, Phys. Rep. **539**, 135 (2014).

[6] C. A. Linhares, A. P. C. Malbouisson, Y. W. Milla, and I. Roditi, First-order phase transitions in superconducting films: A Euclidean model, Phys. Rev. B **73**, 214525 (2006).

[7] L. M. Abreu, A. P. C. Malbouisson, J. M. C. Malbouisson, and A. E. Santana, Large N transition temperature for superconducting films in a magnetic field, Phys. Rev. B **67**, 212502 (2003).

[8] L. M. Abreu, A. P. C. Malbouisson, J. M. C. Malbouisson, and A. E. Santana, Finite-size effects on the chiral phase diagram of four-fermion models in four dimensions, Nucl. Phys. **B819**, 127 (2009).

[9] L. M. Abreu, A. P. C. Malbouisson, and J. M. C. Malbouisson, Finite-size effects on the phase diagram of difermion condensates in two-dimensional four-fermion interaction models, Phys. Rev. D **83**, 025001 (2011).

[10] L. M. Abreu, A. P. C. Malbouisson, and J. M. C. Malbouisson, Nambu-Jona-Lasinio model in a magnetic background: Size-dependent effects, Phys. Rev. D **84**, 065036 (2011).

[11] C. A. Linhares, A. P. C. Malbouisson, and M. L. Souza, A note on the infrared behavior of the compactified Ginzburg–Landau model in a magnetic field, Europhys. Lett. **96**, 31002 (2011).

[12] C. A. Linhares, A. P. C. Malbouisson, J. M. C. Malbouisson, and I. Roditi, Spontaneous symmetry restoration in a field theory at finite chemical potential in a toroidal topology, Phys. Rev. D **86**, 105022 (2012).

[13] F. C. Khanna, A. P. C. Malbouisson, J. M. C. Malbouisson, and A. E. Santana, Finite-size effects on the phase transition in the three-dimensional Gross-Neveu model, Europhys. Lett. **97**, 11002 (2012).

[14] F. C. Khanna, A. P. C. Malbouisson, J. M. C. Malbouisson, and A. E. Santana, Phase transition in the massive Gross-Neveu model in toroidal topologies, Phys. Rev. D **85**, 085015 (2012).

[15] L. M. Abreu, C. A. Linhares, A. P. C. Malbouisson, and J. M. C. Malbouisson, Magnetic effects on spontaneous symmetry breaking/restoration in a toroidal topology, Phys. Rev. D **88**, 107701 (2013).

[16] E. B. S. Corrêa, C. A. Linhares, and A. P. C. Malbouisson, Finite-size, magnetic and chemical-potential effects on first-order phase transitions, Phys. Lett. A **377**, 1984 (2013).

[17] F. C. Khanna, A. P. C. Malbouisson, J. M. C. Malbouisson, and A. R. Santana, *Thermal Quantum Field Theory—Algebraic Aspects and Applications* (World Scientific Publishing Company, Singapore, 2009).

[18] E Elizalde, *Ten Physical Applications of Spectral Zeta Functions*, 2nd ed. (Springer-Verlag, Berlin Heidelberg, 1995).

[19] E. Cavalcanti, C. A. Linhares, and A. P. C. Malbouisson, Properties of size-dependent models having quasiperiodic boundary conditions, Int. J. Mod. Phys. A **33**, 1850008 (2018).

[20] G. Fucci and K. Kirsten, Expansion of infinite series containing modified bessel functions of the second kind, J. Phys. A **48**, 435203 (2015).

[21] S. Weinberg, *The Quantum Theory of Fields: Modern applications* (Cambridge University Press, Cambridge, England, 2013), Vol. 2.

Chapter 6

Effect of boundary conditions on dimensionally reduced field-theoretical models at finite temperature

Published as:
E. Cavalcanti, J.A. Lourenço, C.A. Linhares, and A.P.C. Malbouisson. Physical Review D **100**, 025008 (2019) *Effect of boundary conditions on dimensionally reduced field-theoretical models at finite temperature*

PHYSICAL REVIEW D **100,** 025008 (2019)

Effect of boundary conditions on dimensionally reduced field-theoretical models at finite temperature

E. Cavalcanti,[1,*] C. A. Linhares,[2,†] J. A. Lourenço,[3,‡] and A. P. C. Malbouisson[1,§]

[1]*Centro Brasileiro de Pesquisas Físicas/MCTI, 22290-180 Rio de Janeiro, RJ, Brazil*
[2]*Instituto de Física, Universidade do Estado do Rio de Janeiro, 20559-900 Rio de Janeiro, RJ, Brazil*
[3]*Departamento de Ciências Naturais, Universidade Federal do Espírito Santo, 29932-540 Campus São Mateus, ES, Brazil*

(Received 24 April 2019; published 18 July 2019)

Here we understand *dimensional reduction* as a procedure to obtain an effective model in $D-1$ dimensions that is related to the original model in D dimensions. To explore this concept, we use both a self-interacting fermionic model and self-interacting bosonic model. Furthermore, in both cases, we consider different boundary conditions in space: periodic, antiperiodic, Dirichlet, and Neumann. For bosonic fields, we get the so-defined dimensional reduction. Taking the simple example of a quartic interaction, we obtain that the boundary conditions (periodic, Dirichlet, Neumann) influence the new coupling of the reduced model. For fermionic fields, we get the curious result that the model obtained reducing from D dimensions to $D-1$ dimensions is distinguishable from taking into account a fermionic field originally in $D-1$ dimensions. Moreover, when one considers antiperiodic boundary conditions in space (both for bosons and fermions), it is found that the dimensional reduction is not allowed.

DOI: 10.1103/PhysRevD.100.025008

I. INTRODUCTION

The construction and use of quantum field-theoretical models at dimensions different from the usual space-time in $D = 3+1$ are usual in the literature [1–17]. Its first appearance seems to be in the construction of the Kaluza five-dimensional theory [1] that intended to unify gravity and electromagnetism. Since then, models and theories in $D \neq 4$ have been used in many different situations:

(i) Phenomenology in particle physics considering extra dimensions [2–10];
(ii) Field theories in $D < 4$ [11–17];
(iii) Superstring theory [18–20].

In the context of finite-temperature field theory, it is understood that the regime of very high temperatures is associated with a dimensional reduction of the model. For scalar fields, it is possible to obtain an effective model in dimension $D-1$ that has a temperature-dependent coupling. This effective model is related to the original theory in D dimensions when the temperature is very high [21–24]. One of the uses of the thermal dimensional reduction is to investigate aspects of hot QCD [25–29].

When we consider a system with restriction in one spatial direction, the discussion of dimensional reduction is renewed. For example, in the context of low-dimensional field theories ($D \leq 4$), we can take into account the study of films and surfaces. Let us consider two physical systems: (A) a film with thickness L subjected to a thermal bath with temperature $T = 1/\beta$; (B) a surface (planar system) subjected to the same temperature T. We call a *dimensional reduction* the possibility that the model of the system (A) becomes or brings information about a planar model—like the one of case (B)—if we consider the limiting process to take the length to zero: $L \to 0$.

If we generalize this problem to an arbitrary number of dimensions, we can ask ourselves whether there is a relationship between a model in D dimensions and a model in $D-1$ dimensions; this is the major objective in the present study.

It is a known theoretical result confirmed by experiments that for both bosonic and fermionic systems that undergo a phase transition, and are spatially limited, there is a minimum size below which there is no phase transition [30–32]. This seems to indicate that for systems where at least one of the dimensions is restricted to a compact finite size with a compactification length L, a strict dimensional reduction is not allowed—at least in the context of phase transitions. Recently, in the context of phase transitions, it

*erich@cbpf.br
†linharescesar@gmail.com
‡jose.lourenco@ufes.br
§adolfo@cbpf.br

has been obtained that the minimal size of the system depends on the boundary conditions imposed on the spatial restriction. This analysis was done both for bosonic and fermionic models, and a quasiperiodic boundary condition was applied which interpolates between the periodic and antiperiodic boundary conditions [33].

We have previously found [34] that for bosonic fields at the one-loop level, the so-called dimensional reduction is obtained when one considers periodic boundary condition in space. In this article, we extend this analysis so that we consider a few more boundary conditions: Dirichlet, Neumann, and antiperiodic. Another step is to take into account purely fermionic models, so we can compare them with the bosonic situation. In the context of a thermal dimensional reduction, it is known that dimensional reduction happens for bosonic models [21–24]. The logic is that at high temperatures there occurs a decoupling between static (a zero mode) and nonstatic contributions (nonzero modes). Although this reasoning occurs when dealing with periodic boundary condition, when we refer to antiperiodic boundary condition—as is the case of fermions in the thermal dimensional reduction—we do not have static modes [22]. Therefore, we cannot expect the same behavior both for periodic and antiperiodic boundary conditions. Indeed, it seems that a fermionic model in D dimensions is not related to a model originally built in $D-1$ dimensions [35,36].

II. GENERIC MODEL AND BOUNDARY CONDITIONS

Our aim is to discuss field-theoretical models with self-interaction terms. In this way, we avoid for the moment the combinatorics of many-particle models to focus on the effects of boundary conditions. The basic ingredient to discuss field theories in D dimensions at one-loop level is the one-loop Feynman amplitude. In the scenario of a scalar field theory, the amplitude $\mathcal{I}$ with ρ propagators and zero external momenta is

$$\mathcal{I}_\rho^D(M) = \int \frac{d^D p}{(2\pi)^D} \frac{1}{(p^2+M^2)^\rho},$$

where M is the mass of the scalar field. The D-dimensional integral becomes an integral sum after we introduce boundary conditions on $d < D$ coordinates. The compactification of the imaginary time introduces the inverse temperature $\beta = 1/T$, and the compactification of the spatial directions introduces some finite-lengths L_i. The boundary condition on the imaginary time must be periodic ($a_0 = 0$) for bosons or antiperiodic ($a_0 = 1$). However, there is freedom regarding the boundary condition imposed on the spatial direction. In the context of quantum field theories at toroidal topologies, the use of periodic and antiperiodic boundary conditions [30,31] has been discussed, its extension to quasiperiodic boundary conditions [33], and also the use of Dirichlet and Neumann boundary conditions [37]. We consider a scenario with $d = 2$ compactifications; after computing the remaining $D-2$ integrals using dimensional regularization, we obtain that the one-loop Feynman amplitude for each boundary condition ($b.c.$) is

$$\begin{aligned}&\mathcal{I}_\rho^{D,2}(M;\beta,a_0,L|b.c.)\\&=\frac{\Gamma(\rho-\frac{D}{2}+1)}{(4\pi)^{\frac{D}{2}-1}\Gamma(\rho)\beta L}\sum_{n_0\in\mathbb{Z},n_1\in\mathcal{M}}\left[M^2+\left(\frac{2\pi n_0}{\beta}+\frac{a_0\pi}{\beta}\right)^2+\omega_{n_1}^2\right],\end{aligned} \tag{1}$$

where the domain $\mathcal{M}$ of the sum over the frequencies ω_{n_1} is given in Table I for each boundary condition.

Although we start with a Feynman amplitude for a scalar field, Eq. (2), it can be shown that the one-loop Feynman amplitude of μ fermionic propagators can be written as a combination of scalar one-loop Feynman amplitudes. We take into account a four-fermion coupling given by $a + b\gamma_S$, where γ_S represents the chiral matrix. The one-loop Feynman amplitude in this scenario is

$$\mathcal{J}_\mu^D(M) = \mathrm{tr}\int \frac{d^D p}{(2\pi)^D}\left(\frac{a+b\gamma_S}{i\not{p}+M}\right)^\mu. \tag{2}$$

The relation between $\mathcal{J}_\mu^D$ and $\mathcal{I}_\rho^D$ is obtained in the Appendix A and reads

$$\begin{aligned}\frac{1}{d_\gamma}\mathcal{J}_\mu^{D,d} &= a^\mu\sum_{k=0}^{\lfloor\frac{\mu}{2}\rfloor}\sum_{j=0}^{k}\binom{\mu}{2k}\binom{k}{j}M^{\mu-2j}(-1)^j\mathcal{I}_{\mu-j}^{D,d}(M)+b^\mu(\mu-2\lfloor\mu/2\rfloor)\mathcal{I}_{\mu/2}^{D,d}(M)\\&+\sum_{k=1}^{\lfloor\frac{\mu-1}{2}\rfloor}a^{\mu-2k}b^{2k}\sum_{j=k}^{\lfloor\frac{\mu}{2}\rfloor}\frac{j!(\mu-j-1)!}{(j-k)!k!(\mu-k-j)!(k-j)!}\sum_{\ell=0}^{\lfloor\frac{\mu}{2}-j\rfloor}\binom{\mu-2j}{2\ell}\sum_{n=0}^{\ell}(-1)^n\binom{\ell}{n}M^{\mu-2j-2n}\mathcal{I}_{\mu-j-n}^{D,d}(M)\\&+\sum_{k=1}^{\lfloor\frac{\mu-1}{2}\rfloor}a^{\mu-2k}b^{2k}\sum_{j=\lfloor\frac{\mu}{2}+1\rfloor}^{\mu-k}\frac{j!(\mu-j-1)!}{(j-k)!k!(\mu-k-j)!(k-j)!}\sum_{\ell=0}^{\lfloor\frac{\mu}{2}-j\rfloor}\binom{2j-\mu}{2\ell}\sum_{n=0}^{\ell}\binom{\ell}{n}M^{2j-\mu-2n}\mathcal{I}_{j-n}^{D,d}(M).\end{aligned} \tag{3}$$

TABLE I. Frequencies and domain of sum for each boundary condition in space.

Boundary condition (b.c.)	$\mathcal{M}$	ω_{n_1}
Periodic ($\mathcal{P}$)	$\mathbb{Z}$	$2\pi n_1/L$
Antiperiodic ($\mathcal{A}$)	$\mathbb{Z}$	$(2n_1+1)\pi/L$
Dirichlet ($\mathcal{D}$)	$\mathbb{N}^+$	$\pi n_1/L$
Neumann ($\mathcal{N}$)	$\mathbb{N}$	$\pi n_1/L$

It holds independently of the number of compactified dimensions d. This means that the fermionic scenario is a combination of the relation given by Eq. (3) and the expression of Eq. (1) considering antiperiodic boundary condition in the imaginary time ($a_0 = 1$). Therefore, in the analysis that follows, the bosonic behavior is studied by investigating Eq. (1) with $a_0 = 0$ and the fermionic behavior is studied by investigating Eq. (1) with $a_0 = 1$.

Notice that we can express both the cases of Dirichlet and Neumann boundary conditions in terms of the function with periodic boundary condition in space and a reduced function with just a thermal compactification.

$$\mathcal{I}_\rho^{D,2}(M;\beta,a_0;L|\mathcal{D}) = \frac{1}{2}\mathcal{I}_\rho^{D,2}(M;\beta,a_0;2L|\mathcal{P}) - \frac{1}{2L}\mathcal{I}_\rho^{D-1,1}(M;\beta,a_0), \tag{4}$$

$$\mathcal{I}_\rho^{D,2}(M;\beta,a_0;L|\mathcal{N}) = \frac{1}{2}\mathcal{I}_\rho^{D,2}(M;\beta,a_0;2L|\mathcal{P}) + \frac{1}{2L}\mathcal{I}_\rho^{D-1,1}(M;\beta,a_0). \tag{5}$$

Therefore, we only need to analyze the cases of periodic and antiperiodic boundary conditions in space. For both periodic and antiperiodic boundary conditions in space, the remaining infinite sum in Eq. (1) can be identified as an Epstein-Hurwitz zeta function [38]. After an analytic continuation, this leads to the sum over modified Bessel functions of the second kind $K_\nu(x)$; see Refs. [30,31]. Using for convenience that $\nu = D/2 - \rho$, the amplitude $\mathcal{I}_\rho^{D,2}$ reads

$$\mathcal{I}_\rho^{D,2}(M;\beta,a_0;L) = \frac{(M^2)^\nu\Gamma(-\nu)}{(4\pi)^{\frac{D}{2}}\Gamma(\rho)} + \frac{\mathcal{W}_\nu(M;\beta,a_0;L)}{(2\pi)^{\frac{D}{2}}2^{\rho-2}\Gamma(\rho)}, \tag{6}$$

where, for periodic boundary conditions in space ($\mathcal{P}$), the function $\mathcal{W}_\nu$ is

$$\mathcal{W}_\nu(M;\beta,a_0;L|\mathcal{P}) = \sum_{n=1}^\infty \cos(n\pi a_0)\left(\frac{M}{n\beta}\right)^\nu K_\nu(n\beta M) + \sum_{n=1}^\infty \left(\frac{M}{nL}\right)^\nu K_\nu(nLM) + 2\sum_{n_0,n_1=1}^\infty \cos(n_0\pi a_0)\left(\frac{M}{\sqrt{n_0^2\beta^2+n_1^2L^2}}\right)^\nu \times K_\nu\left(M\sqrt{n_0^2\beta^2+n_1^2L^2}\right), \tag{7}$$

and, for antiperiodic boundary conditions in space ($\mathcal{A}$), the function $\mathcal{W}_\nu$ is

$$\mathcal{W}_\nu(M;\beta,a_0;L|\mathcal{A}) = \sum_{n=1}^\infty \cos(n\pi a_0)\left(\frac{M}{n\beta}\right)^\nu K_\nu(n\beta M) + \sum_{n=1}^\infty (-1)^n\left(\frac{M}{nL}\right)^\nu K_\nu(nLM) + 2\sum_{n_0,n_1=1}^\infty \cos(n_0\pi a_0)(-1)^{n_1}\left(\frac{M}{\sqrt{n_0^2\beta^2+n_1^2L^2}}\right)^\nu \times K_\nu\left(M\sqrt{n_0^2\beta^2+n_1^2L^2}\right). \tag{8}$$

Notice that with the above equations one fully determines the behavior at one-loop level for finite β and finite L both for bosonic and fermionic models in D dimensions with the prescribed boundary conditions. In the following sections, we organize and apply the expressions for each situation under interest.

III. DIMENSIONAL REDUCTION

In this section, let us clarify the discussion of dimensional reduction. There are two main paths to obtain a dimensionally reduced field-theoretical model.

The first path is to take the original Lagrangian in D dimensions, reduce it to $D-1$ dimensions, and then quantize it. This path ignores possible boundary conditions imposed on the removed dimension. The quantization is here understood as the computation of the correction given by the one-loop Feynman amplitudes. If we are dealing with a model with one self-interacting bosonic field, the Feynman amplitude for the dimensionally reduced model in $D-1$ with one compactification corresponding to the inverse temperature $\beta = 1/T$ reads

$$\mathcal{I}_\rho^{D-1,1}(M;\beta,a_0=0) = \frac{(M^2/2)^\nu}{(2\pi)^{\frac{D}{2}}2^{\rho-2}\Gamma(\rho)}\left[\frac{\pi}{M^2\beta}\Gamma(1-\nu) + \frac{\sqrt{\pi}}{M}\sum_{k=0}^\infty \frac{(-1)^k}{\Gamma(k+1)}\Gamma\left(\nu-k-\frac{1}{2}\right) \times \zeta(2\nu-2k-1)\left(\frac{M\beta}{2}\right)^{-2\nu+2k+1}\right]. \tag{9}$$

On the other hand, for a model describing a self-interacting fermionic field, the Feynman amplitude $\mathcal{J}_\rho^{D-1,1}$ is related to $\mathcal{I}_\rho^{D-1,1}(M;\beta,a_0=1)$ through the relation given by Eq. (3), and the function $\mathcal{I}_\rho^{D-1,1}(M;\beta,a_0=1)$ reads

$$\mathcal{I}_\rho^{D-1,1}(M;\beta,a_0=1) = \mathcal{F}_\rho^D(M,\beta;c_1=0,c_2=1/2), \tag{10}$$

where, for future convenience, the function $\mathcal{F}_\rho^D(M,\beta;c_1,c_2)$ is defined as

$$\mathcal{F}_\rho^D(M,\beta;c_1,c_2) = \frac{(M^2/2)^\nu}{(2\pi)^{\frac{D}{2}}2^{\rho-2}\Gamma(\rho)}\frac{\beta}{2\pi}\sum_{k=1}^{\infty}\frac{(-1)^k}{\Gamma(k+1)} \times\Gamma(k+1-\nu)\zeta(2k+2-2\nu)\left(\frac{M\beta}{2\pi}\right)^{2k-2\nu} \times(-1+c_1 2^{2(k-\nu)}+c_2 2^{-2(k-\nu)}). \quad (11)$$

We compare this first path with a different procedure to obtain a dimensionally reduced field-theoretical model. In this second path, we take a quantized version of the model in D dimensions and force the reduction taking the limit $L\to 0$. To explore this, we need to evaluate $\mathcal{I}_\rho^{D,2}$ at a very small length L. We proceed as in Ref. [34] and use a integral representation of K_ν in the complex plane,

$$K_\nu(X) = \frac{1}{4\pi i}\int_{c-i\infty}^{c+i\infty} dt\Gamma(t)\Gamma(t-\nu)\left(\frac{X}{2}\right)^{\nu-2t}. \quad (12)$$

To allow the interchange of the integral and the sum, the value of c must be chosen in such a way that there is no pole located to the right of it [37]. After using this integral representation, we can compute the infinite sums and study the poles. It produces a tedious algebraic manipulation for each of the situations under interested, and the main results are exhibited in the following subsections. Of course, this path splits into different ones as the choice of the boundary condition in the spatial direction might influence the result. Before investigating in further details the behavior as $L\to 0$, let us reinforce that the investigation of the dimensional reduction comes from the comparison of both paths. This comparison may produce three different outcomes.

(i) At first, there might be a well-defined dimensional reduction, meaning that there is a relationship as

$$s(L)\mathcal{I}_\rho^{D,2}(M;\beta,a_0;L|\text{b.c.})|_{L\to 0} = \mathcal{I}_\rho^{D-1,1}(M;\beta,a_0)+\{??\}, \quad (13)$$

where $s(L)$ is some *scale* function that only depends on the finite length L, and we allow the presence of some residual terms.

(ii) A second possibility is that the original model does not produce any relevant behavior as $L\to 0$, and then the procedure of dimensional reduced is ill-defined and not allowed.

(iii) A final possibility that could arise is that a dimensionally reduced model is achieved, but it does not correspond to the expected one.

$$s(L)\mathcal{I}_\rho^{D,2}(M;\beta,a_0;L|\text{b.c.})|_{L\to 0} = \tilde{\mathcal{I}}_\rho^{D-1,1}(M;\beta,a_0)+\{??\}. \quad (14)$$

With this discussion made evident, let us now study each possibility. Bosonic fields are treated in Secs. III A, III B, and III C, while fermionic fields are considered in Secs. III D, III E, and III F.

A. Bosonic field: Periodic boundary conditions in space

This first case was the object of study in a previous article where we explored the subject in further detail [34]. We take the case of periodic boundary conditions, Eq. (7), for $a_0=0$, that is related to bosons, apply the integral representation Eq. (12), and use the following analytic extension [38] of infinite double sum:

$$\sum_{n_0=1,n_1=1}^{\infty}\frac{1}{(n_0^2\beta^2+n_1^2L^2)^t} = -\frac{\zeta(2t)}{2L^{2t}}+\frac{\sqrt{\pi}}{2}\frac{\Gamma(t-1/2)}{\Gamma(t)}\frac{\zeta(2t-1)}{\beta L^{2t-1}} + \frac{2\pi^t}{\Gamma(t)}\sqrt{\frac{L}{\beta}}\frac{1}{(\beta L)^t}\sum_{n_0,n_1=1}^{\infty}\left(\frac{n_0}{n_1}\right)^{t-\frac{1}{2}}K_{t-\frac{1}{2}}\left(2\pi n_0 n_1\frac{L}{\beta}\right), \quad (15)$$

where ζ is the Riemann zeta function. By convention, we first do the sum over n_0 and then the sum over n_1. After this, the function $\mathcal{W}_\nu$ reads

$$\mathcal{W}_\nu(M;\beta,a_0=0;L|\mathcal{P}) = \int_{c-i\infty}^{c+i\infty}\frac{dt}{4\pi i}\Gamma(t)\zeta(2t)\Gamma(t-\nu)\left(\frac{M\beta}{2}\right)^{-2t} + \frac{\sqrt{\pi}L}{\beta}\int_{c-i\infty}^{c+i\infty}\frac{dt}{4\pi i}\Gamma(t-\nu)\Gamma\left(t-\frac{1}{2}\right)\zeta(2t-1)\left(\frac{ML}{2}\right)^{-2t} + \frac{1}{\sqrt{\pi}}\sum_{k=1}^{\infty}\int_{c-i\infty}^{c+i\infty}\frac{ds}{2\pi i}\left(\frac{M\beta}{2\pi}\right)^{2k-2\nu}\left(\frac{\pi L}{\beta}\right)^{-2s} \times\Gamma(s)\zeta(2s)\Gamma\left(s+k-\nu+\frac{1}{2}\right)\zeta(2s+2k-2\nu+1). \quad (16)$$

A detailed treatment demands to investigate Eq. (16) for each different value assumed by 2ν (odd, even, noninteger), as this determines whether we are dealing with single or double poles. However, motivated by previous results and to make the notation clear, we choose here to exhibit only the position of the poles and the power dependencies on β and L. Note that a structure as $\Gamma(u)\zeta(2u)$ means the existence of poles at $u=0,1/2$, and a structure as $\Gamma(u)\eta(2u)$ means only a pole at $u=0$. The analysis of Eq. (16) gives that:

(i) for the first integral we have poles at $t=0$, $t=1/2$, and $t=\nu-j$ with $j\in[0,\infty[$. This corresponds to the dependencies β^0, β^{-1}, and $\beta^{2k-2\nu}$;

(ii) for the second integral there are poles at $t = 1/2$, $t = 1$, and $t = \nu - j$ with $j \in [0, \infty[$. This corresponds to the dependencies β^{-1}, $\beta^{-1}L^{-1}$, and $(L/\beta)L^{2k-2\nu}$;

(iii) the last integral has poles at $s = 0$, $s = 1/2$, $s = \nu - k - 1/2$, and $s = \nu - k$. This corresponds to the dependencies $\beta^{2k-2\nu}$, $(\beta/L)\beta^{2k-2\nu}$, $L^{2k-2\nu}$, and $(L/\beta)L^{2k-2\nu}$.

We are mainly interested in the behavior of $\mathcal{I}^{D,2}$ as $L \to 0$ to see whether there is some function of the inverse temperature $\beta = 1/T$ that could be related to a scenario with one less dimension. To do this, we use some scale function multiplied by the Feynman amplitude,

$$s(L)\mathcal{I}^{D,2}_{\rho}(M;\beta, a_0 = 0; L|\mathcal{P})|_{L\to 0}. \tag{17}$$

In a previous article, we used $s(L) = L$ and split this product into three different parts: one that goes to zero as $L \to 0$ and therefore do not contribute in anything, another component that grows as $L \to 0$ and could be considered a residual contribution coming from high dimension, and a final component that gives a contribution independent of the length L. From the analysis of the poles and the power dependencies on β and L, we can note that the relevant poles are $t = 1$ from the second integral and $s = 1/2$ from the third integral in Eq. (16). Indeed, this gives the simple result

$$\begin{aligned} L\mathcal{I}^{D,2}_{\rho}&(M;\beta, a_0 = 0; L|\mathcal{P})|_{L\to 0} \\ &= \mathcal{I}^{D-1,1}_{\rho}(M;\beta, a_0 = 0) + \text{divergent terms}, \end{aligned} \tag{18}$$

where $\mathcal{I}^{D-1,1}_{\rho}(M;\beta, a_0 = 0)$ is exactly the Feynman amplitude for the reduced scenario with $D - 1$ dimensions and just one compactification related to the temperature. It reads

$$\begin{aligned} \mathcal{I}^{D-1,1}_{\rho}&(M;\beta, a_0 = 0) \\ &= \frac{(M^2/2)^{\nu}}{(2\pi)^{\frac{D}{2}}2^{\rho-2}\Gamma(\rho)}\left[\frac{\pi}{M^2\beta}\Gamma(1-\nu)\right. \\ &\quad + \frac{\sqrt{\pi}}{M}\sum_{k=0}^{\infty}\frac{(-1)^k}{\Gamma(k+1)}\Gamma\left(\nu - k - \frac{1}{2}\right) \\ &\quad \left.\times\,\zeta(2\nu - 2k - 1)\left(\frac{M\beta}{2}\right)^{-2\nu+2k+1}\right]. \end{aligned}$$

This result shows that the dimensional reduction is well defined for a self-interacting bosonic field with periodic boundary conditions, as already discussed in the previous article. For further details, one is referred to Ref. [34] where this relation was obtained with a careful investigation for even, odd, and noninteger D and also the residual divergent terms were fully exhibited. The important aspect to be noted here is that we can get the structure of the function from a quick investigation of the poles. To avoid a lengthy exposition, this procedure is repeated in the following sections to study other cases of interest.

B. Bosonic field: Dirichlet and Neumann boundary conditions in space

As discussed previously, both the Dirichlet [Eq. (4)] and Neumann [Eq. (5)] boundary conditions are a linear combination of a model with periodic boundary condition in space and a dimensionally reduced model. Therefore, as we know that the behavior of the model with periodic boundary conditions in space is given by Eq. (18), we obtain directly that

$$\begin{aligned} L\mathcal{I}^{D,2}_{\rho}&(M;\beta, a_0 = 0; L|\mathcal{D})|_{L\to 0} \\ &= -\frac{1}{4}\mathcal{I}^{D-1,1}_{\rho}(M;\beta, 0) + \text{divergent terms}, \end{aligned} \tag{19}$$

$$\begin{aligned} L\mathcal{I}^{D,2}_{\rho}&(M;\beta, a_0 = 0; L|\mathcal{N})|_{L\to 0} \\ &= \frac{3}{4}\mathcal{I}^{D-1,1}_{\rho}(M;\beta, 0) + \text{divergent terms}. \end{aligned} \tag{20}$$

Just like the scenario with periodic boundary conditions, we obtain that the dimensional reduction is well defined. What changes is the relation between the (D)-dimensional model and the $(D-1)$-dimensional model. The significance of this can be further understood if we follow the discussion of a previous article [34] and consider a bosonic model with quartic interaction given by the coupling constant λ_D. The relationship between the coupling constant of the dimensionally reduced model λ_{D-1} and λ_D is different for each boundary condition,

$$\begin{aligned} \lambda_{D-1} &= \frac{\lambda_D}{L}, && \text{periodic b.c.;} \\ \lambda_{D-1} &= -\frac{\lambda_D}{4L}, && \text{Dirichlet b.c.;} \\ \lambda_{D-1} &= \frac{3\lambda_D}{4L}, && \text{Neumann b.c..} \end{aligned}$$

Notice that for Dirichlet boundary conditions the coupling constant of the dimensionally reduced model changes sign, which raises a question about the vacua stability of this model and motivates a further investigation.

C. Bosonic field: Antiperiodic boundary conditions in space

In this section, we consider bosonic fields $(a_0 = 0)$ with antiperiodic boundary conditions in space. To investigate this, we apply the integral representation of the K_{ν}, Eq. (12), in the function $\mathcal{W}_{\nu}$, Eq. (8), and make use of the analytic extension that reads

$$\sum_{n_0=1,n_1=1}^{\infty}\frac{(-1)^{n_1}}{(n_0^2\beta^2+n_1^2L^2)^t}$$
$$=\frac{1}{2L^{2t}}\eta(2t)-\frac{\sqrt{\pi}}{2}\frac{\Gamma(t-1/2)}{\Gamma(t)}\frac{\eta(2t-1)}{\beta L^{2t-1}}$$
$$+\frac{2\pi^t}{\Gamma(t)}\sqrt{\frac{L}{\beta}}\frac{1}{(\beta L)^t}\sum_{n_0,n_1=1}^{\infty}(-1)^{n_1}\left(\frac{n_0}{n_1}\right)^{t-\frac{1}{2}}K_{t-\frac{1}{2}}\left(2\pi n_0 n_1\frac{L}{\beta}\right), \tag{21}$$

where η is the Dirichlet eta function. By convention, we first do the sum over n_0 and then the sum over n_1. After this, the function $\mathcal{W}_\nu$ reads

$$\mathcal{W}_\nu(M;\beta,a_0=0;L|\mathcal{A})$$
$$=\int_{c-i\infty}^{c+i\infty}\frac{dt}{4\pi i}\Gamma(t)\zeta(2t)\Gamma(t-\nu)\left(\frac{M\beta}{2}\right)^{-2t}$$
$$-\frac{\sqrt{\pi}L}{\beta}\int_{c-i\infty}^{c+i\infty}\frac{dt}{4\pi i}\Gamma(t-\nu)\Gamma\left(t-\frac{1}{2}\right)\eta(2t-1)\left(\frac{ML}{2}\right)^{-2t}$$
$$-\frac{1}{\sqrt{\pi}}\sum_{k=1}^{\infty}\int_{c-i\infty}^{c+i\infty}\frac{ds}{2\pi i}\left(\frac{M\beta}{2\pi}\right)^{2k-2\nu}\left(\frac{\pi L}{\beta}\right)^{-2s}\Gamma(s)\eta(2s)$$
$$\times\Gamma\left(s+k-\nu+\frac{1}{2}\right)\zeta(2s+2k-2\nu+1). \tag{22}$$

We investigate the above equation and obtain the poles for each of the integrals.

(i) First integral: poles at $t=0$, $t=1/2$ and $t=\nu-j$ with $j\in[0,\infty[$. This corresponds to the dependencies β^0, β^{-1}, and $\beta^{2k-2\nu}$.
(ii) Second integral: poles at $t=1/2$ and $t=\nu-j$ with $j\in[0,\infty[$. This corresponds to the dependencies β^{-1} and $(L/\beta)L^{2k-2\nu}$.
(iii) Third integral: poles at $s=0$, $s=\nu-k-1/2$, and $s=\nu-k$. This corresponds to the dependencies $\beta^{2k-2\nu}$, $L^{2k-2\nu}$, and $(L/\beta)L^{2k-2\nu}$.

This means that the case of antiperiodic boundary conditions in space and $a_0=0$ only has dependencies as β^α, $(L/\beta)L^\alpha$, L^α. Therefore, the procedure of taking $L\to 0$,

$$L\mathcal{I}_\rho^{D,2}(M;\beta,a_0=0;L|\mathcal{A})|_{L\to 0}, \tag{23}$$

does not reproduce any behavior of a model with fewer dimensions. This is completely different from the situation with periodic boundary conditions in space, where a relationship between a "film" model (D dimensions) and a "surface" model ($D-1$ dimensions) is clear. Therefore, for a bosonic model with antiperiodic boundary conditions in space, the idea of dimensional reduction is ill defined and does not result in any temperature-dependent function. This is related to the nonexistence of static modes when dealing with antiperiodic boundary conditions [22].

D. Fermionic field: Periodic boundary conditions in space

From this point forward, we proceed to take into account the situation of a fermionic model. We already know that the one-loop Feynman amplitude for fermions is related to the one-loop Feynman amplitude for bosons with $a_0=1$; this relation is given by Eq. (3). At first, we consider periodic boundary conditions in space, given by Eq. (7). To explore the behavior as $L\to 0$, we use the integral representation of K_ν, Eq. (12), and the double sum that arises is treated by an analytic extension

$$\sum_{n_0=1,n_1=1}^{\infty}\frac{(-1)^{n_0}}{(n_0^2\beta^2+n_1^2L^2)^t}$$
$$=-\frac{1}{2L^{2t}}\zeta(2t)+\frac{2\pi^t}{\Gamma(t)}\sqrt{\frac{L}{\beta}}\frac{1}{(\beta L)^t}\sum_{n_0,n_1=1}^{\infty}\left(\frac{n_0}{n_1}\right)^{t-\frac{1}{2}}$$
$$\times\left[-K_{t-\frac{1}{2}}\left(2\pi n_0 n_1\frac{L}{\beta}\right)+2^{\frac{1}{2}-t}K_{t-\frac{1}{2}}\left(2\pi n_0 n_1\frac{L}{\beta}\right)\right]. \tag{24}$$

Hence, the function $\mathcal{W}_\nu$ reads

$$\mathcal{W}_\nu(M;\beta,a_0=1;L|\mathcal{P})$$
$$=-\int_{c-i\infty}^{c+i\infty}\frac{dt}{4\pi i}\Gamma(t)\eta(2t)\Gamma(t-\nu)\left(\frac{M\beta}{2}\right)^{-2t}$$
$$\times\frac{1}{\sqrt{\pi}}\sum_{k=1}^{\infty}\int_{c-i\infty}^{c+i\infty}\frac{ds}{2\pi i}\left(\frac{M\beta}{2\pi}\right)^{2k-2\nu}\left(\frac{\pi L}{\beta}\right)^{-2s}$$
$$\times\Gamma(s)\zeta(2s)\Gamma\left(s+k-\nu+\frac{1}{2}\right)(-1+2^{2s+2k-2\nu+1})$$
$$\times\zeta(2s+2k-2\nu+1), \tag{25}$$

and an analysis of each term gives that

(i) for the first integral there are poles at $t=0$ and $t=\nu-j$ with $j\in[0,\infty[$. This corresponds to the dependencies β^0 and $\beta^{2k-2\nu}$;
(ii) and for the second integral there are poles at $s=0$, $s=1/2$, and $s=\nu-k$. This corresponds to the dependencies $\beta^{2k-2\nu}$, $(\beta/L)\beta^{2k-2\nu}$, and $(L/\beta)L^{2k-2\nu}$.

It can be noted that the relevant contribution comes from the pole $s=1/2$ of the second integral. This is the contribution that survives at $L\to 0$. Making it explicit, we obtain in this limit that

$$L\mathcal{I}_\rho^{D,2}(M;\beta,a_0=1;L|\mathcal{P})|_{L\to 0}$$
$$=\mathcal{F}_\rho^D(M,\beta;c_1=4,c_2=0)+\text{divergent terms}, \tag{26}$$

where the function $\mathcal{F}_\rho^D(M,\beta;c_1,c_2)$ is defined in Eq. (11).

Just as we did when we exhibited the result for the bosonic case ($a_0=0$) in periodic boundary conditions in space, let us concentrate on the behavior as $L\to 0$. To make the comparison clear, we can keep in mind the analogy of heated films (in dimension D with two compactifications) and surfaces (in dimension $D-1$ with one compactification). The heated film described by a fermionic model is given by (26) when the film thickness is very small. However, the surface described by the same fermionic model reads

$$\mathcal{I}_{\rho}^{D-1,1}(M;\beta,a_0=1) = \mathcal{F}_{\rho}^{D}(M,\beta;c_1=0,c_2=1/2)+\text{divergent terms}, \tag{27}$$

which is completely different.

Therefore, in the case of a fermionic model, there is no direct relationship between models in different dimensions. This result resembles the discussion that the procedure of dimensional reduction and quantization does not commute for fermionic models [36] and that the dimensional reduction behaves differently for bosons and fermions [35].

E. Fermionic field: Dirichlet and Neumann boundary conditions in space

As a next step, we investigate the fermionic field at different spatial boundary conditions. Just as done in Sec. III B for bosonic fields in Dirichlet and Neumann boundary conditions, we apply in Eqs. (4) and (5) the known result for periodic boundary conditions, Eq. (26), and the dimensionally reduced fermionic model given by Eq. (10). This gives, respectively, for Dirichlet and Neumann boundary conditions that

$$L\mathcal{I}_{\rho}^{D,2}(M;\beta,a_0=1;L|\mathcal{D})|_{L\to 0} = \frac{3}{4}\mathcal{F}_{\rho}^{D}(M,\beta;c_1=4/3,c_2=1/3)+\text{divergent terms}, \tag{28}$$

$$L\mathcal{I}_{\rho}^{D,2}(M;\beta,a_0=1;L|\mathcal{N})|_{L\to 0} = -\frac{1}{4}\mathcal{F}_{\rho}^{D}(M,\beta;c_1=-4,c_2=1)+\text{divergent terms}. \tag{29}$$

These results reinforce that, as found in Sec. III D, the fermionic field does not undergo a dimensional reduction as bosonic fields. We can, indeed, obtain a dimensionally reduced model, as expressed in Eqs. (28) and (29). However, it has no relation with the otherwise expected result given by Eq. (10).

F. Fermionic field: Antiperiodic boundary conditions in space

At last, let us consider a fermionic model ($a_0=1$) with antiperiodic boundary conditions in space [Eq. (12)]. After using the integral representation of Eq. (12), we use the following analytic extension of the double sum:

$$\sum_{n_0=1,n_1=1}^{\infty}\frac{(-1)^{n_0+n_1}}{(n_0^2\beta^2+n_1^2L^2)^t} = \frac{1}{2L^{2t}}\eta(2t)+\frac{2\pi^t}{\Gamma(t)}\sqrt{\frac{L}{\beta}}\frac{1}{(\beta L)^t}\sum_{n_0,n_1=1}^{\infty}(-1)^{n_1}\left(\frac{n_0}{n_1}\right)^{t-\frac{1}{2}} \times\left[-K_{t-\frac{1}{2}}\left(2\pi n_0 n_1\frac{L}{\beta}\right)+2^{\frac{1}{2}-t}K_{t-\frac{1}{2}}\left(2\pi n_0 n_1\frac{L}{\beta}\right)\right], \tag{30}$$

and obtain the expression for the function $\mathcal{W}_{\nu}$,

$$\begin{aligned}\mathcal{W}_{\nu}(M;\beta,a_0=1;L|\mathcal{A}) &= -\int_{c-i\infty}^{c+i\infty}\frac{dt}{4\pi i}\Gamma(t)\eta(2t)\Gamma(t-\nu)\left(\frac{M\beta}{2}\right)^{-2t} \\ &\quad -\frac{1}{\sqrt{\pi}}\sum_{k=1}^{\infty}\int_{c-i\infty}^{c+i\infty}\frac{ds}{2\pi i}\left(\frac{M\beta}{2\pi}\right)^{2k-2\nu}\left(\frac{\pi L}{\beta}\right)^{-2s}\Gamma(s)\eta(2s) \\ &\quad\times\Gamma\left(s+k-\nu+\frac{1}{2}\right)(-1+2^{2s+2k-2\nu+1}) \\ &\quad\times\zeta(2s+2k-2\nu+1).\end{aligned} \tag{31}$$

Studying the poles for each integral in Eq. (31), we obtain that

(i) first integral: poles at $t=0$ and $t=\nu-j$ with $j\in[0,\infty[$. This corresponds to the dependencies β^0 and $\beta^{2k-2\nu}$;

(ii) second integral: poles at $s=0$ and $s=\nu-k$. This corresponds to the dependencies $\beta^{2k-2\nu}$ and $L^{2k-2\nu}$.

Therefore, for antiperiodic boundary conditions in space and $a_0=1$ there is no mixed dependency on β and L. Also, just like the case of antiperiodic boundary conditions in space for bosons discussed in Sec. III C the procedure of dimensional reduction is ill defined.

This result shows that the use of antiperiodic boundary conditions in space forbids the procedure of dimensional reduction both for bosonic and fermionic fields. This might be an indication of a topological aspect, independent of the nature of the field.

IV. CONCLUSION

We discussed in Sec. III that there were three possible outcomes when one investigates the procedure of dimensional reduction as proposed in this article. In the remaining sections, we found examples of all the following three categories:

(i) Well-defined dimensional reduction.

This happens for bosonic fields in periodic, Dirichlet, and Neumann boundary conditions where there is a simple relation between a model in D dimensions that is dimensionally reduced and a model in $D-1$ dimensions. See Secs. III A and III B.

(ii) Ill-defined dimensional reduction.
This happens for antiperiodic boundary conditions in space, both for bosonic and fermionic fields. See Secs. III C and III F.

(iii) Dimensional reduction to a different model.
This happens for fermionic fields in periodic, Dirichlet, and Neumann boundary conditions where the model in D dimensions that is dimensionally reduced has no relation with a model originally constructed in $D-1$ dimensions. See Secs. III D and III E.

We remark that from the perspective of the decoupling of heavy fields [21,22], what we call a "dimensional reduction," could also be understood as identifying whether there are static modes related to the compactified dimension in the model under analysis. It means that for periodic, Dirichlet, and Neumann boundary condition we get a static mode related to the system size L, while for antiperiodic boundary condition there are only nonstatic modes.

We found that the previous article [34] was indeed a special case (bosonic field, periodic boundary condition in space) and now we exhibit a bigger picture of the problem. The procedure of dimensional reduction indeed depends on the imposed boundary conditions and the nature of the field. Nevertheless, there are yet some open questions. The behavior of fermionic fields passing through a dimensional reduction might be explained by the fact that fermions are dependent on the number of spatial dimensions. Moreover, the forbidden dimensional reduction for models with antiperiodic boundary conditions in space is perhaps a topological aspect of dimensionally reducing a Möbius strip, which would explain the independence on the nature of the fields.

ACKNOWLEDGMENTS

The authors thank the Brazilian agency Conselho Nacional de Desenvolvimento Científico e Tecnológico (CNPq) for partial financial support.

APPENDIX: RELATION BETWEEN FERMIONIC AND BOSONIC INTEGRALS

The one-loop Feynman amplitude for self-interacting fermionic field with coupling $a+b\gamma_S$ is

$$\mathcal{J}_\nu^D(m) = \mathrm{tr}\int \frac{d^D p}{(2\pi)^D}\left(\frac{a+b\gamma_S}{i\not{p}+m}\right)^\nu = \mathrm{tr}\int \frac{d^D p}{(2\pi)^D}\left(\frac{(a+b\gamma_S)(-i\not{p}+m)}{p^2+m^2}\right)^\nu. \quad \text{(A1)}$$

Here we use the notation of Ref. [23] for the Euclidean Dirac matrices. To compute the trace in a systematic way, we define $v=-ip^\mu\gamma_\mu+m$, $\tilde{v}=ip^\mu\gamma_\mu+m$ and note that $v\gamma_S=\tilde{v}\gamma_S$. Organizing the trace $\mathcal{T}_\nu=\mathrm{tr}[(a+b\gamma_S)v]^\nu$ in such a way that all γ_S matrices are on the left, we have

$$\mathcal{T}_1(a,b) = av + b\gamma_S v, \quad \text{(A2a)}$$

$$\mathcal{T}_2(a,b) = a^2v^2 + ab\gamma_S(\tilde{v}v+v^2) + b^2\gamma_S^2\tilde{v}v, \quad \text{(A2b)}$$

$$\mathcal{T}_3(a,b) = a^3v^3 + a^2b\gamma_S(\tilde{v}^2v+\tilde{v}v^2+v^3) + ab^2\gamma_S^2(\tilde{v}^2v+2\tilde{v}v^2) + b^3\gamma_S^3\tilde{v}v^2, \quad \text{(A2c)}$$

$$\mathcal{T}_4(a,b) = a^4v^4 + a^3b\gamma_S(\tilde{v}^3v+\tilde{v}^2v^2+\tilde{v}v^3+v^4) + a^2b^2\gamma_S^2(\tilde{v}^3v+2\tilde{v}^2v^2+3\tilde{v}v^3) + ab^3\gamma_S^3(2\tilde{v}^2v^2+2\tilde{v}v^3) + b^4\gamma_S^4\tilde{v}^2v^2. \quad \text{(A2d)}$$

From these we can infer some relations regarding the trace $\mathcal{T}_\nu$ for any ν. The component with $b=0$ and $a\neq 0$ contributes as

$$\mathcal{T}_\nu(a,0) = a^\nu v^\nu,$$

and the component with $a=0$ and $b\neq 0$ behaves as

$$\mathcal{T}_\nu(0,b) = b^\nu\gamma_S^\nu(\tilde{v}v)^{\lfloor\nu/2\rfloor}v^{\nu-2\lfloor\nu/2\rfloor}.$$

The mixed terms are a little bit more intricated. First, we adopt another notation defining some function $f_j^{(i)}(\tilde{v},v)$,

$$\mathcal{T}_\nu(a,b)-\mathcal{T}_\nu(a,0)-\mathcal{T}_\nu(0,b) = \sum_{\sigma=1}^{\nu-1}a^{\nu-\sigma}b^\sigma\gamma_S^\sigma f_\sigma^{(\nu-\sigma)}(\tilde{v},v),$$

where the function $f_j^{(i)}(\tilde{v},v)$ can be shown to satisfy the following difference equations:

$$f_{2\ell}^{(i)}(\tilde{v},v) = \frac{\tilde{v}v}{\ell!}\frac{\partial}{\partial v}f_{2\ell-1}^{(i)}(\tilde{v},v), \quad \text{(A3)}$$

$$f_{2\ell+1}^{(i)}(\tilde{v},v) = \frac{\tilde{v}v}{\ell!}\frac{\partial}{\partial\tilde{v}}f_{2\ell}^{(i)}(\tilde{v},v). \quad \text{(A4)}$$

Therefore, once we obtain one of these functions all others are obtained recursively. The simpler one is the case $f_1^{(i)}$ which is associated with $a^ib\gamma_S$ and can be directly written as

$$f_1^{(i)} = \sum_{k=0}^{i}\tilde{v}^{i-k}v^{k+1}.$$

With this in hand, we use the difference equations and obtain the generalization that

$$f_j^{(i)}(\tilde{v},v)=\sum_{k=0}^{i}\frac{(k+\lfloor j/2\rfloor)!}{k!\lfloor j/2\rfloor!}\frac{(i-k+\lfloor\frac{j+1}{2}\rfloor-1)!}{(i-k)!(\lfloor\frac{j+1}{2}\rfloor-1)!}\tilde{v}^{i+j-k-\lfloor\frac{j+1}{2}\rfloor}v^{k+\lfloor\frac{j+1}{2}\rfloor}.$$

Substituting back, we obtain that the complete trace is

$$\begin{aligned}\mathrm{tr}[(a+b\gamma_S)v]^\nu=\mathrm{tr}\Bigg[&a^\nu v^\nu+b^\nu\gamma_S^\nu(p^2+m^2)^{\lfloor\frac{\nu}{2}\rfloor}v^{\nu-2\lfloor\frac{\nu}{2}\rfloor}\\&+\sum_{\sigma=1}^{\nu-1}a^{\nu-\sigma}b^\sigma\gamma_S^\sigma\sum_{k=0}^{\nu-\sigma}\frac{(k+\lfloor\frac{\sigma}{2}\rfloor)!}{k!\lfloor\frac{\sigma}{2}\rfloor!}\frac{(\nu-k-1-\lfloor\frac{\sigma}{2}\rfloor)!}{(\nu-k-\sigma)!(\lfloor\frac{\sigma+1}{2}\rfloor-1)!}\tilde{v}^{\nu-k-\lfloor\frac{\sigma+1}{2}\rfloor}v^{k+\lfloor\frac{\sigma+1}{2}\rfloor}\Bigg].\end{aligned}\tag{A5}$$

Therefore, the trace operation becomes simply

$$\mathrm{tr}(\tilde{v}v)^n(v^2)^m=\mathrm{tr}(\tilde{v}v)^n(\tilde{v}^2)^m=d_\gamma(m^2+p^2)^n(m^2-p^2)^m,$$

where d_γ is the dimension of the gamma matrix.

After computing the full trace and making some algebraic manipulation, we obtain

$$\begin{aligned}\frac{1}{d_\gamma}\mathrm{tr}[(a+b\gamma_S)v]^\nu=&\,a^\nu\sum_{k=0}^{\lfloor\frac{\nu}{2}\rfloor}\binom{\nu}{2k}m^{\nu-2k}(-p^2)^k+b^\nu(p^2+m^2)^{\frac{\nu}{2}}(\nu-2\lfloor\nu/2\rfloor)\\&+\sum_{k=1}^{\lfloor\frac{\nu-1}{2}\rfloor}a^{\nu-2k}b^{2k}\sum_{j=k}^{\lfloor\frac{\nu}{2}\rfloor}\frac{j!(\nu-j-1)!}{(j-k)!k!(\nu-k-j)!(k-j)!}(p^2+m^2)^j\sum_{\ell=0}^{\lfloor\frac{\nu}{2}-j\rfloor}\binom{\nu-2j}{2\ell}m^{\nu-2j-2\ell}(-p^2)^\ell\\&+\sum_{k=1}^{\lfloor\frac{\nu-1}{2}\rfloor}a^{\nu-2k}b^{2k}\sum_{j=\lfloor\frac{\nu}{2}+1\rfloor}^{\nu-k}\frac{j!(\nu-j-1)!}{(j-k)!k!(\nu-k-j)!(k-j)!}(p^2+m^2)^{\nu-j}\sum_{\ell=0}^{\lfloor\frac{\nu}{2}-j\rfloor}\binom{2j-\nu}{2\ell}m^{2j-\nu-2\ell}(-p^2)^\ell.\end{aligned}\tag{A6}$$

As a final manipulation we use that

$$(-p^2)^\ell=\sum_{n=0}^{\ell}(-1)^n\binom{\ell}{n}(p^2+m^2)^n m^{2\ell-2n},$$

and now we can relate the fermionic scenario with the bosonic one,

$$\begin{aligned}\frac{1}{d_\gamma}\mathcal{J}_\nu^D=&\,a^\nu\sum_{k=0}^{\lfloor\frac{\nu}{2}\rfloor}\sum_{j=0}^{k}\binom{\nu}{2k}\binom{k}{j}m^{\nu-2j}(-1)^j\mathcal{I}_{\nu-j}^D(m^2)+b^\nu(\nu-2\lfloor\nu/2\rfloor)\mathcal{I}_{\nu/2}^D(m^2)\\&+\sum_{k=1}^{\lfloor\frac{\nu-1}{2}\rfloor}a^{\nu-2k}b^{2k}\sum_{j=k}^{\lfloor\frac{\nu}{2}\rfloor}\frac{j!(\nu-j-1)!}{(j-k)!k!(\nu-k-j)!(k-j)!}\sum_{\ell=0}^{\lfloor\frac{\nu}{2}-j\rfloor}\binom{\nu-2j}{2\ell}\sum_{n=0}^{\ell}(-1)^n\binom{\ell}{n}m^{\nu-2j-2n}\mathcal{I}_{\nu-j-n}^D(m^2)\\&+\sum_{k=1}^{\lfloor\frac{\nu-1}{2}\rfloor}a^{\nu-2k}b^{2k}\sum_{j=\lfloor\frac{\nu}{2}+1\rfloor}^{\nu-k}\frac{j!(\nu-j-1)!}{(j-k)!k!(\nu-k-j)!(k-j)!}\sum_{\ell=0}^{\lfloor\frac{\nu}{2}-j\rfloor}\binom{2j-\nu}{2\ell}\sum_{n=0}^{\ell}\binom{\ell}{n}m^{2j-\nu-2n}\mathcal{I}_{j-n}^D(m^2).\end{aligned}$$

This relation also holds if one considers compactified dimensions. One must only be careful that the conditions imposed on $\mathcal{I}$ will be, in this case, the conditions that would be imposed on the fermionic integral. Therefore, if one introduces a compactification of the imaginary time to introduce temperature, it must have antiperiodic boundary condition as we are dealing with fermions.

[1] T. Kaluza, Int. J. Mod. Phys. D **27**, 1870001 (2018).
[2] A. A. Khan *et al.* (*CP*-PACS Collaboration), Phys. Rev. D **64**, 114506 (2001).
[3] D. Chakraverty, K. Huitu, and A. Kundu, Phys. Lett. B **558**, 173 (2003).
[4] K. Agashe, G. Perez, and A. Soni, Phys. Rev. Lett. **93**, 201804 (2004).
[5] A. Karch, E. Katz, D. T. Son, and M. A. Stephanov, Phys. Rev. D **74**, 015005 (2006).
[6] M. Blanke, A. J. Buras, B. Duling, K. Gemmler, and S. Gori, J. High Energy Phys. 03 (2009) 108.
[7] C. D. Fosco, A. P. C. Malbouisson, and I. Roditi, Phys. Lett. B **609**, 430 (2005).
[8] L. Da Rold and A. Pomarol, Nucl. Phys. **B721**, 79 (2005).
[9] G. Panico, M. Serone, and A. Wulzer, Nucl. Phys. **B739**, 186 (2006).
[10] G. Panico, M. Serone, and A. Wulzer, Nucl. Phys. **B762**, 189 (2007).
[11] G. 't Hooft, Nucl. Phys. **B75**, 461 (1974).
[12] S. Hands, J. High Energy Phys. 09 (2015) 047.
[13] B. Rosenstein, B. Warr, and S. H. Park, Phys. Rep. **205**, 59 (1991).
[14] S. Hands, A. Kocic, and J. B. Kogut, Ann. Phys. (N.Y.) **224**, 29 (1993).
[15] B. Rosenstein, B. J. Warr, and S. H. Park, Phys. Rev. D **39**, 3088 (1989).
[16] K. G. Klimenko, Z. Phys. C **54**, 323 (1992).
[17] K. G. Klimenko, Teor. Mat. Fiz. **90**, 3 (1992) [Theor. Math. Phys. **90**, 1 (1992)].
[18] P. Horava and E. Witten, Nucl. Phys. **B475**, 94 (1996).
[19] J. H. Schwarz, Phys. Rep. **89**, 223 (1982).
[20] O. Aharony, S. S. Gubser, J. M. Maldacena, H. Ooguri, and Y. Oz, Phys. Rep. **323**, 183 (2000).
[21] T. Appelquist and R. D. Pisarski, Phys. Rev. D **23**, 2305 (1981).
[22] N. P. Landsman, Nucl. Phys. **B322**, 498 (1989).
[23] J. Zinn-Justin, *Quantum Field Theory and Critical Phenomena*, 4th ed. (Clarendon Press, Oxford, 2002).
[24] H. Meyer-Ortmanns and T. Reisz, *Principles of Phase Structures in Particle Physics* (World Scientific Publishing Company, Singapore, 2007).
[25] S. Nadkarni, Phys. Rev. D **27**, 917 (1983).
[26] E. Braaten and A. Nieto, Phys. Rev. D **53**, 3421 (1996).
[27] P. Bialas, A. Morel, B. Petersson, K. Petrov, and T. Reisz, Nucl. Phys. **B581**, 477 (2000).
[28] T. Zhang, T. Brauner, A. Kurkela, and A. Vuorinen, J. High Energy Phys. 02 (2012) 139.
[29] A. Bazavov *et al.* (HotQCD Collaboration), Phys. Rev. D **90**, 094503 (2014).
[30] F. C. Khanna, A. P. C. Malbouisson, J. M. C. Malbouisson, and A. R. Santana, *Thermal Quantum Field Theory—Algebraic Aspects and Applications* (World Scientific Publishing Company, Singapore, 2009).
[31] F. C. Khanna, A. P. C. Malbouisson, J. M. C. Malbouisson, and A. E. Santana, Phys. Rep. **539**, 135 (2014).
[32] C. A. Linhares, A. P. C. Malbouisson, Y. W. Milla, and I. Roditi, Phys. Rev. B **73**, 214525 (2006).
[33] E. Cavalcanti, C. A. Linhares, and A. P. C. Malbouisson, Int. J. Mod. Phys. A **33**, 1850008 (2018).
[34] E. Cavalcanti, J. A. Lourenço, C. A. Linhares, and A. P. C. Malbouisson, Phys. Rev. D **99**, 025007 (2019).
[35] S.-z. Huang and M. Lissia, Phys. Lett. B **349**, 484 (1995).
[36] L. P. R. Ospedal and J. A. Helayël-Neto, Phys. Rev. D **97**, 056014 (2018).
[37] G. Fucci and K. Kirsten, J. Math. Phys. (N.Y.) **59**, 033503 (2018).
[38] E. Elizalde, Lect. Notes Phys. **855**, 1 (2012).

Chapter 7

Conclusions

Now this is not the end. It is not even the beginning of the end. But it is, perhaps, the end of the beginning.

– Winston Churchill

In this final chapter, I present some further developments and final remarks for the research developed. It is mainly a quick comment on unpublished results and a letter of intentions for future research.

7.1 Renormalon poles

The investigation of renormalon poles arose as a consequence of the broader interest in the summability of quantum field theories. The discussion on this topic is in the introduction at sections 1.3 and 1.9 and the paper reproduced in Chap. 4. Furthermore, the behavior of the renormalon poles as temperature is increased evidences the relevance on the topic of dimensional reduction and motivates us to consider the influence of other parameters as a finite length and boundary conditions. As discussed in Sec. 1.10 we took a break in the investigation of renormalon to understand more properly the question of dimensional reduction. The consequence of this investigation are the papers reproduced in chapters 5 and 6. As could be expected, a next step (*in development*) is to return to the investigation of renormalon poles. There are some open inquiries to addressed:

1. Does the disappearance of renormalons happen just in the limit of dimensional reduction, or is there some finite temperature in which occurs this change of behavior?
2. Are there other parameters that can influence the location or the residues of the renormalon poles?
3. Is the observed behavior a characteristic of the chosen model or a general aspect inherent of all field theoretical models that have renormalons?

Although not yet published, there are partial answers to these inquiries as can be seen in the following.

To address the first inquiry, we can note that an essential element to produce the renormalon pole, in the model under consideration at the article, is the asymptotic behavior of the internal "bubbles" as $\ln \ell$, where ℓ is the momenta that enter the bubble. We can look at it both from an analytical or numerical perspective, but the basic idea is that the dominance of the asymptotic behavior is related to the ratio ℓ/T. This ratio is unphysical as ℓ is the momenta of integration, and we can make sense out of it only if the ratio ℓ/T tends to zero of infinity. For zero temperature and low temperatures, $T \ll \ell$, and we can assume that for extremally high temperatures, $T \gg \ell$. Therefore, there are only the regimes already considered during the article: zero temperature, low temperatures, and very high temperatures. This perspective indicates that the renormalon disappearance occurs only when the dimensional reduction happens. This means the nonexistence of a "transition temperature".

The second inquiry, of whether another parameter could influence the renormalon poles, can lead to a large number of assumptions to be tested. As far as we know, the specialized literature did not make any direct investigation of this yet. Of course, we can always assume, and perhaps even be satisfied, by the formal perspective that "if we can do; we must do". However, to understand the underlying motivation, we must remember the concept of adiabatic continuity conjecture discussed in Sec. 1.10.

The idea is to obtain the nonperturbative solution of a field-theoretical model. As we already explained, the existence of the renormalons in the model introduces a problem in this procedure. Let us assume a field-theoretical model with one circle compactification of length L. We see that there is a disappearance of the renormalons if we get to the regime of dimensional reduction (the limit as $L \to 0$). Therefore, in this regime, the series is summable, and we can obtain the nonperturbative solution. What if we adjust the value of L? One proposition is that the nonperturbative solution for finite L or even $L \to \infty$ is related to the solution obtained in the limit $L \to 0$ *if* the system does not undergo a phase transition. That is the idea behind the adiabatic continuity conjecture. Therefore, one needs to avoid phase transitions in the parameter L so that the conjecture holds. One scheme to ensure this is to apply spatial periodic boundary conditions for fermions and spatial antiperiodic boundary conditions for bosons. Notice that the freedom to choose the spatial boundary condition is what make the circle compactification useful. The boundary condition related to the introduction of finite temperature, on the other hand, would be restricted by the KMS condition.

The above considerations motivates the investigation of the dependence with, for example, different boundary conditions or chemical potential as these parameters could help to get a "path" from low L to high L. As could be inferred, the investigation in

Chap. 6 was a preparatory step to consider temperature, finite length, and four different boundary conditions (periodic, antiperiodic, Dirichlet and Neumann). A first (and somewhat easy) step is to take into account, using our simplified model of scalar field theory, two scenarios: 1 - finite temperature and chemical potential; 2 - finite size and quasiperiodic boundary conditions.

By quasiperiodic (or anyonic) boundary condition we mean the use of a parameter (θ) that allows to interpolates between a periodic boundary condition ($\theta = 0$) and an antiperiodic boundary condition ($\theta = 1$).

The computation is very similar to the procedure at the article reproduced in Chap. 4, and the conclusion of this first step analysis states that both scenarios make almost no difference. The introduction of a finite chemical potential μ does not modify the location of the poles neither the number of renormalons, it only modifies the residues. In the scenario with a spatial restriction and employing a quasiperiodic boundary condition, we obtain a similar result, the only difference being that there is a specific configuration at which the residues vanish.

The scope of validity of the results requires the investigation of different field-theoretical models, and we do not have an indication so far of what to expect. However, with this intention in mind, we already considered both bosonic and fermionic models in our investigation of dimensional reduction, as exhibited in Chap. 6.

7.2 Hadronic Phenomenology

As is evident in Chap. 3, the model discussed is just a first step. To fully develop the work, we should take into account the time evolution of the hadronic multiplicities. However, as pointed out in the article itself, there are some missing features, as we have only investigated the lowest partial wave.

However, this research line still uses the hypothesis that the interaction with the hadron gas represents a relevant contribution to understand the charmonium J/ψ behavior. As commented in the introduction, recent experiments at LHC are still evaluating, which are the most relevant contributions. Some new information might arise with the data from pA collisions. In these collisions, although without a QGP phase, there is an observed suppression in the abundance of charmonia.

We stopped this investigation for a while, as we considered that a more useful path would be to consider the J/ψ regeneration in the QGP phase. The reported results so far seem to indicate that the hadron gas phase is not responsible for the observed phenomena.

7.3 Dimensional Reduction

As already commented, this topic was just a brief a detour, but we found some open topics unnoticed by the literature, and there is yet a few questions to address. So far, we got a relationship between a model in D dimensions and its dimensionally-reduced version in $D-1$. Moreover, we know that this relation depends on the nature of the field (bosonic or fermionic) and the boundary condition imposed on the restricted dimension.

However, our discussion stops at one-loop order. It remains as a next challenge to extend the study to more loops, ideally in a format valid for any number of loops. A possible path to take this into account requires first that we express an arbitrary Feynman diagram in D dimensions with d compactifications, an extension of the known parametric representation of graphs to the scenario of toroidal topologies. With this in hand, we can investigate the topic on a more general ground.

Furthermore, as this theme of dimensional reduction is somewhat related to the topic of films and surfaces, a generalization to a nonrelativistic version might be relevant and is under current development.

7.4 Final remarks

As pointed out in the introduction, there is a *large picture* where everything discussed throughout this manuscript becomes related. I consider that the first step towards it is to take into account an effective quark-meson model that could describe the transition from the QGP to the hadrons gas. A candidate, as indicated by the recent literature, is to consider the chiral Polyakov Quark Meson (PQM) model (also called Polyakov Linear Sigma Model, PLSM). After choosing a model, we can first study it from a formal perspective. The path is to evaluate its nonperturbative results from the perturbative series by investigating the Borel summability of the theory and, if needed, apply the program of resurgence to "cure" the ambiguities that come from the renormalons. Then, we could extract phenomenological predictions about the behavior of heavy quarkonia inside the quark-gluon plasma, hadron gas, or also the mixed phase.